MECHANISTIC DISSECTION OF VPS45'S FUNCTION(S) USING MUTATIONS UNDERPINNING SEVERE CONGENITAL NEUTROPENIA.

Blythe Wright

Doctor of Philosophy

UNIVERSITY OF YORK
BIOLOGY
February 2025

i. Abstract

Severe congenital neutropenia (SCN) is a rare haematological disorder defined by a reduction in neutrophils, the white blood cells that fight infection. SCN patients are susceptible to opportunistic bacterial infections that become life-threatening. In 2013, Stepensky and colleagues identified the first mutation in the *VPS45* gene associated with SCN V, these patients displayed an increase in apoptosis (programmed cell death) in their neutrophils and resistance to treatment. Most SCN patients have regular granulocyte-colony stimulating factor (G-CSF) treatment to manage symptoms, however patients with SCN V are subject to much more invasive bone marrow transplants to treat their condition. In addition to this SCN causing *VPS45* mutation, 4 more have since been identified. Until this point Vps45 had been well-characterised as a membrane trafficking protein in yeast and more recently has been implicated in autophagy, whether these functions are related to SCN is unknown.

In this project I investigated how Vps45 is involved in increased apoptosis in cells using the model organism, *Saccharomyces cerevisiae* (budding yeast) by characterising the different roles of Vps45. Using yeast strains with *VPS45* mutations analogous to the mutations identified in SCN V patients, I used three physiological assays to investigate the role of Vps45 in membrane trafficking, autophagy and apoptosis. By dissecting the roles of Vps45 in different processes in the cell I have identified a potential model for Vps45's role in protection from apoptosis, characterising this role of Vps45 and its known interactors in different mechanisms will eventually lead to a more suitable treatment for SCN V patients.

ii. Acknowledgements

Thank you to the BBSRC White Rose PhD programme for funding this project and to Prof. Dani Ungar and Dr. Chris Stefan for an engaging and thoughtful VIVA discussion.

I would like to thank many people for helping me during my PhD, particularly my supervisors. Prof. Nia Bryant and Dr. Chris MacDonald have supported me academically and emotionally throughout my time at York. Their understanding of my health struggles has helped me to strive to complete my research to the best of my abilities despite any problems along the way. This also applies to my TAP supervisor Prof. Dani Ungar who has helped me in hard times but academically has always given me his time and support helping me to produce my best work in my progression meetings. I would also like to thank Dr. Dimi Kioumourtzoglou for his help getting me set up in the J0 lab in 2020 which during COVID lockdowns was incredibly difficult. Dr. Dave Mentlak (Safety Dave) has always kept us safe in the lab during and after COVID and has always been the best person to sound ideas off and is always genuinely interested in your work, wanting to help as much as he can.

To Dr. Pete O'Toole and Dr. Karen Hogg at the University of York Technology Facility, thank you for providing me with an enjoyable and informative 3-month placement programme. Also, thank you to Karen and Dr. Grant Calder for all their help with my imaging and cytometry woes and queries.

I really appreciate Ann Mathe, Patricia McNamara and Monica Bandeira for all their help with supporting me through all my health support and adjustments, allowing me to finish this PhD as I always dreamed to. Thank you.

Thank you to Dr. Anna Basu and Janice Pearse, even though I've strayed from patient-based research, their passion and care for patients inspired me to continue my academic career.

Dr. Nathan Clark for providing the ERC data that spurred my mechanistic thinking from early on. To Josie Ayre, Alex Swinden and Daniel Newsome the patient Masters' students who I tried to navigate zoom guidance for in my first year and then the Undergraduate students (Tara Best, Sandra Manoj, Isabelle Sutherland, Gemma Rowbotham, Ashleigh Martin and Allice Poore) who reminded me that I do enjoy sharing my love of research, it's just a lot easier when it's face to face.

Thank you to Dr. Katherine Paine and Dr. Kamilla Laidlaw who were always supportive and helpful with any yeasty questions I had when I first began, and throughout. The 'Yeast Gang' made life in the lab a lot more enjoyable particularly when there wasn't much to look forward to after work. Dr. Nisreen Chahid, thank you for being my first friend in York and my virtual companion when times were strange and unfamiliar. I am very grateful for meeting Dr. Ben West and Dr. Jordan Tzvetkov while in J0, they always supported me in my lab difficulties and have made my time in the city of York more enjoyable, especially since making friends in first year was incredibly difficult. I am also grateful to Dr. Alex Scott and Dr. Evie Farnham whose virtual social gatherings made my COVID transition less lonely.

Thank you to my friend/housemate Dr. Josie Monaghan for giving me somewhere to live (the best house in York I think) and for being the most supportive friend that I really needed. Dr. Sophie James, living parallel lives until about 3 months before you left York was not ideal but thanks to the internet you are able to make me laugh constantly. Thank you to Dr. Alex Brown and Dr. Christopher Markwell, every biologist needs at least one physicist to help them zoom out of the tiny stuff for a second. Thank you to my undergraduate cohort (Annie, Lisa, Carl, Moh, Helen, Curtis and David) and the cell signalling masters girls (Claudia, Charlotte and Izzy) for making my progression through further education so fun. Though, I think 10 years of extra learning is probably too long.

I would like to thank my mum and dad for supporting me throughout, listening to my woes and always being there for me. Especially my Grandma Brown who without her generosity I would have never been able to fill out my dreams of being a fully-fledged scientist. I would like to thank the Whitaker family for being my biggest cheerleaders and finally to Ed Whitaker for loving me and looking after me when I needed help the most, I couldn't have done it without you.

This thesis is dedicated to Carl Bradford, a brilliant scientist who would have been the only "lay" person to take the time to read this because that is just who he was.

iii. Declaration

I declare that this thesis is a presentation of original work, and I am the sole author. This work has not been previously presented for a degree or other qualification at this University or elsewhere. All sources are acknowledged as references.

Blythe Wright (February 2025)

iv. Table of Contents

v. List of Tables

vi. List of Figures

vii. Abbreviations

(w/v)	Units Weight per Unit Volume
°C	Degrees Celsius
~	Approximately
µ	Micro (prefix)
11BR	Atg11 Binding Region
A	Amps
AIM	Atg8 Interacting Motif
ALP	Alkaline Phosphatase
ANC	Absolute Neutrophil Count
ANOVA	Analysis of Variance
Ape1	Aminopeptidase I
APS	Ammonium Persulfate
Atg	Autophagy-related Protein
AUC	Area Under the Curve
Bec-1	Beclin-1
BMT	Bone Marrow Transplant
BPS	Bathophenanthroline Disulfonate
CaCl2	Calcium Chloride
CMAC	7-amino-4-chloromethylcoumarin L-arginine amide
CORVET	Class C Core Vacuole/Endosome Tethering Complex
CPY	Carboxypeptidase Y
CVT	Cytoplasm-to-Vacuole Targeting
DIC	Differential Interference Contrast
DNA	Deoxyribonucleic Acid
EDTA	Ethylenediaminetetraacetic Acid
ER	Endoplasmic Reticulum
ERC	Evolutionary Rate Covariation
ESCRT	Endosomal Sorting Complex Required for Transport
FASTA	Amino Acid Sequence
FERARI	Endosomal Recycling and Rab Interactor Complex
FYVE	Fab1-YOTB-Vac1-EEA1 PI3P Binding Domain
g	Gram
GAPDH	Glyceraldehyde-3-Phosphate Dehydrogenase
G-CSF	Granulocyte Colony-Stimulating Factor
G-CSFR	Granulocyte Colony-Stimulating Factor Receptor

GDP	Guanosine Diphosphate
gDNA	Genomic DNA
GFP	Green Fluorescent Protein
GTP	Guanosine Triphosphate
GTPase	GTP Hydrolase
H_2O_2	Hydrogen Peroxide
HA	Human Influenza Haemagglutinin Protein
HCl	Hydrochloric Acid
His	Histidine
HOPS	Homotypic Fusion and Vacuole Protein Sorting
L	Litre
LB	Lysogeny Broth
Leu	Leucine
m	milli (prefix)
MVB	Multivesicular Body
OD_{600}	Optical density at 600 nm
PAS	Pre-autophagosomal Structure
PBS	Phosphate Buffered Saline
PCR	Polymerase Chain Reaction
PE	Phosphatidylethanolamine
PEG	Polyethylene Glycol
PGK	Phosphoglycerate Kinase
PI3P	Phosphatidylinositol-3-Phosphate
PVC	Pre-vacuolar Compartment
Rab	Small GTPases
ROS	Reactive Oxygen Species
rpm	Rotations Per Minute
SC	Synthetic Complete
SCN	Severe Congenital Neutropenia
SD-N	Synthetic Nitrogen Free Media
SDS	Sodium Dodecyl Sulfate
SDS-PAGE	Sodium Dodecyl Sulfate Polyacrylamide Gel Electrophoresis
SGD	Saccharomyces Genome Database
SM	Sec1/Munc18-like protein
SNARE	Soluble N-ethylmaleimide-Sensitive-Factor Attachment Protein Receptor
t-SNARE	Target-SNARE

TAE	Tris-Acetate-EDTA
TBST	Tris-Buffered-Saline-Tween®20
TE	Tris-EDTA
TEMED	N,N,N’,N’-Tetramethylethylenediamine
TGN	Trans-Golgi Network
TOR	Target of Rapamycin
Tris	Tris(hydroxymethyl)aminomethane
Ura	Uracil
V	Volts
v-SNARE	Vesicle-SNARE
VPS	Vacuolar Protein Sorting
xg	G-force
YPD	Yeast Extract Peptone Dextrose Media

1 Introduction

1.1 Vps45 and vesicle traffic

1.1.1 SNARE binding biology

Trafficking of cellular material in eukaryotic cells often requires vesicles in, for example, uptake from the external environment at the cellular membrane and exchange between membrane bound cellular compartments (organelles). The soluble N-ethylmaleimide-sensitive factor attachment protein receptor (SNARE) protein superfamily are required for mediating fusion of vesicles to organelles and provide specificity of these events (Scales *et al*., 2000). SNARE proteins are associated with membranes, with many having C-terminal transmembrane domains, though others may be attached by lipid modifications (Jahn *et al*., 2023). The cytoplasmic portion of the SNARE protein holds the N-terminal domain and the SNARE motif which contributes to the fusion of two opposing membranes (Misura *et al*., 2002).

Of the SNARE family there are two main sub-types: t-SNAREs and v-SNAREs. t-SNAREs are found on the target membrane of the organelles and have a corresponding v-SNARE found on the vesicle membrane holding the desired cellular material (Söllner *et al*., 1993). The SNARE motif consists of a coiled-coil domain that is required for SNARE complex formation; when three t-SNARE domains and a v-SNARE interact, the SNARE motifs rearrange into a parallel four-helix bundle (Antonin *et al*., 2002; Poirier *et al*., 1998; Sutton *et al*., 1998). The parallel arrangement of the helix bundle anchors the vesicle to the target membrane bringing the two membranes together (Hanson *et al*., 1997). Bi-lipid membranes brought into close proximity dimple towards each other with the proximal membranes creating a hemi-fusion and eventually a fusion pore. After membrane rupture, and the vesicle contents can deposit into the desired organelle (**Figure 1.1**) (Markin *et al*., 1984; Ungar and Hughson, 2003).

Syntaxins, a type of t-SNARE, possess a single transmembrane domain, a SNARE domain and a regulatory N-terminal domain (Habc) (Poirier *et al*., 1998). The N-terminus of syntaxins do not influence the specificity of SNARE complex

binding (Bethani *et al*., 2007), however, the N-terminus is thought to influence the rate of binding, by interacting with other factors (Dulubova *et al*., 2001; Misura *et al*., 2000; Munson *et al*., 2000) such as Sec1/Munc18-like (SM) proteins (Jahn and Südhof, 1999). In some t-SNAREs removal of the N-terminal domain leads to an increase in fusion events (Parlati *et al*., 1999) suggesting that SNARE co-effectors can promote SNARE binding as chaperones or activators as well as negatively regulate the fusion process. Conformation switches syntaxins from "open" to "closed", wherein the Habc domain folds back on the SNARE domain, regulating the binding of SNAREs to form their cognate complexes and aid vesicle docking (Dulubova *et al*., 1999).

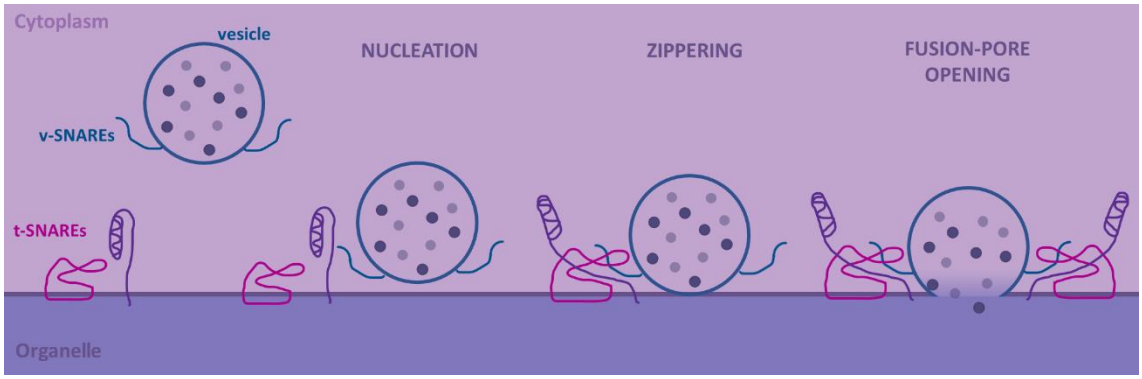

Figure 1.1 *- The mode of action of SNARE binding; Vesicles with a v-SNARE approach the organelle membrane containing t-SNAREs. Nucleation: the t-SNARES and v-SNAREs bind, docking the vesicle to the organelle membrane. Zippering: the coiled complexes of the SNAREs "zip" together, locking the two membranes together. Lipid molecules flow between membranes in a connecting stalk creating a hemifusion state. Fusion-pore opening: tight binding of the SNAREs and movement of lipids forms a new bilayer, which widens and ruptures creating the fusion-pore where the contents of the vesicle can mix with the luminal contents of the organelle (Chen and Scheller, 2001).*

1.1.2 Vps45 is an SM protein required for SNARE binding

SM proteins are a family of proteins that regulate SNARE mediated membrane fusion (Carr and Rizo, 2010). Vps45 is a Sec1 homolog, among four yeast SM proteins, Sec1, Sly1 and Vps33 (Eisemann *et al*., 2020). Vps45's role as an SM protein has been well characterised in budding yeast, *Saccharomyces cerevisiae,* where it regulates binding of syntaxin Tlg2 to its corresponding SNARE complex (Bryant and James, 2001). Vps45 has also been shown to aid assembly of SNARE complexes through interacting with the endosomal t-SNARE Pep12 (Cowles *et al*., 1997). Vps45 binds to a 30 amino acid long sequence in

the N-terminal domain of Tlg2 to aid SNARE complex assembly, a sequence that does not exist in Pep12 (Dulubova *et al*., 2002) indicating that Vps45 aids different SNARE assemblies through its role as an SM protein in different modes of action.

Vps45 cycles on and off membranes in vesicle traffic in a protein phosphatase (PP1) dependant manner controlling the fusion of the vesicles to the target membrane (Bryant and James, 2003). Vps45 stabilises the syntaxin Tlg2 promoting assembly with cognate endosomal v-SNARE proteins, Tlg1 and Vti1. In the absence of Vps45, Tlg2 is downregulated and unavailable to bind to its cognate SNARE binding partners (Bryant and James, 2001). Vps45 binds to Tlg2 through the N-terminal peptide of the syntaxin inserting into the hydrophobic pocket of the SM protein. Although they can also interact without the N-terminal binding of Tlg2 suggesting that SM proteins use different modes for assembly and disassembly of their cognate SNARE complexes (Carpp *et al*., 2006) the high-affinity pocket binding mechanism of Vps45 to Tlg2 is important for regulation of Tlg2 levels in the cell (Carpp *et al*., 2007). As an SM protein Vps45 is involved in a "switch" of Tlg2 from a closed to an open conformation which facilitates Tlg2's ability to form a functional SNARE complex (Struthers *et al*., 2009). The second binding site of Vps45 to Tlg2 requires a closed conformation of Tlg2 that is independent of the N-terminal domain (Furgason *et al*., 2009). In mammalian cells the N-peptide of syntaxin 16 (Tlg2 mammalian ortholog (Struthers *et al*., 2009)) is also required for the high-affinity binding to mammalian Vps45 (Burkhardt *et al*., 2008).

1.1.3 vps mutants in yeast

Vacuolar sorting protein (*vps*) yeast mutants exhibit abnormal sorting or delivery of vacuolar proteins to the vacuole and represent a large number of factors discovered by genetic screening (Bankaitis *et al*., 1986; Robinson *et al*., 1988; Rothman *et al*., 1989; Rothman and Stevens, 1986). Distinct *vps* mutants were categorised into 6 classes, A-F based on different phenotypes such as vacuolar morphology and ability to traffic vacuolar hydrolases (Banta *et al*., 1988; Raymond *et al*., 1992). *vps45Δ* mutants are characterised as 'Class D' based on their abnormally large vacuole, defects in mother-daughter vacuolar inheritance and missorting of multiple vacuolar hydrolases (Cowles *et al*., 1994).

Cowles *et al*. discovered that in *vps45Δ* cells, vesicles accumulate in clusters associated with the vacuole indicating that Vps45 is involved in vesicle docking/fusion events and was thought to act in Golgi to endosome transport (Cowles *et al*., 1994).

Vps45 is a peripheral membrane protein that co-fractionates with post-Golgi membranes, and its deletion causes secretion of CPY, therefore it is widely accepted that Vps45 is involved in Golgi to vacuole transport (Piper *et al*., 1994). In rats the role of Vps45 was also shown to bind to syntaxin homologs in traffic between the Golgi, the pre-lysosomal compartment and the lysosome (Pevsner *et al*., 1996). In Chinese hamster ovary cells, Vps45 was identified as a Sec1 homolog with high identity to the Vps45 observed in *Saccharomyces cerevisiae* and binds specifically to the mammalian syntaxin 6, which shares homology with yeast Pep12 (Bock *et al*., 1997; Tellam *et al*., 1997). Human Vps45 has high expression in the brain indicating that this protein was also involved in Golgi-synaptic vesicle membrane traffic (El-Husseini *et al*., 1997). Since, Vps45 has been shown to regulate vesicle traffic between the Golgi and lysosomes and the recycling of plasma membrane receptors in human cells (Rahajeng *et al*., 2010).

1.1.4 CPY traffic

The delivery of vacuolar hydrolases such as carboxypeptidase Y (CPY) relies on cycling of the CPY receptor Vps10 (Marcusson *et al*., 1994) between the Golgi and the prevacuolar-endosomal compartment (Cooper and Stevens, 1996; Stack *et al*., 1995). Golgi-derived vesicles containing Vps10 fuse with the prevacuolar compartment, this requires t-SNARE Pep12 and v-SNARE Vti1 and is facilitated by SM protein Vps45 and the GTPase Vps21 (**Figure 1.2**) (Cowles *et al*., 1994; Fischer von Mollard and Stevens, 1999; Horazdovsky *et al*., 1994; Piper *et al*., 1994).

Precursors of CPY are secreted from the cell into the extracellular medium when mutant strains are defective in delivery of CPY to the yeast vacuole (Bankaitis *et al*., 1986). CPY is synthesised as a precursor enzyme at the endoplasmic reticulum(ER) (p1CPY, 67 kDa), at the Golgi the inactive enzyme is modified by oligosaccharides (p2CPY, 69 kDa) and then cleaved into the active/mature form (mCPY, 61 kDa) (Stevens *et al*., 1982; Valls *et al*., 1987) following delivery to

the vacuolar lumen and processing by the aspartyl protease Pep4 (Vida *et al*., 1990). CPY has a 30 amino acid segment, a vacuolar sorting signal, deletion of this signal leads to missorting of this protein (Johnson *et al*., 1987).

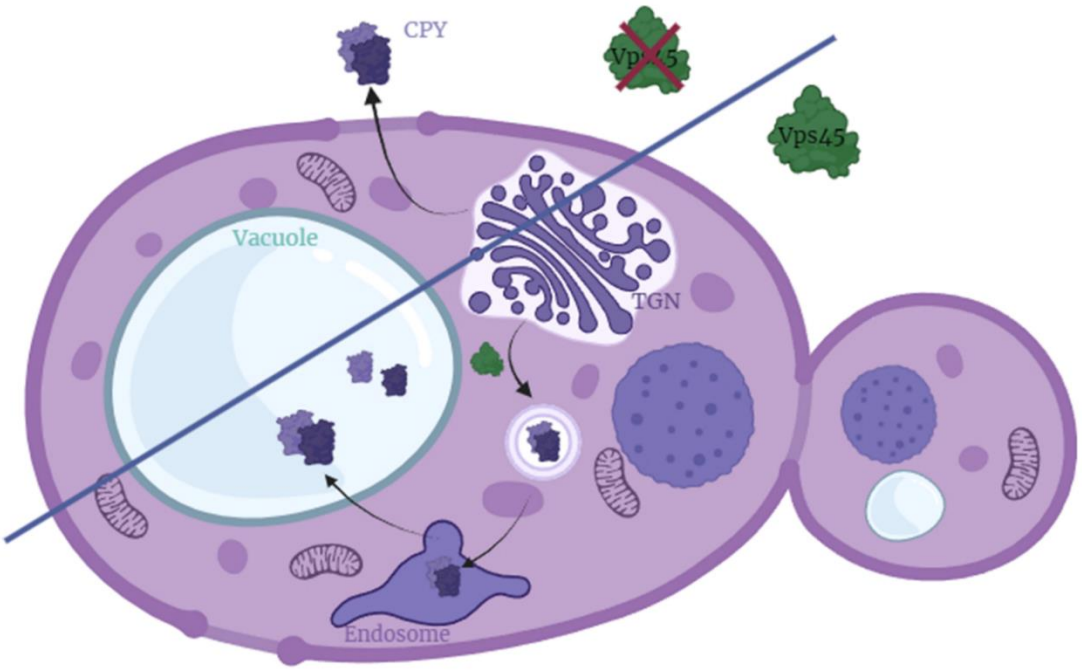

Figure 1.2 *- Loss of Vps45 leads to removal of p2CPY from the cell and into the extracellular space; When CPY cannot be trafficked through the endosomal system the inactive enzyme is secreted from the cell.*

Alkaline phosphatase (ALP) is another vacuolar enzyme which follows a separate pathway from the Golgi to the vacuole, bypassing the pre-vacuolar compartment (Conibear and Stevens, 1998). ALP is also cleaved into its active form at the vacuole, by Pep4 (Klionsky and Emr, 1989). ALP and Vam3 are trafficked from the Golgi though this route independently of Vps45 and Pep12 indicating that Golgi-derived vesicles do not fuse with the prevacuolar compartment (Piper *et al*., 1997). However, this process does require Vti1 and Vti1 is present at the vacuolar membrane implying that it is required for retrograde traffic (Bryant *et al*., 1998b). Vti1 binds with t-SNARE Pep12 to traffic Golgi derived vesicles to the prevacuolar compartment and the t-SNARE, Sed5, in traffic from the ER to the Golgi (Parlati *et al*., 2002; von Mollard *et al*., 1997).

1.1.5 The CVT Pathway

The cytoplasm-to-vacuole (CVT) pathway is a form of selective autophagy, initially identified as selectively transporting vacuolar hydrolases to the vacuole.

The formation of the CVT vesicle requires the SNARE protein Tlg2 and the SM protein Vps45 (Abeliovich *et al*., 1999). CVT cargo is enclosed in the CVT vesicle which is ~150 nm (compared to ~500 nm for the autophagosome). The known CVT cargos are prApe1, Ams1, Ape4, Lap3 and Ty1. Ape1 is a vacuolar hydrolase and principal cargo of the CVT pathway (Cueva *et al*., 1989). Ape1 is the only cargo of the CVT vesicle that is required for the vesicle structure formation (Shintani *et al*., 2002). The structure of Ape1 consists of two main parts: the enzymatic component (mApe1) and the propeptide (mApe1 + propeptide = prApe1). prApe1 is processed into the enzymatically active form (mApe1) by the vacuolar proteinase Prb1 (Klionsky *et al*., 1992) upon entry to the vacuole. The Ape1 enzyme is evolutionarily conserved from bacteria to eukaryotes, although the CVT pathway is not evolutionarily conserved (Meijer *et al*., 2007) it is beneficial for studying the method of selective autophagy throughout species.

After synthesis the precursor prApe1 folds into a homododecamer (Kim *et al*., 1997). The propeptide of prApe1 facilitates assembly of prApe1 into dodecamers forming the Ape1 complex, an aggregate required for the template of CVT vesicles (Quinones *et al*., 2012). The Ape1 complex is recognised by Atg19 through propeptide of prApe1 and binding with the coiled-coil region of Atg19 (Scott *et al*., 2001). Atg19 recruits Atg8 and Atg11 through the AIM (Atg8 family interacting motif) region of Atg8 and Atg11 binding region (11BR) of Atg19 (Noda *et al*., 2010) leading to the CVT complex. The recruitment of autophagy machinery requires Atg19-Atg11 and leads to membrane wrapping of the CVT complex into the CVT vesicle (Yorimitsu and Klionsky, 2005). Upon delivery to the vacuole, fusion of the CVT vesicle outer membrane with the vacuole requires the SNAREs Vam3 and Vti1, docking by Vps18 and the Rab GTPase Ypt7 (Fischer von Mollard and Stevens, 1999). The Ape1 complex is released into the vacuole upon fusion with the CVT vesicle, prApe1 is processed into a mature form mApe1 (**Figure 1.3**) (Klionsky *et al*., 1992).

Atg8 is an ubiquitin-like protein that is covalently coupled to a phosphatidylethanolamine (PE) and localised to the isolation membranes and autophagosomes (Ichimura *et al*., 2000). It has two functions, autophagosome formation and tethering of cargos selectively to the isolation membrane (Xie *et*

al., 2008). The isolation membrane is a precursor for the phagophore and eventually the double-membraned autophagosome, which Atg complexes to expand the lipid bilayer (Reggiori, 2005). Atg8 has specific amino acid residues required for vesicle formation and cargo sequestration (Ho *et al*., 2009). Atg8-PE interacts with Atg19 allowing for the isolation membrane to enclose the Ape1 complex into the CVT vesicle (Sawa-Makarska *et al*., 2014). Atg19 is the sole receptor of Ape1 though does bind to other CVT vesicle cargo, Ams1 and Ty1, delivering them to the vacuole via the CVT pathway. Binding of Atg19 to prApe1 limits the size of the Ape1 complex (Yamasaki *et al*., 2016) therefore regulating the CVT vesicle as well as aiding the formation of the CVT vesicle. Upon completion of the CVT vesicle Atg8-PE is removed from the outer membrane by Atg4 (Kirisako *et al*., 2000) any remaining Atg8 on the inner membrane is delivered to the vacuole and degraded.

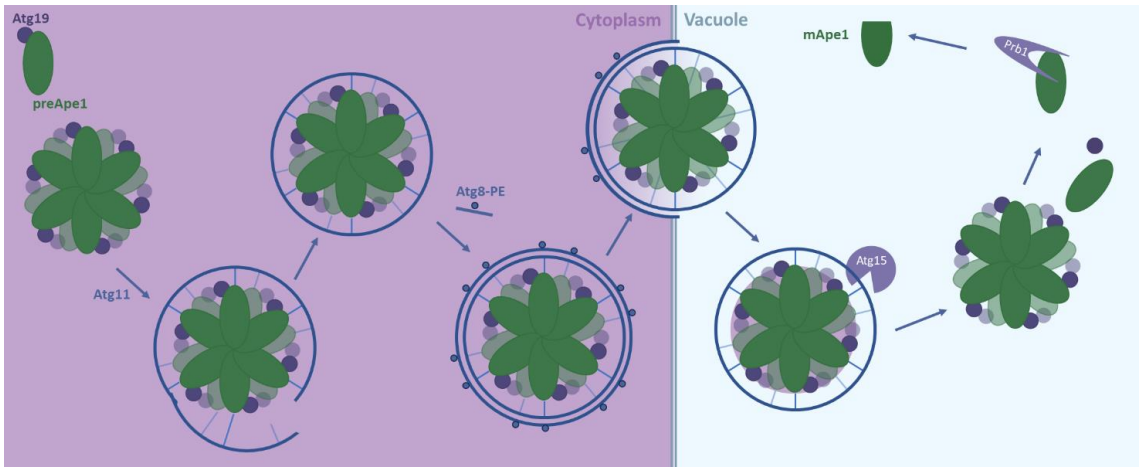

Figure 1.3 *- The CVT vesicle; (1) prAPe1 folds into a homodimer, the propeptide of prApe1 facilitates assembly into the dodecamer aggregate (2) The propeptide of Ape1 binds to Atg19. (3) Atg19 facilitates binding to Atg11 and Atg8. (4) The CVT vesicle fuses with the vacuolar membrane where Atg8-PE is released by Atg4. (5) Atg15, a phospholipase, degrades the CVT body upon delivery to the vacuolar lumen. (6) Ape1 dodecamer dissembles and the propeptide is removed by Prb1 forming the mature enzyme.*

Atg11 is a scaffold protein associated with the pre-autophagosomal structure and is critical in recruiting core autophagy machinery to different selective cargos including Ape1 (Kanki *et al*., 2009; Okamoto *et al*., 2009). The 11BR of Atg19 is phosphorylated by Hrr25 kinase in order to recruit Atg11 to the Ape1 complex (Pfaffenwimmer *et al*., 2014). Phosphoregulation of Atg11-receptor

interaction is a general mechanism of selective autophagy in nutrient rich conditions (Kim *et al*., 2001).

Atg34 was identified as an Atg19 family protein and contains a coiled-coil, the 11BR and AIM domain (Suzuki *et al*., 2010). However, Atg34 is unable to bind to Ape1 and cannot compensate for defects in CVT pathway with dysfunctional Atg19. Atg32 is a transmembrane protein that is associated with the mitochondrial outer membrane and the cytosolic N-terminus contains a well-conserved AIM or LIR (LC3 interacting region) in mammals (Noda *et al*., 2008). Binding of Atg32 to Atg8 is phosphorylation dependant (Farré *et al*., 2013). Conversely, Atg34 binds to Ams1 not Ape1, though this is only triggered during starvation (Suzuki *et al*., 2010). The degradation of mitochondria requires Atg32 and Atg11 (Okamoto *et al*., 2009), Atg32 phosphorylated by CK2 for binding with Atg11 in mitophagy (Kanki *et al*., 2013), but it is not required for non-selective autophagy or the CVT pathway (Kanki *et al*., 2009).

1.1.6 The CVT pathway vs Autophagy

The CVT pathway and autophagy have similarities in their mechanism and machinery, while the CVT pathway is a consistent part of yeast cell metabolism, autophagy is induced under stress. For autophagy to take place a series of events need to occur, beginning with the nucleation of the phagophore at the pre-autophagosomal structure (PAS). The phagophore expands sequestering cargo for delivery to the vacuole eventually closing and forming the double membrane of the autophagosome. Upon arrival at the vacuole the autophagosome fuses with the vacuolar membrane realising the autophagic body into the lumen of the vacuole. Here, the inner vesicle membrane is degraded by vacuolar hydrolases, the contents of the autophagic body is released and the contents degraded. Whereas, in the CVT pathway the contents of the vesicle is required for vacuolar cargo to be delivered to the vacuole where it becomes enzymatically active required for vacuolar function (Lynch-Day and Klionsky, 2010).

In the absence of nutrients, the suggested switch to completion of the larger autophagosome from the CVT vesicle is thought to be induced by the Atg1-Atg13-Atg17 starvation complex as opposed to Atg11. Atg11 is critical for PAS

organisation in starvation after growth phase in yeast and Atg11 levels are directly related to the efficiency of the CVT pathway (Geng and Klionsky, 2008).

1.1.7 Autophagy

Autophagy etymologically combines the auto, "self" and phage, "eat" in Greek to describe the evolutionarily conserved self-preservation process. Macroautophagy refers to the double-membraned vesicle; the autophagosome which non-selectively engulfs portions of the cytoplasm, to transport to the lysosome for degradation (Medzhitov and Janeway, 2002). Selective autophagy refers to targeted degradation or organelle specific autophagy. Here we shall focus on macroautophagy and therefore just autophagy hereafter.

Autophagy is defined as all cellular processes that involve the sequestering of intracellular material with the intention of degradation at the lysosome/vacuole where its macromolecular constituents are recycled (Klionsky, 2013). In eukaryotes autophagy is induced by inhibition of the target of rapamycin (TOR) kinase (Cutler *et al*., 1999), a serine-threonine protein kinase that is inactivated in nutrient poor conditions. In yeast there are two TOR homologs and Tor1 is involved in the TORC1 complex which is required for autophagy induction (Ganley *et al*., 2009) through activation by PI3P (Dann and Thomas, 2006). Whereas Tor2 is a phospholipid kinase required for cytoskeleton organisation that is involved in cell cycle arrest (Helliwell *et al*., 1994).

Human Beclin-1 and the yeast homolog Atg6/Vps30 are scaffold proteins bound in a lipid kinase complex (Kang *et al*., 2011). They contain a unique and conserved domain that is required for controlling autophagosome size and number. Atg14 is required for autophagy dependent phosphorylation of Beclin-1 (Bcl-1) (Fogel *et al*., 2013). The autophagy machinery Atg8 in yeast has 2 mammalian homologs; light chain 3 (LC3) and γ-aminobutyric acid receptor associated proteins (GABARAP) that become conjugated to lipids in the autophagosome membrane and therefore act as a marker for autophagy induction (Johansen and Lamark, 2020; Lystad and Simonsen, 2019). Core autophagy machinery such as Atg8 that has been characterised and observed in yeast allow for insight into the function of their mammalian homologs in autophagy in human cells.

1.1.8 Sequestration of the mitochondria for mitophagy

Removal of surplus high energy material such as the mitochondria is triggered by low energy conditions. Mitochondria play a key role in cell homeostasis and therefore require intra-organelle homeostasis via intra-mitochondrial chaperones and proteases that remove misfolded, damaged or excess proteins from the organelle (Koppen and Langer, 2007). Mitochondria are the main source of reactive oxygen active species (ROS) as by-products from complex I and III of the electron transport chain (Dröse and Brandt, 2008). Excess ROS can lead to protein modifications, lipid peroxidation, and DNA damage, which in excess leads to dissipation of the mitochondrial membrane potential and cell death by the release of pro-apoptotic proteins (Kroemer *et al*., 2007).

In the instance that mitochondrial damage cannot be controlled at this level higher level mechanistic steps are taken to limit damage and improve function. Mitochondrial fission is required to segregate dysfunctional mitochondria from functional mitochondria (Twig *et al*., 2008), mitochondria unable to fuse with intact organelles in the mitochondrial network are therefore removed via mitophagy (Priault *et al*., 2005). In yeast the mitochondrial membrane protein Uth1 is required for sequestering dysfunctional mitochondria for mitophagy (Kissová *et al*., 2004). Mitophagy appears to occur at a specialised phagophore preassembly site which is spatially separate from the CVT vesicle or non-selective autophagosome (Kanki *et al*., 2009). Mitophagy activation by outer membrane interactors leads to autophagosome formation surrounding the damaged mitochondria, and is important in apoptosis (Onishi *et al*., 2021).

Mitochondrial removal in mammalian cells has been shown to be cargo protein binding specific and requires the mitochondrial protein NIX an outer membrane protein that directly binds to LC3/GABARAP (Atg8 in yeast) (Schweers *et al*., 2007). This leads to removal of mitochondrion through the accumulation of PINK1 on the outer membrane caused by the reduction of membrane potential, which recruits PARKIN to the outer membrane where it ubiquitinylates other outer membrane proteins leading to removal of dysfunctional mitochondria (Ziviani *et al*., 2010).

In yeast mitophagy is simultaneous with non-selective autophagy and induced at stationary phase in media containing glycerol or lactate (Kanki and Klionsky, 2008). Mitophagy can also be induced through TOR kinase inhibition by nitrogen starvation or by rapamycin treatment (Kanki and Klionsky, 2008).

1.1.9 Autophagy and apoptotic flux

Crosstalk between apoptotic and autophagic factors have been indicated in the literature, for example Beclin-1 (Bec1), the mammalian ortholog of Atg6, is part of a complex with PI3K that initiates autophagy by PI3P activation of mTOR. Binding of Bec1 to the anti-apoptotic Bcl-2 at the ER requires dissociation in order for Bec1 to initiate autophagy (Maiuri *et al*., 2010). Caspase mediated cleavage of Bec1 is required for crosstalk of apoptosis and autophagy (Kang *et al*., 2011). Like mammalian cells, yeast apoptosis also displays certain characteristics such as DNA breakage, chromatin condensation, ROS accumulation and cytochrome c release from mitochondria (Fröhlich and Madeo, 2000). In yeast, apoptosis can be induced by intercellular factors and extracellular factors like H_2O_2 exposure, though high levels can induce necrosis (Madeo *et al*., 1999). Necrosis in comparison to apoptosis is the release in intracellular contents due to the rupture of the cellular membrane as opposed to apoptosis (known as programmed cell death) which is more contained. In some organisms autophagy induction can mediate a further regulated cell death mechanism known as autophagic cell death, evidence suggests that autophagy can induce cell death in yeast under prolonged starvation conditions (Falcone and Mazzoni, 2016). Autophagy induced cell death is implicated as a caspase independent cell death mechanism (Gozuacik and Kimchi, 2004).

1.1.10 Apoptosis

Yeast lacks *BAX* and *BCL* genes though does contain orthologs of the main mammalian apoptotic regulators (Falcone and Mazzoni, 2016). When induced in mammalian cells, Bax expression induces mitochondrial network disorganisation and induction of Atg8 mediated autophagy as opposed to apoptotic indicators such as an increase in Yca1, the yeast metacaspase (Kissová *et al*., 2006).

ROS accumulation in yeast cells leads to apoptosis in a caspase dependant manner, in the absence of Yca1 apoptosis is prevented (Madeo *et al*., 2002). In yeast, ROS are mainly produced by the mitochondria during aerobic respiration

as a result of electron reactivity with oxygen after they have been leaked by the respiratory chain (Longo *et al*., 1996). ROS accumulation can lead to oxidative damage of nucleic acids, proteins and lipids and in high concentrations can lead to apoptosis or necrosis in higher concentrations. The mitochondria release cytochrome c and this signals apoptotic cell death.

1.2 Identification of VPS45 SCN mutants

1.2.1 Severe Congenital Neutropenia

Neutropenic patients usually present as children who have an absolute neutrophil count (ANC) of less than $0.2x10^9$/L, usually suffering from seemingly preventable severe bacterial infections in childhood (Kostman, 1975). Neutropenic patients become infected by microorganisms that are usually part of their endogenous flora, allowing for susceptibility to bacterial and less commonly parasitic viral and fungal infections. Susceptibility to fungal infections increases with their prolonged use of antibiotic treatments (Hou *et al*., 2023). Treatment to increase neutrophil count using regular granulocyte-colony stimulating factor (G-CSF) injections was introduced in the 1990's (Dale *et al*., 1993).

Severe congenital neutropenia (SCN) was initially described in 1956 by Kostmann in Sweden, an autosomal recessive disorder characterised by the reduction in neutrophils and increased susceptibility to bacterial infections (Kostmann, 1956). Neutropenia that lasts for longer than a few months can be caused by congenital bone marrow defects (Boxer and Dale, 2002). Severe congenital neutropenias are a group of genetic disorders in which the patients' neutrophils and haematopoietic precursor cells undergo apoptosis (Klein, 2009). This causes a reduction in circulating white blood cells (neutrophils) in the bloodstream (Alotaibi and Albarkheel, 2020). *ELA2* or *HAX1* are examples of non-syndromic variants of the disease whereas some patients' experience syndromic disease due to the function of the genes where the mutations are present, such as glucose metabolism control (*G6PC3*), lysosomal function (*LYST*) or mitochondrial proteins (*AK2*) (Klein, 2009). These mutations are categorised by symptoms and for example SCN V is the category for patients with mutations in the *VPS45* gene. SCN V is a syndromic condition characterized

mainly by the presence of bone marrow fibrosis, impaired cell migration, and increased apoptosis in blood cells, which often leads to the secondary symptoms of recurrent bacterial and fungal infections, abnormally large platelets, osteosclerosis and enlarged kidneys (Meerschaut *et al*., 2015).

Neutrophil elastase is a proteinase that is required in early development, and it is thought that mutations in this enzyme cause increased apoptosis in neutrophil precursors and interrupt neutrophil differentiation (Ancliff *et al*., 2001). In neutropenia caused by mutations in the *ELA2* gene, the reduction in neutrophils was caused by increased apoptosis of the myeloid progenitor cells of the bone marrow. Some patients also moved on to develop acute myeloid leukaemia (AML), these patients did not have an increase in apoptosis in most white blood cell lineages in comparison to AML free neutropenia patients (Boxer and Dale, 2002). All of the SCN patients who developed AML in the study had acquired cytoplasmic domain G-CSF receptor mutations (Boxer, 2006). *HAX1* mutations also lead to SCN (Klein *et al*., 2007) prior to this it was well known that *HAX1* is an anti-apoptotic protein and is involved in the intrinsic/mitochondrial apoptotic pathway (Cilenti *et al*., 2004). The intrinsic cell death pathway is initiated by internal signals in the cell which in turn leads to the release of cytochrome c from the mitochondria.

1.2.2 T224N mutation discovery and involvement in apoptosis

The first *VPS45* SCN mutation published was the mutation causing a threonine-224 to Asparagine (T224N) residue change. In 2013, it was reported that there were 2 Palestinian families who presented with neutropenia, myelofibrosis (bone marrow scarring) and bone marrow failure (Stepensky *et al*., 2013). The 3 patients and 2 older siblings had typical development initially then between the ages of 1 – 7 months they began presenting with recurrent bacterial infections, pneumonia and soft tissue infections. Laboratory work established low red blood cell, white blood cell and platelet counts with abnormal blood cell morphology. Progression of the disease in patients led to enlarged kidneys and spleen. Treatment of patients with G-CSF was unsuccessful and therefore 2 patients underwent a bone marrow transplant. 1 child was later diagnosed with a behavioural developmental disorder. Flow cytometry analysis of patient neutrophils demonstrated an increased spontaneous apoptosis and increased

susceptibility to apoptosis through reduced mitochondrial potential. Bone marrow aspirations showed increased activation of caspase-3 (Stepensky *et al*., 2013).

Vps45 protein is of highest abundance in mononuclear blood cells and neutrophils (Rajasekariah *et al*., 1999). As *vps45Δ* yeast are associated with vacuolar trafficking in yeast, investigations into the lysosomes of patient cells were completed, they established that patient lysosomes were reduced under normal and starvation conditions (Stepensky *et al*., 2013). The absence of functional lysosomes in the patients identifies Vps45 as critical in endosomal-lysosomal traffic in humans as seen in yeast (Stepensky *et al*., 2013). It is critical for neutrophils to have functional endosomal-lysosomal trafficking as protein recycling is crucial for neutrophil function (Kinchen and Ravichandran, 2008).

Stepensky *et al.* hypothesised that the absence of Vps45 in SCN patients perturbed delivery of cargo through the endosomal system which in turn 'backs up' secretory pathways leading to ER stress triggering apoptosis (Stepensky *et al*., 2013). The susceptibility of SCN V patient neutrophils to apoptosis could be due to the lack of Bcl-2 present (Iwai *et al*., 1994) and increase in apoptotic myeloid cells due to defective clearance from poor lysosomal function.

In *vps45Δ* yeast expressing a *VPS45* plasmid harbouring a T238N mutation, analogous to the human T224N mutation, showed a reduction in levels of the Vps45 cognate SNARE protein Tlg2 (Stepensky *et al*., 2013). This indicates that the mutations observed in SCN patients might be explained by an analogous response conserved in yeast.

1.2.3 SCN V patients require bone marrow transplants as G-CSF treatments are unsuccessful.

SCN was almost always fatal until the effective development of G-CSF treatment regimes, G-CSF stimulates the production of more neutrophils through increased proliferation at all stages of granulopoiesis (Lord *et al*., 1989). It promotes the movement of progenitor cells through the bone marrow niche through MMP-9 activation which leads to bone marrow repopulation and translocation (Heissig *et al*., 2002). The majority of SCN patients respond to G-

CSF treatment, pushing their ANC towards the normal range (2.5-7x10^9/L) and allowing them to survive until adulthood. Although progression into AML diagnosis has been implicated due to the stimulation of the bone marrow to over-produce cells at an increased rate (Schaffer and Klein, 2008). Treatment also delays apoptosis through inhibiting the mitochondrial-dependant activation of caspase-3 (Maianski *et al*., 2002). Indicating that G-CSF has anti-apoptotic effect in the cell.

Hematopoietic stem cell transplants commonly known as bone marrow transplants (BMT) are the only current treatment for patients with SCN V. This is due to the patients' distinct inability to respond to the commonly used G-CSF treatment given to patients with neutropenia. G-CSF is considered to be the main treatment for idiopathic neutropenia and is often used to increase white blood cell counts in neutropenia patients (Jakubowski *et al*., 1989). Bone marrow transplants are used to replace the patients' entire immune system in order to eradicate the cells primarily affected by the *VPS45* mutations. Bone marrow donors are usually siblings but in the instance of shared genetic conditions a haplotype donor (parental and rejection is more likely) or non-related donor (much harder to find) is required. The SCN V patients often do not respond well to the bone marrow transplants (Meerschaut *et al*., 2015; Stepensky *et al*., 2013; Vilboux *et al*., 2013) but are successful eventually.

1.2.4 SCN mutations and presentation in patients

As well as the discovery of the T224N mutation in *VPS45* causing SCN, 4 more disease causing mutations have been identified. Five Palestinian and Moroccan families with children who all presented with poor weight gain, enlarged spleens and kidneys as well as recurrent infections and/or abscesses (Meerschaut *et al*., 2015). All had neutropenia which was resistant to stimulation by G-CSF treatment, nucleated red blood cells and bone marrow stress. Electron microscopy identified 2 patients had increased mitochondria in the neutrophils. Cell migration in these patients' cells was also diminished when assessed using scratch assays, and FACS (fluorescent activated cell sorting) showed that mutant *VPS45* patient cells expressed much lower levels of β1-integrin on the cell surface. Blood cell motility requires β1-integrin (Werr *et al*., 1998). Bone marrow samples also showed 14x higher rates of apoptosis in *VPS45* mutant

cells using flow cytometry (Meerschaut *et al*., 2015; Shah *et al*., 2017; Vilboux *et al*., 2013).

Levels of endogenous Vps45 and Rabenosyn-5 (homolog of yeast Vac1) were reduced by half in patient fibroblasts. GTPase Rab5 recruits Vps45 and Rabenosyn-5 to the endosome through a FYVE finger domain (Nielsen *et al*., 2000). Vps45 in yeast is involved in endosomal trafficking pathways and human Vps45 in neutrophils is also crucial for protein trafficking and release of inflammatory mediators (Rajasekariah *et al*., 1999). Human Vps45 and Rabenosyn-5 are involved in β1-integrin trafficking in the cell (Rahajeng *et al*., 2010) lower protein levels in these patients explain the reduction of surface membrane β1-integrin and therefore the reduction in motility of these cells. Vilboux *et al*. however, did not associate the increase in apoptosis in these patients with the increased ER stress due to lack of functional recycling as Stepensky *et al*. did in their analysis of the T224N patients (see 1.2.2) but rather that the accumulation of vesicles from perturbed delivery to the plasma membrane could lead to increased apoptosis (Vilboux *et al*., 2013). Of these patients four had the T224N *VPS45* mutation and 2 had a novel E238K mutation, who both experienced neurological defects not seen in the T224N *VPS45* SCN patients (Vilboux *et al*., 2013).

Meerschaut *et al*., supported the identification of neurological defects alongside SCN with the publication of a case report stating that a child with the E238K mutation had neurological developmental problems as well as SCN. The patient presented with *Staphylococcus aureus* sepsis and blood work showed neutropenia and abnormal red blood cells (size, shape, count and colour). The patient was unsuccessfully treated with G-CSF and then a bone marrow transplant which was successful. The patient had a similar ophthalmological and neurological phenotype to the T224N *VPS45* SCN patients discussed above (Stepensky *et al*., 2013), the absence of enlarged kidneys in this patient although they had an enlarged liver, suggesting that SCN V patients are susceptible to organomegaly of multiple types not just confined to the kidneys (Meerschaut *et al*., 2015).

In 2017, Shah *et al*. identified a mutation causing P468L residue change in *VPS45* leading to neutropenia, the patient presented with a fever, was diagnosed with neutropenia and treated with G-CSF, the neutropenia continued, and she developed anaemia and then bone marrow failure. The patient was treated with a bone marrow transplant (Shah *et al*., 2017). The patient also experienced global developmental delay, likely explained by the high expression of Sec1/Munc18 proteins in the brain (Halachmi and Lev, 1996).

In 2020, Alotaibi and Albarkheel identified a previously unidentified *VPS45* mutation causing the L410P residue change. The Saudi sibling patients both had recurrent upper respiratory tract infections and chronic inflammation of the gums. The sisters were both administered G-CSF treatment twice weekly. The publication emphasised the importance of neutrophils in oral health and first line of defence in protection from pathogenic microorganisms (Alotaibi and Albarkheel, 2020). A final patient in Boston, MA, USA has a P253L residue change which was identified during a panel to identify his mild case of neutropenia by Dr. Mary Munson and Dr. Peter Newberger (Newburger, 2018).

1.2.5 Autophagic mediation of neutrophils

Neutrophils are circulating leukocytes that are required in protection from infection during acute inflammation. During activation neutrophils use various methods to irradicate the potential bacterial infection, in addition to the most commonly known phagocytosis, such as autophagy, degranulation and release of reactive oxygen species (ROS) (Henson and Johnston, 1987; Nathan, 2003; Savill and Haslett, 1995).

Autophagy is important in neutrophil function as the autophagosome engulfs unwanted material, such as bacteria that have been phagocytosed. However, neutrophils can use multiple methods for pathogen elimination in addition to phagocytosis and autophagy, such as xenophagy and autophagy arrest after pathogen mishandling (Yu and Sun, 2020).

1.2.6 Mitochondrial mechanisms in neutrophils

The mitochondrial pathway of cell death is significant in neutrophils due to the fact there are fewer in comparison to most somatic cells. Generally, the mitochondria play three roles within the cell: housing the mitochondrial genome,

generating ATP as energy for the cell and facilitating intrinsic apoptosis (Maianski *et al*., 2002). Production of ATP through the electron transport chain/respiration is unimportant in the neutrophil as neutrophils get their energy directly through the fast turnover of glucose in glycolysis, due to the nature of their role in killing bacteria in hypoxic microenvironments. The production of lactate through glycogenolysis increases by 60% during phagocytosis in respect to the environment and energy requiring process (Borregaard and Herlin, 1982). In addition to the abnormal use of the mitochondria, neutrophils also undergo respiratory burst, which is a non-mitochondrial abrupt release of reactive oxygen species or ROS which requires relatively large volumes of oxygen (Klebanoff, 2005) which in turn explains neutrophil's ability to use glycolysis for ATP energy when oxygen is low. This suggests that the mitochondria are potentially sensitive to triggering apoptosis in neutrophils (van Raam *et al*., 2006). As well as the fact that some SCN variants are caused by mitochondrial mutations such as in Pearson's Syndrome (Rotig *et al*., 1989).

1.3 Aims and Hypothesis

1.3.1 Aims for the project.

My main aims for this project were to understand the effects of SCN mutations identified in human *VPS45* using the model organism budding yeast. I wanted to analyse the apoptotic phenotype seen in the neutrophils of the patients and in each results chapter try to dissect the mechanism for this increase in susceptibility to apoptosis. The absence of treatment for this disorder is a driving force in moving towards understanding the underlying mechanism of this disease. Bone marrow transplants are usually a last resort treatment, though for SCN V, at the moment, this is the gold standard. Due to this, understanding neutrophils susceptibility to apoptosis by using model organism will aid the future of a more targeted treatment for patients diagnosed with this disease.

1.3.2 Hypothesis

My initial hypothesis prompted the theoretical routes taken in Chapter 3 and Chapter 4. I postulated that in the absence of Vps45 autophagy mediated by Vps45's role in membrane trafficking is compromised, which leads to the increase in susceptibility to apoptosis in these cells (**Figure 1.4**). I theorised

that in times of stress Vps45's reported role in autophagy and membrane trafficking leads to cell dysfunction and eventually apoptosis when the protein is mutated or absent. I therefore wanted to establish the link between Vps45's role in autophagy and apoptosis.

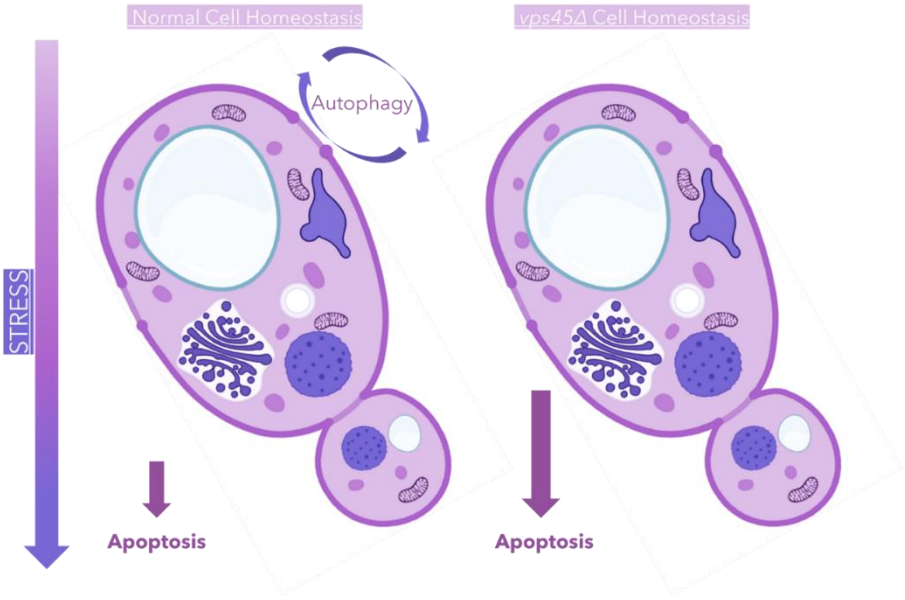

Figure 1.4 *- Dysfunctional autophagy in vps45Δ cells leads to apoptosis in yeast.*

1.3.3 Chapter 3 Aims

Residues mutated in SCN patients are highly conserved across eukaryotes. By creating yeast strains expressing mutant alleles of Vps45, I first wanted to analyse assess the levels of Vps45 and membrane trafficking function of mutations associated with SCN in yeast. Next, I wanted to analyse defects in apoptosis and autophagy individually before further investigation into any potential links.

1.3.4 Chapter 4 Aims

I wanted to establish any potential effectors of Vps45 in apoptosis. Firstly, through identifying any known interactors of Vps45 that are associated with increased susceptibility to apoptosis. Then by analysing these proteins roles in any of the pathways that Vps45 has been associated with.

1.3.5 Chapter 5 Aims

My main aim of Chapter 5 was to expand on any of relevant data that appears valuable from my first two research chapters. As well as dissect the Evolutionary Rate Covariation (ERC) data given to the Bryant Lab by Dr. Nathan Clark. ERC

analysis of evolutionary relationships between proteins allows for identification of proteins that may have had similar evolutionary stresses as Vps45 (see 2.13). This allows for the identification of potential new effectors of Vps45.

2 Materials and Methods

2.1 Materials

2.1.1 Reagents

- 30% H_2O_2 (10386643, Fisher Scientific)
- 6x DNA loading dye (R0611, Thermo Fisher)
- β- mercaptoethanol (M-6250, Sigma)
- Bathophenanthroline Disulfonate (B1375, Sigma)
- Circular nitrocellulose membrane (10401116, Life Sciences)
- CMAC (Y7531, Thermo Fisher)
- G418 Disulfate (108321-42-2, TOKU-E)
- Gel Blotting paper (GB 005, Cytiva)
- GeneRuler 1kb Plus DNA ladder (SM1333, Thermo Fisher)
- 'Hi-Pure' Low EEO agarose (300-300, BioGene)
- MitoTracker™ CMXRos (M46752, Thermo Fisher)
- Nitrocellulose membrane (GE10600003, Cytiva)
- Phenol:chloroform:isoamyl alcohol (25:24:1) (77617, Sigma)
- Precision Plus Protein™ ladder (161-0373, BIORAD)
- Salmon sperm (3040476, R&D systems)
- SuperSignal™ West Pico PLUS Chemiluminescent Substrate (34578, Thermo Fisher)
- SYBR™ Safe DNA stain (S33102, Thermo Fisher)
- Zymolyase (085L, GB Biosciences)

2.1.2 Kits

- GeneJET Gel Extraction Kit (K0692, Thermo Scientific)
- Monarch® Plasmid DNA Miniprep Kit Protocol (T1010, New England Biolabs)

2.1.3 Solutions

- 70% polyethylene glycol (PEG):
  - 35 g PEG-3350
  - To 50 mL with milliQ water (autoclave)

- Elution buffer: (10 mM TrisCl, pH 8.5)
- LiTE Sorbitol:
    - 100 mM lithium acetate
    - 10 mM Tris.HCl (pH 7.5)
    - 1 M sorbitol
    - 1 mM EDTA
    - 200 µM calcium chloride (filter sterilised)
- Phosphate Buffered Saline (PBS):
    - 85 mM NaCl
    - 1.7 mM KCl (pH 7.4)
    - 5 mM Na_2HPO_4
    - 0.9 mM KH_2PO_4
- Ponceau S Stain:
    - 0.2% (w/v) Ponceau S
    - 1% (v/v) glacial acetic acid
- SDS-PAGE Resolving Buffer:
    - 75 mM Tris-HCl (pH 8.8)
    - 0.2% (w/v) SDS (sodium dodecyl sulphate)
- SDS-PAGE Running Buffer:
    - 20 mM glycine
    - 62 mM Tris-Base
    - 0.1% (w/v) SDS
- SDS-PAGE Stacking Buffer:
    - 25 mM Tris-HCl (pH 6.8)
    - 0.2% (w/v) SDS
- Semi-Dry Transfer Buffer:
    - 24 mM Tris base (pH 8.3)
    - 20 mM glycine
    - 0.1% (w/v) SDS
    - 20% (v/v) ethanol
- TAE Buffer:
    - 40 mM Tris-Acetate (pH 8)
    - 1 mM EDTA (Ethylenediaminetetraacetic acid)
- TBST:
    - 20 mM Tris-HCl (pH 7.5)

    - 137 mM NaCl
    - 0.1% (v/v) Tween®-20
- TE Buffer:
    - 10 mM Tris (pH 8.0)
    - 1 mM EDTA
- TE Lite:
    - 20 mM Tris (pH 8.0)
    - 0.1 mM EDTA
- TWIRL buffer:
    - 50 mM Tris-HCl (pH 6.8)
    - 5% (w/v) SDS
    - 8 M urea
    - 10% (v/v) glycerol
    - 0.2% (w/v) bromophenol blue
- Yeast freezing buffer:
    - 40% glycerol
    - 0.05% NaCl

* SDS gels required addition of acrylamide and were polymerised by addition of ammonium persulfate (APS) and N, N, N’, N’ - tetramethylenediamine (TEMED).

2.1.4 Media

- LB media:
    - 4 g peptone (18322-500G-F, Sigma)
    - 2 g yeast extract (LP0021, OXOID)
    - 2 g sodium chloride
    - 400 mL milliQ water
- YPD media:
    - 1% (w/v) yeast extract (LP0021, OXOID)
    - 2% (w/v) peptone (18322-500G-F, Sigma)
    - 2% (w/v) D-glucose (G8270, Sigma)
    - 400 mL milliQ water
- Synthetic complete (SC) media:
    - 8 g D-glucose (G8270, Sigma)
    - 2.8 g Yeast Nitrogen Base without amino acids (CYN0402, Formedium)

    - X mg Complete amino acids (DCS0019, Formedium)
    - 400 mL milliQ water
- SD-N media:
    - 8 g D-glucose (G8270, Sigma)
    - 4.4g Minimal medium w/o amino acids w/o ammonium chloride (FMM0601, Formedium)
    - 400 mL milliQ water
- SD-His media:
    - 8 g D-glucose (G8270, Sigma)
    - 2.8 g Yeast Nitrogen Base without amino acids (CYN0402, Formedium)
    - X mg -His drop-out (DSCK1003, Formedium)
    - 400 mL milliQ water
- SD-Leu media:
    - 8 g D-glucose (G8270, Sigma)
    - 2.8 g Yeast Nitrogen Base without amino acids (CYN0402, Formedium)
    - X mg -Leu drop-out (DSCK2504, Formedium)
    - 400 mL milliQ water
- SD-Ura media:
    - 8 g D-glucose (G8270, Sigma)
    - 2.8 g Yeast Nitrogen Base without amino acids (CYN0402, Formedium)
    - X mg -Ura drop-out (DSCK1009, Formedium)
    - 400 mL milliQ water
- Ethanol/Glycerol media:
    - 386 mL SC media
    - (3%) 12 mL ethanol
    - (3%) 12 mL glycerol
- Bathophenanthroline Disulfonate (BPS) media:
    - 400 mL SC media
    - (150 µM) 37 mg BPS
- $CaCl_2$ media:
    - 400 mL SC media
    - (100 mM) 4.439g $CaCl_2$

*X mg refers to changing specifications of the stock product.

All growth media was sterilised through autoclaving immediately after preparation, before use. Antibiotics were routinely added as required for selection following sterilization when the medium had cooled to 60°C or below. The final concentrations of these were: 100 µg/mL Ampicillin or 250 µg/mL G418 sulphate. For solid media, 2% (w/v) agar (A/1080/53, Thermo Fisher) was added prior to autoclave sterilisation.

2.1.5 Antibodies

Table 2.1 *- Antibodies used in this project for Western Blotting and CPY assay.*

Primary Antibodies				
Antibody	**Raised**	**Source**	**Code**	**Working Dilution**
α-Vps45	rabbit	Bryant Lab		1:50
α-Tlg2	rabbit	Bryant Lab		1:500
α-GFP	mouse	Sigma	G6539	1:1000
α-CPY	mouse	ThermoFisher	10A5B5	1:500
α-GAPDH	mouse	Ambion	AM4300	1:1000
α-PGK1	mouse	Bryant Lab		1:20,000
α-HA	mouse	Roche	12CA5	1:1000
Secondary Antibodies				
αMouse	HRP-conjugated	Cell Signalling	7076S	1:2000
αRabbit	HRP-conjugated	Cell Signalling	7074S	1:2000

2.1.6 E. coli Strains

This project used One Shot™ TOP10 Chemically Competent *E. coli* cells (C404003, ThermoFisher) for plasmid expansion and transformation.

Genotype: F$^-$*mcr*A Δ(*mrr-hsd*RMS-*mcr*BC) φ80*lac*ZΔM15 Δ*lac*X74 *rec*A1 *ara*D139 Δ(*ara-leu*)7697 *gal*U *gal*K λ–*rps*L(StrR) *end*A1 *nup*G.

2.1.7 S. cerevisiae Strains

CMY650 (shown in red, **Table 2.2**) was initially used for all experiments, until we established that the *tlg2Δ* phenotype was not rescued by *TLG2*

overexpression, leading to the formation of the His5+ *tlg2Δ::his5*$^{+}$ strain. CMY refers to the Chris MacDonald yeast strain database at the University of York.

Table 2.2 *- Yeast strains used in this project.*

Yeast Database	Parental Strain	Genotype	Source	Name
CMY56	BY4742	MAT*α, his3Δ leu2Δ lys2Δ ura3Δ*	BY4742 (Brachmann *et al*., 1998)	wildtype
CMY1356	BY4742	*vps45-his5*$^{+}$	MacDonald Lab	*vps45*$^{his5+}$
CMY657	BY4742	*vps45Δ::KanMX4*	MacDonald Lab	*vps45Δ*
CMY650	BY4742	*tlg2Δ::KanMX4*	MacDonald Lab	*tlg2Δ*
	BY4742	*tlg2Δ::his5*$^{+}$	Bryant Lab	*tlg2Δ*
CMY2211	BY4742	*pep12Δ::KanMX4*	MacDonald Lab	*pep12Δ*
CMY2205	BY4742	*vac1Δ::KanMX4*	MacDonald Lab	*vac1Δ*
CMY2206	BY4742	*vps21Δ::KanMX4*	MacDonald Lab	*vps21Δ*
CMY1381	BY4742	*vps45*^{T238N}*-his5*$^{+}$	MacDonald Lab	T238N
CMY1957	BY4742	*vps45*^{P485L}*-his5*$^{+}$	Bryant Lab	P267L
CMY1426	BY4742	*vps45*^{P267L}*-his5*$^{+}$	MacDonald Lab	P485L
CMY2207	BY4742	*atg8Δ::KanMX4*	MacDonald Lab	*atg8Δ*
CMY2209	BY4742	*atg1Δ::KanMX4*	MacDonald Lab	*atg1Δ*
CMY2212	BY4742	*pep4Δ::KanMX4*	MacDonald Lab	*pep4Δ*
	BY4742	*mef2Δ::KanMX4*	MacDonald Lab	*mef2Δ*
	BY4742	*ptm1Δ::KanMX4*	MacDonald Lab	*ptm1Δ*
	BY4742	*yhl017wΔ::KanMX4*	MacDonald Lab	*yhl017wΔ*

2.1.8 Primers

Oligonucleotides were designed using Snapgene Viewer® v6.0.2 and were manufactured by Integrated DNA Technologies (IDT, UK). Oligos were dissolved in nuclease-free water to generate a 100 µM stock solution. Bold bases refer to the base change that introduces a mutation and the sequence specific to the *loxP-his5-loxP* cassette for removal of the *TLG2* gene by homologous recombination. The blue base refers to the introduction of the *Avr*II (R0174S, NEB) restriction enzyme cut site to improve screening of *VPS45*-E252K mutants before sending for sequencing (**Table 2.3**).

Table 2.3 *- Oligonucleotides used for this project.*

PCR oligos	**Oligo sequence (5'-3')**
Upstream *VPS45*	*CGTCATTACAGTTAGTTAACGTTCG*
Downstream *VPS45*	*GACCGGGGTTCGACTCCCCGTATCGG*
P485L mutant oligo	*GAATGAATTCTAAGAGCAACACCGCTGAAAACGTCTATATG CAACATATT**tt**GGAAATTTCGTCATTACTAACAGATC*
Oligo for P485L sequencing	*CCAGATATACAGGTATGAAGGAGC*
E252K mutant oligo (with AvrII RE site)	*CCTTGGACCTACCAATCAATGATCAAT**a**AGTATATAGGCATT AAGCGGAATATAGTTGATTTATCGAAAGTGCCTAG**g**ATTGAT AAAGACC*
E252K mutant oligo	*CCTATAACACCTTTACTTCAACCTTGGACCTACCAATCAATG ATCAAT**a**AGTATATAGGCATTAAGCGGAATATAG*
Oligo for E252K sequencing	*CCAGATATCAGGTATGAAGGAGC*
L422P mutant oligo	*CCAGCTCAGACAAAATCCGTCAACTAGTTGAGATTC**c**GTCTC AACAACTTCC*
Oligo for L422P sequencing	*GCAAAGCATATGGCTATAGTGGGGG*
TLG2 Knockout 5' (**his5 cassette**)	*CGGCAAGACAGGAAAGTCTCCAATTGATGTACATTTTATCGC **CGCCAGCTGAAGCTTCGTACGC***
TLG2 Knockout 3' (**his5 cassette**)	*CGCGATGCGGTACCGTGAAAGTTTTGTCATCAAAGTAGGTC ATCC**GCATAGGCCACTAGTGGATCTG***
5' *TLG2* Genotype	*GTTGGACCGGTTTGTATTGGGC*
3' *TLG2* Genotype	*GAACAATCCTTACGGATTTAGG*
Upstream *TLG2*	*GCGTATAGATTATAGCAGAATAGACTATAAGTACGGC*
Downstream TLG2	*CCATATTTTATCATCTTCAGGAACTACTTATGCACAATATTCG TTCGCC*
Upstream *PEP12*	*CCCCTATAAAACAGGCCTGC*
Downstream *PEP12*	*CGGCGTAGAAATATTATGAGAGAGCCC*
Upstream *VAC1*	*GACCGACCTAAAGAGCAAAGCCGG*
Downstream *VAC1*	*GCGTGGAGATTCCGCGAATGATCG*
Upstream *VPS21*	*GGGGCTTTTTGCTAAAACAATATCCCCG*
Downstream *VPS21*	*CCCTCTCCTTTCTAGGTACG*

2.1.9 Plasmids

Table 2.4 *- Plasmids used in this project. *General Biosystems 2024 Order. Numbered identifiers refer to the Bryant Lab plasmid -80°C stocks and pCM refers to the Chris MacDonald plasmid library at the University of York.*

Plasmid Name	Identifier	Genotype	Source
Cen Parent	76	YCplac111	Nia Bryant
Cen *VPS45*	69	YCplac111 expressing Vps45-HA from *VPS45* promoter	Nia Bryant
Cen T238N	70	YCplac111 expressing Vps45-T238N-HA from *VPS45* promoter. C*A(713) & A*T(714)	Nia Bryant
Cen P267L	90	YCplac111 expressing Vps45-P267L-HA from *VPS45* promoter. C*T(800)	Nia Bryant
Cen P485L		YCplac111 expressing Vps45-P485L-HA from *VPS45* promoter. C*T(1454)	GB 2024*
Cen E252K		YCplac111 expressing Vps45-P485L-HA from *VPS45* promoter. G*A(754)	GB 2024*
Cen L422P		YCplac111 expressing Vps45-L422P-HA from *VPS45* promoter. T*C(1265) & G*A(1266)	GB 2024*
2µ Parent	68	YEp352	Nia Bryant
2µ *VPS45*	67	YEp352 expressing Vps45-HA from *VPS45* promoter.	Nia Bryant
2µ T238N	71	YEp352 expressing Vps45-T238N-HA from *VPS45* promoter. C*A(713) & A*T(714)	Nia Bryant
2µ P267L		YEp352 expressing Vps45-P267L-HA from *VPS45* promoter. C*T(800)	GB 2024*
2µ P485L		YEp352 expressing Vps45-P485L-HA from *VPS45* promoter. C*T(1454)	GB 2024*

2µ E252K		YEp352 expressing Vps45-E252K-HA from *VPS45* promoter. G*A(754)	GB 2024*
2µ L422P		YEp352 expressing Vps45-L422P-HA from *VPS45* promoter. T*C(1265) & G*A(1266)	GB 2024*
2µ *TLG2*	96	YEp352 expressing Tlg2-HA from *TLG2* promoter.	Nia Bryant
2µ *PEP12*	97	YEp352 expressing Pep12 from PEP12 promoter.	Nia Bryant
2µ *VAC1*	98	YEp352 expressing VAC1 from Vac1 promoter.	Nia Bryant
2µ *VPS21*	99	YEp352 expressing Myc-Vps21 from VPS21 promoter.	Nia Bryant
GFP-Ape1	pCM290	pRS416 expressing GFP-Ape1 from the APE1 promoter.	Daniel Klionsky
mTurquoise2-Cit1	pCM1181	pRS315 expressing CUP1-Cit1-mTurquoise2 from the CUP1 promoter.	Chris MacDonald
His5+ Integration Plasmid		pUG27 expressing loxP-his5-loxP cassette.	Chris MacDonald (Gueldener *et al*., 2002)

2.1.10 Computer Software

- ImageJ v1.52p (Rasband, W.S., U. S. National Institutes of Health, Bethesda, Maryland, USA
- PyMOL Molecular Graphics System, v2.0 (Schrödinger LLC, New York, New York, USA.)
- CLC Sequence Viewer v8.0 (Qiagen Bioinformatics, Aarhus, Denmark.)
- Snapgene Viewer® v6.0.2 (Dotmatics, Boston, Massachusetts, USA.)
- GraphPad Prism v9.0 (Dotmatics, Boston, Massachusetts, USA.)
- BioRender.com (Ontario, Canada)

2.1.11 External Company Services Used

- Eurofins (Genotyping by Sanger Sequencing)
- General Biosystems (Plasmid Construction)

- Plasmidasaurus (Plasmid Sequencing)
- Integrated DNA Technologies (Oligonucleotide construction)

2.2 General Cell Culture

2.2.1 Culture of E. coli

Bacterial cultures were grown in standard 50 mL Falcon tubes (5 to 10 mL culture) at 37°C in LB media with shaking at 220 rpm. Plates for solid culture were made from the same media composition supplemented by 2% agar.

2.2.2 Culture of S. cerevisiae

Yeast cultures were first left to grow on a plate at 30°C and in either rich media YPD or SC media. Agar plates for cellular culture were made from the same media composition supplemented by 2% agar. Generally, in preparation for experiments 5 mL of culture in a glass culture tube with loose polystyrene cap (Starlab) were left at 30°C overnight with shaking of 220 rpm. In the morning 1 mL of culture would be added to 4 mL of fresh media to promote growth of yeast from starvation into log phase. Yeast cells were used in log phase for all experiments unless stated otherwise.

2.2.3 Yeast Growth assays

Overnight culture of yeast was normalised to OD_{600} 0.6, a 1 in 5 serial dilution was completed in water in a 96-well plate. 3 µL of each yeast inoculation was added to the appropriate selective agar plates using a paper template on the underside of the plate. Plates were left to dry for 5 to 10 minutes and incubated at 30°C and photographed after 24, 48 and 72 hours of incubation.

2.3 General Molecular Biology Methods

2.3.1 DNA Preparations

Single colonies of yeast were inoculated in YPD and grown overnight at 30°C. Cells were centrifuged at 5000 rpm for 2 mins. The pellet was resuspended in 500 µL of TE buffer and 5 µL of β-mercaptoethanol (1% v/v) and 5 µL of zymolyase (25 µg/µL) were added. The cells were incubated at 37°C for ~4 hours. 500 µL of phenol:chloroform:isoamyl alcohol (25:24:1) was added and vortexed for 10 mins. The cells were then centrifuged at 13,000 xg for 10 mins.

The aqueous phase was then added to 500 µL of phenol:chloroform:isoamyl alcohol (25:24:1) vortexed and centrifuged again. 50 µL 3 M sodium acetate was added to the aqueous phase with 1 mL of 100% ethanol prior to freezing at -80°C. The pellet was washed 4 times with 70% ethanol and then resuspended in 100 µL TE Lite and left to resuspend overnight at 25°C.

2.3.2 DNA Amplification by Polymerase Chain Reaction (PCR)

PCR was performed routinely to amplify DNA sequences of interest, either for integrations or for gene sequencing. Appropriate forward and reverse DNA primers were used in each experiment (**Table 2.3**). The following protocol was followed to set up PCR reactions, usually 25µl total volume (**Table 2.5**). Reactions were performed in thin wall PCR tubes and using a thermocycler, conditions were dependent on the desired product (**Table 2.6** and **Table 2.7**). The melting point of the primers was estimated to set the annealing temperature for individual reactions. Molecular weight, amount and relative purity of PCR products was checked by agarose gel electrophoresis (section 2.3.3).

Table 2.5 - *PCR reaction mixture.*

Reagent	Volume (µL)
PCRBIO Ultra Mix (PB010620-040-0, PCRBIO)	12.5
10 mM Forward Primer	1
10 mM Reverse Primer	1
gDNA (100 ng)	1
Nuclease Free Water	9.5
Total	**25**

Table 2.6 *- Thermocycler conditions for gene amplification.*

Step	Temperature (°C)	Time (Minutes:Seconds)
Initial Denaturation	95	01:00
Denaturation*	95	00:20
Annealing*	~55	00:20
Elongation*	72	~01:30
X 25 cycles*		
Final Elongation	72	05:00
Hold	4	-

Table 2.7 - *Thermocycler conditions for amplicon production required for homologous recombination.*

Step	Temperature (°C)	Time (Minutes:Seconds)
Initial Denaturation	95	05:00
Denaturation*	95	00:30
Annealing*	48	00:15
Elongation*	72	01:30
X 30 cycles*		
Final Elongation	72	05:00
Hold	4	-

2.3.3 Ethanol Precipitation

200 µL of PCR product were supplemented with 10 µl salmon sperm, 15 µL of 3 M sodium acetate (pH 5.5) and 1 mL of 100% ethanol and kept at -80°C for 30 mins. The solution was centrifuged at 13,000 xg for 10 mins and supernatant was removed. The pellet was washed three times with 1 mL of 70% ethanol and left to dry for 3 mins at 42°C before adding 30 µL of TE.

2.3.4 Agarose Gel Electrophoresis

Gels were prepared by dissolving powdered agarose in TAE buffer by boiling in a microwave. Agarose gel concentration varied from 0.8-2% (w/v) depending on the size of DNA fragments to be resolved. Agarose solution was allowed to cool to approximately 60°C prior to the addition of SYBR™ Safe DNA at a 1 in 10,000 dilution. The molten solution was poured into a cassette with the appropriate comb and left to set at room temperature before being immersed into a tank containing TAE buffer. DNA samples were prepared by addition of DNA loading dye and loaded on the gel alongside a DNA ladder to provide reference for the size of the resolved DNA fragments. Gels were routinely run at 120 volts, typically for 40 minutes and DNA fragments were visualised using a blue-light transilluminator.

2.3.5 DNA Gel Extraction and Purification

DNA fragments that had been resolved by agarose gel electrophoresis were visualized using a blue-light transilluminator. The fragment of interest was identified by size and excised using a clean scalpel. The agarose gel piece containing the DNA fragment was placed into a sterile Eppendorf tube and DNA

was extracted using the GeneJET Gel Extraction Kit (K0691, Thermo Scientific) following the manufacturer's instructions. Extracted and purified DNA was eluted from the column using 50 µL high purity sterile nuclease free water.

2.4 General Protein Methods

2.4.1 Bacterial Transformation

10 µl of chemically competent bacterial cells were thawed on ice for 30 mins prior to transformation and then mixed with ~1 µg plasmid DNA. Cells were incubated on ice for 30 minutes, heat shocked at 42°C for 30 seconds and then returned to the ice for 5 minutes before 900 µL of LB media was added. Cells were left to recover for 40 minutes at 37°C with 220 rpm shaking before spreading on an LB agar plate containing 100 µg/mL ampicillin.

2.4.2 Mini-prep of Bacterial Plasmids.

5 mL bacterial culture in LB was grown at 37°C with antibiotic overnight from a single colony with shaking at 220 rpm. Plasmid DNA was extracted from the culture using the Monarch® Plasmid DNA Miniprep Kit (T1010, NEB) and following the supplier's recommendations. DNA was eluted with 100 µL elution buffer, warmed to 50°C. DNA concentration was measured using a nano-drop spectrophotometer (NanoDrop™ 2000/2000c, ThermoFisher) and then routinely stored at -20°C.

2.4.3 Competent Yeast

Competent yeast cells were prepared by harvesting approximately 1.5 OD_{600} yeast by centrifugation at 600 xg and washed in 5 mL LiTE Sorbitol before being resuspended in 1 mL LiTE Sorbitol and incubated at 30°C with shaking for 1 hour. The cells were frozen in 50% (v/v) yeast freezing buffer at -70°C until use.

2.4.4 Yeast Transformation

100 µL of yeast was thawed on ice before adding to 5 µL of 10 mg/mL salmon sperm and ~500 ng of plasmid DNA; 150 µL of 70% PEG-3350 was added and mixed. The cells were left on the shaker at 30°C for 45 mins and then heat shocked for 20 mins at 42°C before transfer to ice. The cells were centrifuged at low speed for 1 min and the supernatant discarded. The pellet was

resuspended in ~200 µL water and spread on selective media agar plates. Single colonies were used for experiments after 36 hours of growth.

2.4.5 Preparation of Yeast Cell Lysates

1 mL of overnight yeast culture were diluted in 9 mL of fresh YPD medium and grown for ~4 hours to enter exponential phase. Yeast cultures were then centrifuged at 5000 xg for 5 mins. Pellets were then resuspended in 100 µL of TWIRL buffer containing 10% (v/v) β- mercaptoethanol per unit of OD_{600}. The samples were incubated at 65°C for 15 minutes, vortexed, centrifuged for 10 seconds, and stored at -20°C.

2.4.6 SDS-PAGE

Yeast lysates were incubated at 65°C and vortexed before loading to wells of a stacking gel and discontinuous SDS-PAGE was used to resolve lysates on a 12% acrylamide gel in SDS buffer. Electrophoresis was typically complete after ~90 mins at 120 V. Gels typically included a Precision Plus Protein™ ladder for determination of molecular weight. Gels were removed from the apparatus and then prepared for immunoblotting.

2.4.7 Semi-Dry Protein Transfer

Filter paper and nitrocellulose membrane were soaked in semi-dry transfer buffer for five minutes prior to assembly in the semidry machine. Transfer was completed by assembling filter paper, the membrane, the gel and a second piece of filter paper. Bubbles were removed by using a roller after application of each component. Samples were transferred from the gel to the nitrocellulose membrane using a semidry machine for 50 mins at 0.3 A. Membrane was checked for protein using Ponceau S staining then rinsed with TBST for 15 minutes to remove the stain before western blotting.

2.4.8 Western Blotting (protein immunodetection)

The membrane was blocked in 5% milk in TBST for 1 hour at room temperature. The membrane was then incubated overnight with primary antibody at 4°C. The membrane was washed with TBST three times and incubated with secondary antibody for 2.5 hours, washed again and then imaged using Chemiluminescence Substrate and the iBrightTM (FL1000, Invitrogen) imaging system. Primary antibodies are shown in **Table 2.3** were applied in 3% milk in

TBST. Secondary antibodies used were anti-rabbit HRP conjugate and anti-mouse HRP conjugate at 1/2000 dilution in 5% milk in TBST.

2.4.9 Estimation of Protein Concentration

The percentage of protein in comparison to controls was calculated using Image J (1.52p, National Institutes of Health, USA). The region of interest was selected for each well or dot, the intensity of the area was measured in the software and background removed. Using a control as a baseline of 100(%), intensities of each well or dot were normalised to represent levels in proportion to the control.

2.5 Homologous Recombination of VPS45 SCN mutants

2.5.1 Homologous Recombination

A *his5*$^{+}$ deletion cassette was integrated downstream of the *VPS45* open reading frame to create strain CMY1356. Genomic DNA of this strain was then isolated for use in PCR-based generation of *VPS45* mutants for integration. Oligonucleotides were designed to amplify the *VPS45-his5*$^{+}$ sequence with suitable sites for homologous recombination at the endogenous *VPS45* locus of wildtype strains. These oligos were also designed to incorporate a point mutation, such as the *VPS45*-P485L mutation. The PCR product was ethanol precipitated (2.3.3) and the amplicon was then transformed into the yeast as described in 2.4.4 into BY4742 wildtype yeast. The transformed yeast was selected using selection plates lacking histidine.

2.5.2 Determination of VPS45-P485L Colonies

Single colony transformants grown on the -His selection plates before gDNA extraction (2.3.1) and the *VPS45-his5*$^{+}$ gene amplified via PCR, ethanol precipitated and then run on a 1% (w/v) high quality agarose gel (2.3.4 and 2.3.5). Firstly, strains were genotyped to confirm the successful integration of the *his5*$^{+}$ selection cassette generated from pUG27 (Gueldener *et al*., 2002) downstream of *VPS45*. Amplicons containing the *VPS45* gene with *his5*$^{+}$ cassette were gel extracted using the GeneJET Gel Extraction Kit (K0691, Thermo Scientific) using the manufacturer instructions and sent for sequencing. The corresponding colonies frozen down for -70°C stocks and use in further experiments.

2.5.3 Genotyping Potential SCN Colonies

Sequencing of DNA was provided by Eurofins Genomics TubSeq Sanger Sequencing service, the service was used routinely as a verification step after DNA cloning. Results were analysed using the CLC Sequence Viewer to establish the integration of the single base pair mutation in the *VPS45-his5*$^{+}$ gene. Samples were prepared following the supplier's recommendation. Typically, 15 µL pre-mixed reaction sample in Eppendorf tubes, containing ~50 ng/µL a plasmid DNA and the desired sequencing primer at 10 µM.

2.6 Creation of the tlg2Δ Strain.

2.6.1 Homologous Recombination

PCR was performed to amplify a segment of DNA containing regions specific to the *TLG2 5′* and *3′ UTR* and the *loxP-his5*$^{+}$*-loxP* cassette using the pUG27 plasmid (Gueldener *et al.*, 2002). The PCR product was ethanol precipitated (2.3.3) and the amplicon was then transformed into the yeast as described in 2.4.4 into wildtype yeast. The transformed yeast was selected using histidine selection plates.

2.6.2 Qualification of tlg2Δ Colonies

Single colony transformants grown on the -His selection plates before gDNA extraction (2.3.1) and the *TLG2* gene amplified via PCR then run on a 1% (w/v) agarose gel (2.3.4). Amplicons containing the *TLG2* gene rather than *loxP-his5+-loxP* cassette were distinguished by their difference in molecular weight. The corresponding colonies frozen down for -70°C stocks and use in further experiments.

2.7 CPY Secretion Assay

2.7.1 Preparation of Samples

Overnight culture of yeast was normalised to 0.6 OD_{600}. 3 µL of yeast inoculation was added to a YPD agar plate, once dried a nitrocellulose membrane was laid on the plate. The plate was incubated overnight at 30°C.

2.7.2 Immunoblotting

The membrane was washed with milliQ water and then blocked in 5% milk in TBST for 1 hour at 25°C. 1:500 dilution of CPY antibody in 3% Milk in TBST was added to the membrane for 1.5 hours at room temperature. Membrane was then washed three times with TBST and then a 1:2000 dilution of secondary antibody in 3% Milk in TBST was added to the membrane for 2 hours. The membrane was washed 3 times in TBST and then imaged using Chemiluminescence Substrate and the iBrightTM (FL1000, Invitrogen) imaging system.

2.7.3 Analysis and Presentation

Estimation of CPY secretion levels calculated using the method in 2.4.9.

2.8 Hydrogen Peroxide Sensitivity (Halo) Assay

2.8.1 Preparation of Samples

Overnight culture of yeast was normalised to 1.0 OD_{600}. 1.5 mL of this culture was added to YPD agar plates. The excess overnight culture was removed from the agar, and the plates left to dry. Single circles of filter paper were soaked in 10 µL of H_2O_2 at 5%, 2%, 1% or 0% (w/v) concentrations before transfer to agar plates and incubation for 48 hours at 30°C.

2.8.2 Analysis and Presentation

The images are captured after 3 days and then processed using Image J and processed using the methods described in **Figure 2.1**.

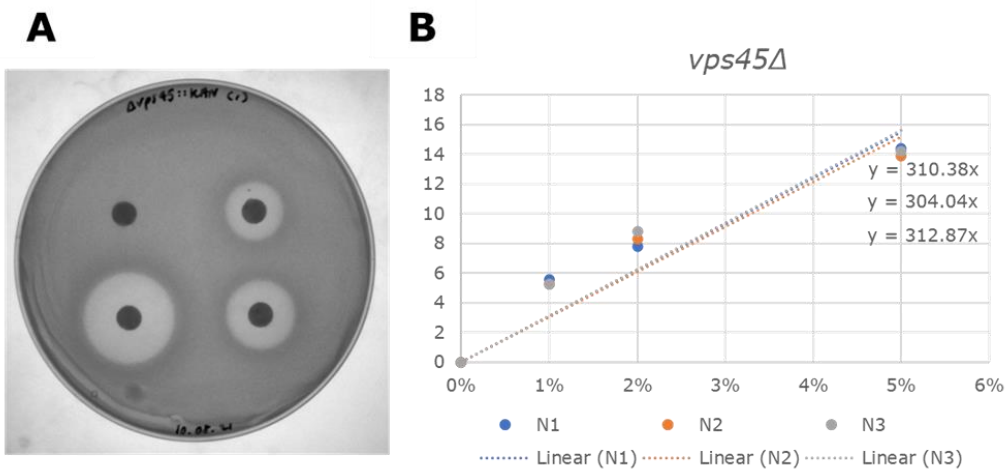

Figure 2.1- *Apoptotic phenotype observations in Wildtype and vps45Δ yeast; (A) Discs of filter paper are soaked in 0%, 1%, 2% and 5% w/v of H_2O_2 and*

placed on lawns of yeast. The area of H_2O_2 sensitivity is measured, the area is an arbitrary data point using Image J (1.52p, U. S. National Institutes of Health, Bethesda, Maryland, USA) which is plotted on a graph for each H_2O_2 concentration. (B) The gradient of the graph (m in y=mx+c) is recorded to incorporate all concentrations of H_2O_2 and the fold change is calculated for each data point, assuming that the wildtype strain has a H_2O_2 sensitivity of 1. The mean is then plotted with the standard error of the mean (+/-SEM) as seen in the results.

2.9 Recovery From Nitrogen Starvation Assay

2.9.1 Preparation of Samples

0.6 OD_{600} of overnight yeast cultures were grown over several hours until they reach log phase 1.0 OD_{600}. Cells were centrifuged at 4000 xg for 10 mins, all YPD was removed from the pellet. Cells were resuspended in 5 mL milliQ water, then centrifuged again. Cells were washed twice more. All water was removed from the pellet and the cells were resuspended in 5 mL of media lacking nitrogen (SD-N).

2.9.2 Sample Handling

The cells in SD-N media were shaken at 26°C for five days. A 100 µL sample of cells was taken daily and suspended in 900 µL of YPD media. The yeast samples were diluted down to avoid overcrowding on the plate and 100 µL was spread evenly over the YPD plates. The cells were left to grow at 30°C in the incubator for 3 days before colonies were counted.

2.9.3 Analysis and Presentation

Recovery from nitrogen starvation was calculated by calculating the percentage change in colonies grown on day 0 against the 5 days following. The AUC was then calculated from the line-graph of the daily growth over the 5 days and re-plotted as a bar chart where the AUC is a percentage of the wildtype control.

2.10 Microscopy

2.10.1 GFP-Ape1 Analysis

Appropriate strains transformed with the GFP-Ape1 plasmid were grown to mid-log phase in selection media, 5 µL of CMAC vacuolar stain added 30 mins prior to experiment to 1 mL of cell suspension at 30°C. After cells were centrifuged

at 600 xg and washed in water 3 times and resuspended in 30 µL synthetic complete media. Before imaging 1 µL of suspension was added to a slide. Using laser scanning confocal microscopes LSM 880 equipped with an Airyscan module (Zeiss) with a 63x Differential Interference Contrast (DIC) objective and a 1.4 numerical aperture. The argon laser excitation was 488 nm with emission filter set to 495 – 550 nm (for GFP) and 561 nm with 570–620 nm emission filter (for CMAC) was used. Micrographs were analysed using Image J.

2.10.2 Mitochondrial Analysis

Appropriate strains transformed with the mTurquoise2-Cit1 plasmid were grown to mid-log phase in selective media. 30 minutes prior to experiment, 1 mL of cells had 100 µM CuCl added to activate the CUP1-mTurquoise2 promoter and 1 µM of CMXRos MitoTracker™ was added. After cells were centrifuged at 600 xg and washed in water 3 times and resuspended in 30 µL SC media. Live yeast cells were imaged using the 63×/1.4 objective lenses on the LSM 880 Zeiss microscope, with 488 nm (mTurquoise2) and 633 nm (MitoTracker™ CMXRos) wavelength argon lasers. Intensity and gain were optimised and kept for each experiment. Micrographs were analysed using Image J.

2.11 Flow Cytometry

Cells were prepared by 10 mL of log-phase cells being centrifuged at 600 xg and washed in PBS 3 times before resuspending in 1 mL of PBS. 10 µM of MitoTracker™ CMXRos was added 15 mins before experiment and cells left at 30°C. Intensity from MitoTracker™ CMXRos (Yellow 610 nm excitation laser, 720/50 nm emission filter) labelled live cells at room temperature was recorded using a CytoFLEX LX355 flow cytometer (Beckman Coulter) and intensity measurements from gated cells measured with CytExpert (Beckman Coulter). 10,000 cells, gated for fluorescence positive yeast cells (using forward/side scatter), were flowed at ~600 V to maintain a rate of approximately 500 – 1000 cells measured per second. Unlabelled / non-expressing cells were used for background calibration.

2.12 Visualisation of the 3D Structure of Vps45

The 3D structure of Vps45 was visualised using PyMOL software. The FASTA sequence of the *Homo sapiens* and *Saccharomyces cerevisiae* were input into

the system and aligned with the *Chaetomium thermophilum* crystal structure using the RCSB Protein Data Bank, and database identifier 6XJL. The Tlg2/Vps45 and Syntaxin 16/hVps45 binding structures were estimated using the same method and the identifier 6XMD (Eisemann *et al*., 2020).

2.13 ERC Data

2.13.1 ERC Data Delivery

Evolutionary Rate Covariation (ERC) is the analysis of evolutionary relationships between proteins using their genes rate of evolution compared to another (**Figure 2.2A**). This is calculated using the methods described in (Clark *et al.*, 2012). Dr. Nathan Clark provided the *YGL095C* (*VPS45)* gene profile matrix against 4309 genes found in the Saccharomyces Genome Database (SGD). Using this matrix, he converted the gene profile for *VPS45* using Fisher Transform to determine the statistical relationship between *VPS45* and the proteins of the matrix (Little *et al*., 2024).

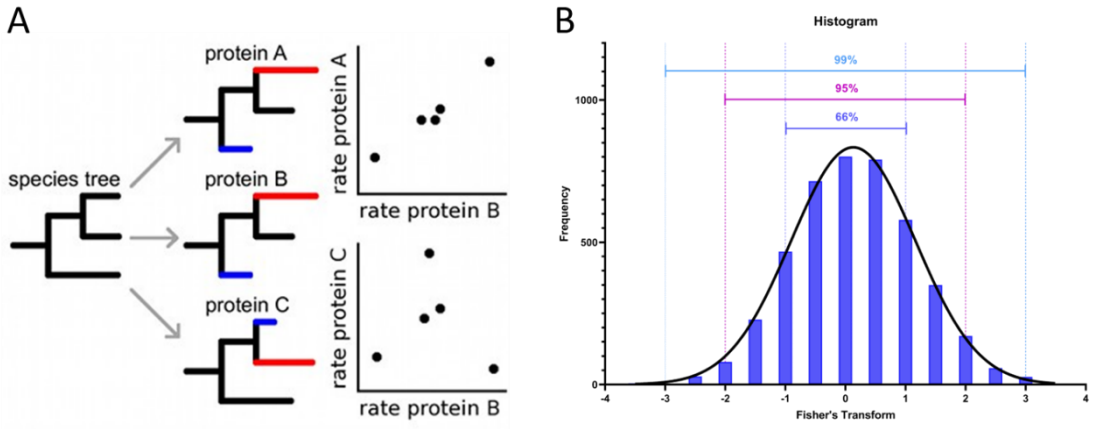

Figure 2.2 *- Understanding the ERC data concept and the VPS45 dataset; (A) ERC analysis explained, the rate of evolution comparing protein A and B is high due to the similar evolution due evolutionary pressure. Whereas protein B and C has a lower ERC value due to their rate of evolution being less similar. Image taken from ("ERC Analysis," 2023) (B) The ERC data creates a rubric of the ERC relationships that compare all genes to one another, the data sent to us by Nathan Clark had been Fisher Transformed, this analyses the relationship and considers skewed data, then estimates confidence intervals. In this histogram the Fisher Transformed ERC data is graphed so that all yeast genes can be accounted and their ERC relationship to VPS45. Values higher than 2 are in the top 5% confidence interval of the data meaning that they are highly likely to be related to VPS45. Likewise values higher than 3 are in the top 1%.*

2.13.2 ERC Data Management

Using the Fisher transformed data kindly provided by Dr. Nathan Clark the Bryant lab was able to determine the relationship of *VPS45* and other genes. Being able to rank them as having a high ERC value and this being statistically significant (**Figure 2.2B**). Using this information, genes that had a positive ERC value were ranked (>3.0 and >2.0) and analysed the location and/or role of the protein using the proteins' profile on the website UniProt.

3 SCN mutations in Vps45 are functional in endosomal traffic and autophagy but are defective in apoptosis.

3.1 Introduction

3.1.1 Vps45 facilitates SNARE binding as an SM protein.

Vacuolar protein sorting 45 (Vps45) protein is a member of the Sec1/Munc18-like (SM) protein family; SM proteins regulate SNARE complexes through physical interactions with SNARE proteins (Misura *et al*., 2000). The SNARE complex consists of 4 α-helices, these helices intertwine and coil together forcing two membranes in close proximity to create the fusion of lipids in the bilayer-membranes (Nichols *et al*., 1997). Membrane fusion allows mixing of the vesicular contents with the lumen of the designated organelle. Only specific combinations of these proteins can form functional SNARE complexes (McNew *et al*., 2000), accounting for specificity between the transfer of cargo of different organelles.

Vps45 has been reported to hold the SNARE Tlg2 in an open conformation (Eisemann *et al*., 2020) allowing Tlg2 to form a functional SNARE complex with Snc2 (Furgason *et al*., 2009). In mammalian cells Vps45 binds to syntaxin 16 (Tlg2 orthologue) (Struthers *et al*., 2009) to allow for binding to cognate SNARE protein VAMP4 (Kreykenbohm *et al*., 2002). Through its role as an SM protein, Vps45 is required for endosomal membrane traffic (Dulubova *et al*., 2002). This enables macromolecules to be transported to the vacuole in yeast and the lysosome in mammalian cells; loss of Vps45 results in accumulation of vesicles in the cytosol (Cowles *et al*., 1994; Piper *et al*., 1994).

Vps45 has been well studied in yeast and multiple phenotypes have been characterised previously which I intend to expand on in this chapter. For example, *vps45Δ* mutant yeast display increased oxidative stress sensitivity (Brown *et al*., 2006) and display a defect in doubling time and growth defect at 39°C in comparison to other *vps* mutants (Shanks *et al*., 2012).

3.1.2 Phenotyping mutant yeast – CPY traffic

The vacuolar hydrolase Carboxypeptidase Y (CPY) is translocated into the lumen of the ER before trafficking through the Golgi apparatus to the trans-Golgi network (TGN). In wildtype cells, CPY is trafficked to the vacuole via a pre-vacuolar compartment where it is cleaved into its mature form which is enzymatically active in the low pH of the vacuolar lumen (Conibear and Stevens, 1998). Vps45 is required for the transport of the vacuolar hydrolase CPY to the vacuole (Bryant *et al*., 1998b). In *vps* mutants, including *vps45Δ* cells, CPY is not trafficked from the TGN to the pre-vacuolar compartment and is instead secreted from the cell (**Figure 1.2**) (Coonrod and Stevens, 2010). This phenotype can be observed using a CPY assay. Using antibody chemiluminescence we can observe the release of CPY from the cells and image this (Methods 2.7). When CPY traffic is dysfunctional the anti-CPY antibody indicates the secretion of CPY from the yeast cells. The fidelity of membrane traffic through the endosomal system to the yeast vacuole uses CPY secretion as a quantifiable phenotype.

3.1.3 Phenotyping mutant yeast – H_2O_2 sensitivity

Yeast lacking *VPS45* display multiple phenotypes in addition to missorting CPY, these include a temperature sensitive growth defect and increased sensitivity to high salt and oxidative stress (Piper *et al*., 1994). Yeast lacking functional *VPS45* are more susceptible to apoptosis as observed by increased sensitivity to H_2O_2, using the H_2O_2 sensitivity assay developed in the Bryant lab we can quantify potential increased levels of apoptosis observed in yeast. How this assay is quantified is shown in Methods 2.8.

3.1.4 Phenotyping mutant yeast – autophagy studies

Under conditions of nutrient deprivation eukaryotic cells recycle non-essential components to promote cell survival. This process of autophagy is also triggered in response to cellular stresses (Anding and Baehrecke, 2017). Autophagosomes are double membraned vesicles containing material to be recycled and are indicators of autophagy. They are targeted to the vacuole where their contents are degraded to recycle constituent components (Kim and Klionsky, 2000). When yeast is starved of nitrogen they enter autophagy (Klionsky *et al*., 2021). Therefore, n this thesis I use a nitrogen starvation assay to assess yeast strains' ability to recover after induction of autophagy (section 2.9).

Vps45 is required for the delivery of vacuolar hydrolase Ape1 to the vacuole through mediation of the cytoplasm to vacuole targeting (CVT) vesicle (Kirisako *et al*., 2000). The CVT pathway is considered to be a type of selective autophagy (Lynch-Day and Klionsky, 2010) in yeast and the movement of Ape1 throughout the cell is often used as a marker of autophagy. After transformation of a plasmid expressing vacuolar Ape1 with an N-terminal GFP-tag allows the localisation of Ape1 to be visualised via microscopy. Under normal conditions Ape1 is trafficked through the cell via the CVT pathway to the vacuole where it is cleaved into an active aminopeptidase. Ape1 travels through the cell via the autophagosome after autophagy induction. Ape1 progresses through the cell to the vacuole and maturation of the Ape1 enzyme at the vacuole is used as an indicator of autophagy function. When Ape1 traffic is dysfunctional GFP-Ape1 can be visualised in bright puncta usually at the surface of the vacuole. Movement of Ape1 to the vacuole through the CVT pathway leads to a diffuse pattern through the vacuole.

Vps45's role as an SM protein in membrane traffic have been implicated in autophagy. Vps45 interacts with Pep12 to traffic cellular material from the Golgi to the endosome (Burd *et al*., 1997) and Pep12 displays an autophagic mutant phenotype (Kanki and Klionsky, 2008). In *pep12Δ* mutant cells, a cognate syntaxin of Vps45, Ape1 accumulates outside the vacuole in autophagosomes (Chen *et al*., 2014). Pep12 is also known to interact with Vps21, a Rab GTPase, which is involved in the double membrane closure of the autophagosome in preparation for delivery to the vacuole (Chen *et al*., 2014). Vps45's binding partner Tlg2 interacts with Sec22 in order to transport Atg9 (Nair and Klionsky, 2011). Atg9 is trafficked from the TGN to endosomes under stress conditions; it is the only transmembrane Atg protein and is required to form autophagosome from the phagophore (Feng *et al*., 2016; Feng and Klionsky, 2017; Orsi *et al*., 2012).

3.1.5 VPS45 SCN mutation phenotypes in patients.

In 2013, Stepenksy *et al*. identified a mutation in the *VPS45* gene that is causative of the disease SCN. However, the identification that *VPS45* was involved in increased apoptosis in humans was novel. Prior to this paper Vps45

was a well characterised vacuolar sorting protein (*vps*) and known for its role in the CVT pathway. SCN mutations can be found in various genes, such as the *ELANE*, *HAX1* or *LYST* genes (Skokowa *et al*., 2017). In recent years five mutations in the human gene *VPS45* have been identified in SCN patients, each resulting in single amino acid changes: T224N (Stepensky *et al*., 2013), P468L (Shah *et al*., 2017), E238K (Meerschaut *et al*., 2015), P253L (unpublished (Newburger, 2018)), L410P (Alotaibi and Albarkheel, 2020).

3.1.6 SCN mutations are conserved across species.

Vps45 is a highly conserved protein throughout species (Bock *et al*., 2001), patients with SCN lack lysosomes of normal morphology (Stepensky *et al*., 2013), indicating that Vps45 is required in the endosomal-lysosomal pathways as in yeast. All five of the residues in SCN patients are highly conserved amino acids throughout evolution (**Figure 3.1C**). Each of these SCN related residues are conserved in the yeast homologue Vps45 (**Figure 3.1A/B**) and therefore yeast is a suitable model organism to observe the effects of these mutations on the function of Vps45. Due to three of the five of these mutations being in the SNARE binding cleft of the protein, where Vps45 binds to Tlg2 in particular (Furgason *et al*., 2009), it is to be expected that these residue changes will have an effect on the fidelity of Vps45 and its binding partners.

3.2 Aims and Hypothesis

3.2.1 Hypothesis

My hypothesis is that the SCN mutant yeast will display similar phenotypes to the *vps45Δ* yeast as the mutations are in the hinge region of the protein above the SNARE binding cleft. This model predicts that the ability of the mutant Vps45 protein to bind to its cognate SNARE protein(s) will be affected and therefore the same trafficking phenotypes as in yeast lacking the protein completely will be present. The data shown in Stepensky *et al*. shows an increase in apoptosis in neutrophils in patients that have *VPS45*-T224N mutant Vps45. Due to the high conservation of the Vps45 protein throughout species I therefore hypothesise that all SCN mutants and *vps45Δ* yeast will also display an increase in apoptosis as seen in the patients observed in the forementioned paper (Stepensky *et al*., 2013).

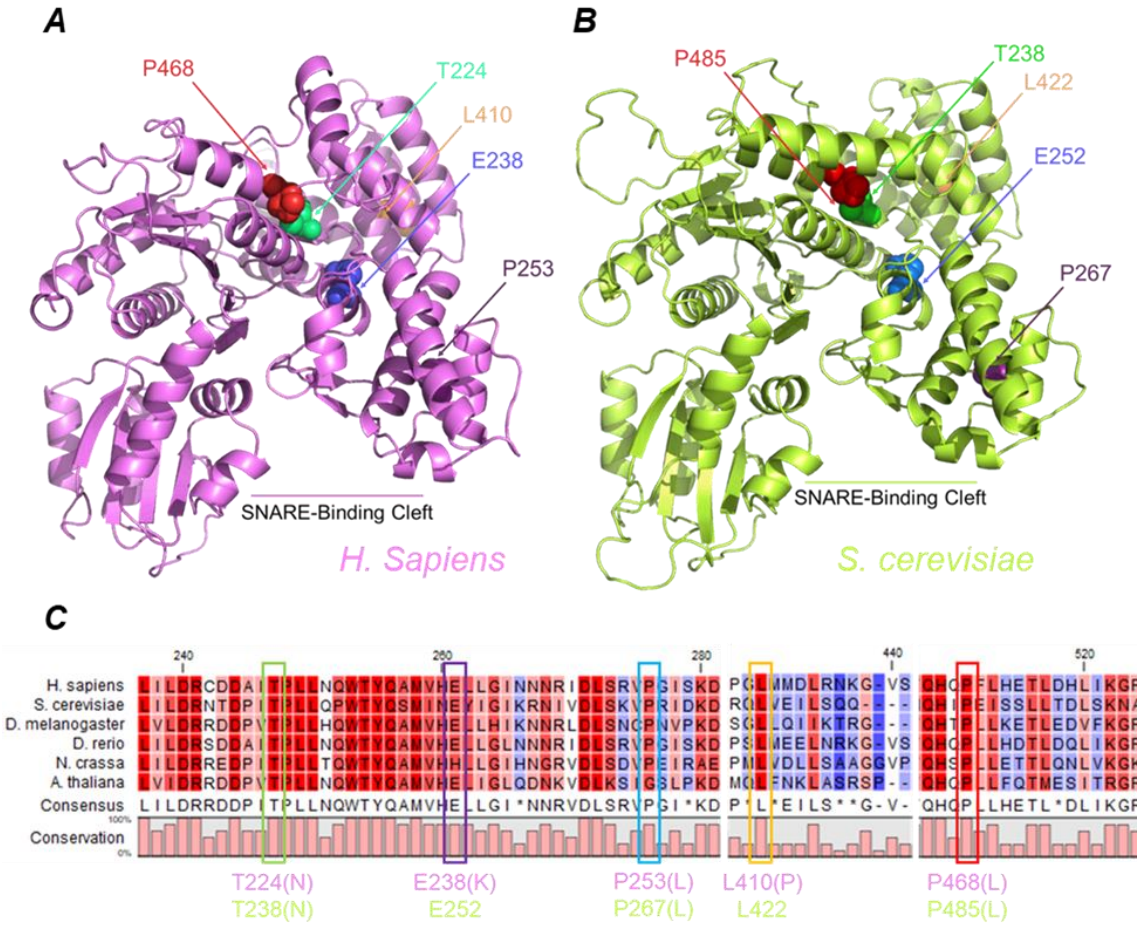

Figure 3.1 *– SCN causing residue changes are conserved residues throughout evolution; (A + B) 3D PyMOL models of human Vps45 (A) and yeast Vps45 (B), each image shows the five Vps45 SCN disease causing mutations and the amino acid position in the 3D model using PyMOL (PyMOL Molecular Graphics System, V 2.0, Schrödinger, LLC) FASTA sequences from UniProt were input into PyMOL and then aligned with the crystal structure of Vps45 from C. thermophilum (Eisemann et al., 2020) using the RCSB Protein Data Bank, and database identifier 6XJL. (C) Vps45 amino acid sequence consensus and conservation of Vps45 SCN mutations across species visualised using CLC Sequence Viewer (Qiagen Bioinformatics, V8.0, Aarhus).*

3.2.2 Aims for Chapter 3

Using mutant yeast that have integrated *VPS45* SCN mutations I will characterise the phenotypes of all these mutants to dissect the roles of Vps45 within the cell. Using standard yeast cell biology techniques and the CPY secretion, H_2O_2 sensitivity and recovery from nitrogen starvation assays described, to analyse the phenotypes of the SCN mutant yeast. Using the H_2O_2 assay I will determine whether the apoptotic phenotype observed in SCN *VPS45*-

T224N patients is (1) observable in yeast and translatable into the model organism yeast and (2) if Vps45 plays a previously unidentified role in apoptosis in yeast as seen in patients and (3) whether the T238N, P267L and P485L *VPS45* SCN mutant yeast display an apoptotic defect as seen in the T224N Vps45 in patient neutrophils.

Vps45 has also been identified as a potential player in autophagy (Burman and Ktistakis, 2010) prior to the identification of *VPS45* mutations being pathogenic. Therefore, I chose to look at the *VPS45* SCN mutant yeast's ability to recover from autophagy using the nitrogen starvation assay and movement of Ape1 through the cell. The link between autophagy and apoptosis is unclear and complex, the current literature seems to suggest a fine line between the self-preservation through autophagy and selecting to go through apoptosis. The recurrent links between autophagy and apoptosis lead to my overall hypothesis that loss of Vps45 function results in reduced protection from apoptosis caused by inability to promote cell survival through autophagy. Therefore, the addition of the SCN causing mutations leads to restriction of Vps45 in the processes required for a cell to have sufficient protection from apoptosis through autophagy.

3.3 Results

3.3.1 SCN mutations are integrated into the yeast genome to form SCN mutant yeast strains.

To analyse the consequences of the genetic mutations in patients with SCN, introduction of the analogous mutation into the genome of yeast allows the effect of the mutation at endogenous levels (as opposed to overexpression via a plasmid) to be assessed. Formation of these strains through homologous recombination is described in the methods section 2.5. The lab successfully introduced 3 SCN analogous mutations into the yeast genome to alter the amino acid sequence of the Vps45 protein (**Figure 3.2**), two previous mutant strains introduced by the MacDonald Lab. The generation of the third mutant using this procedure allows me to make comparisons with all three mutants producing the SCN Vps45 at endogenous levels.

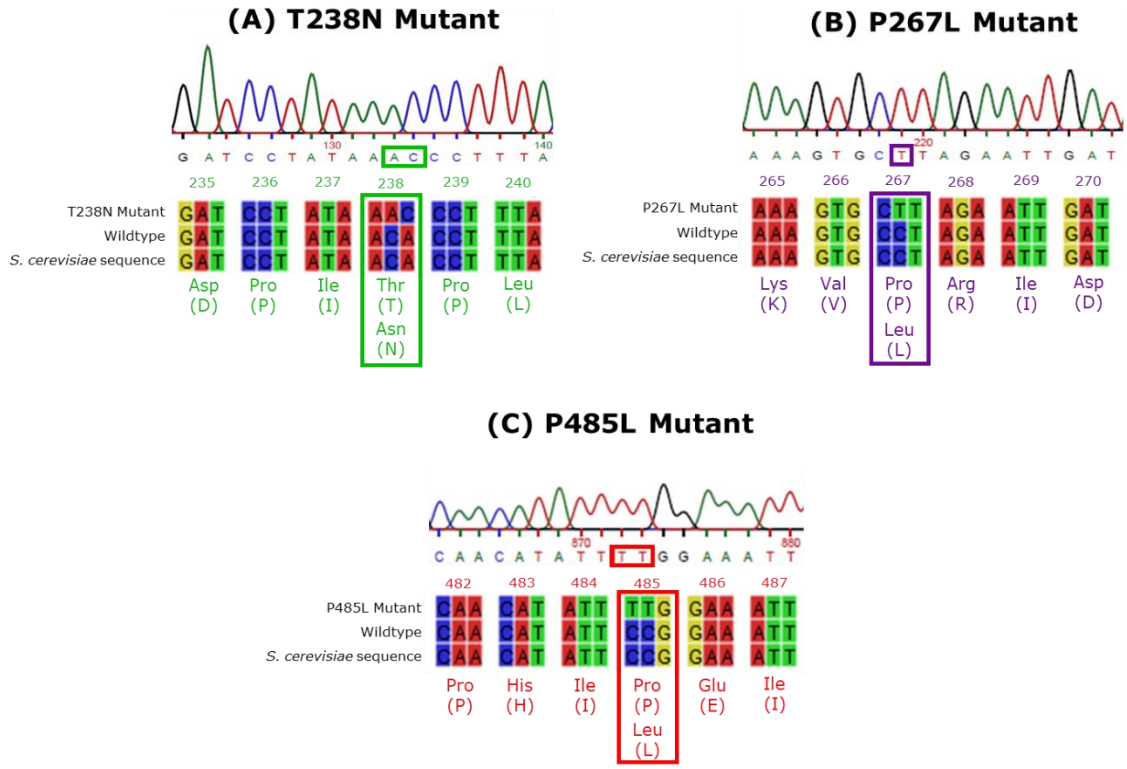

Figure 3.2 *-Sequencing Data of the VPS45 SCN integrated mutant yeast strains; the sequence from the Sanger sequencing by Eurofins© is shown indicating the individual nucleotides, below this is how the gene is translated into the amino acid sequence, visualised by CLC Sequence Viewer (V.8.0, Qiagen, Denmark). The mutations are introduced into the genome of BY4742 wildtype yeast. (A) MacDonald lab; ACA (threonine) is now AAC (aspargine) at position 238 (B) MacDonald Lab; CCT (proline) is now CTT (leucine) at position 267 (C) Bryant lab; CCG (proline) is now TTG (leucine) at position 485.*

3.3.2 Decrease of cell size in vps45Δ cells also seen in mutant yeast

An observed morphological phenotype of *vps45Δ* by Dr. Dimi Kioumourtzoglou in the Bryant lab was a decrease in cell size compared to wildtype yeast when observed under the microscope. I wanted to determine whether the *VPS45* SCN mutant strains displayed this same morphology. Using confocal light microscopy, the cell area of 1000 cells were recorded and plotted (**Figure 3.3**). The significance of this data indicates that the mutations in the *VPS45* gene leading to residue changes have morphological effects on the cell. Vps45 is a class D *vps* protein meaning that the loss of the protein leads to a large singular vacuole (Cowles *et al*., 1994) as opposed to a dynamic smaller vacuole, which was also observed (but not quantified) in the SCN mutants in this experiment.

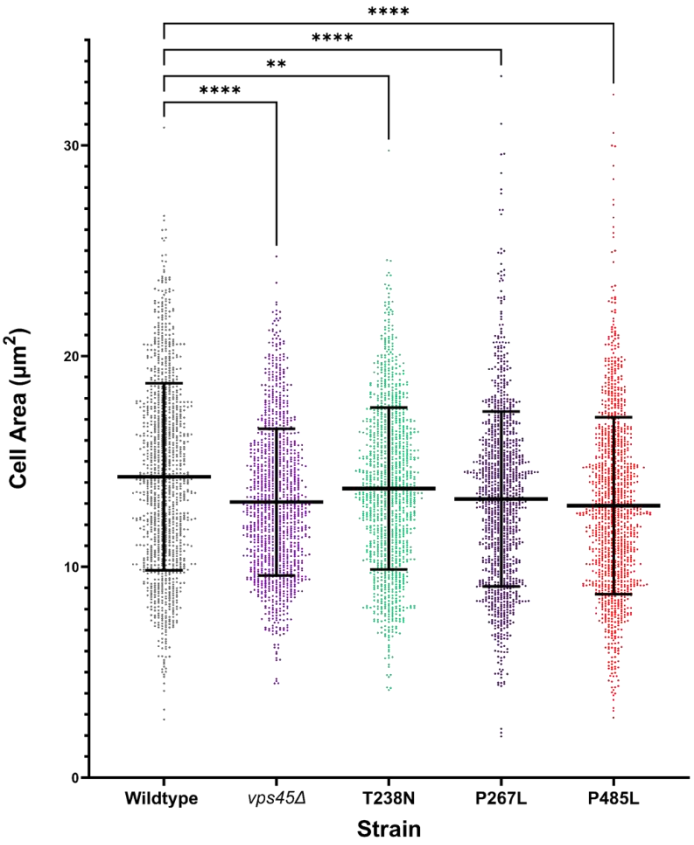

Figure 3.3 *-Cell Size and the VPS45 mutant yeast strains; The graph displays the mean and standard deviation (SD) of the Wildtype BY4742, vps45Δ, T238N, P267L and P485L yeast strains. One-way ANOVA statistical analysis was completed, and all four strains were statistically significantly different from the wildtype yeast (P<0.01 (**), P<0.0001 (****)).*

3.3.3 SCN mutant yeast display reduced Vps45 levels

Using western blotting I wanted to determine the levels of SCN Vps45 (**Figure 3.4**). In comparison to the wildtype yeast lysates SCN mutant lysates all display lower levels of the Vps45 protein. The *VPS45*-T238N mutation only had ~70% of the levels of Vps45 while the *VPS45*-P267L and *VPS45*-P485L mutants had ~80% and ~60% respectively. The *VPS45*-T238N and *VPS45*-P485L had statistically significantly lower levels of Vps45 in the cell lysates than the wildtype control. This data strengthens the importance of the integrated mutations as opposed to the use of overexpression plasmids while collating the majority of the data for this chapter.

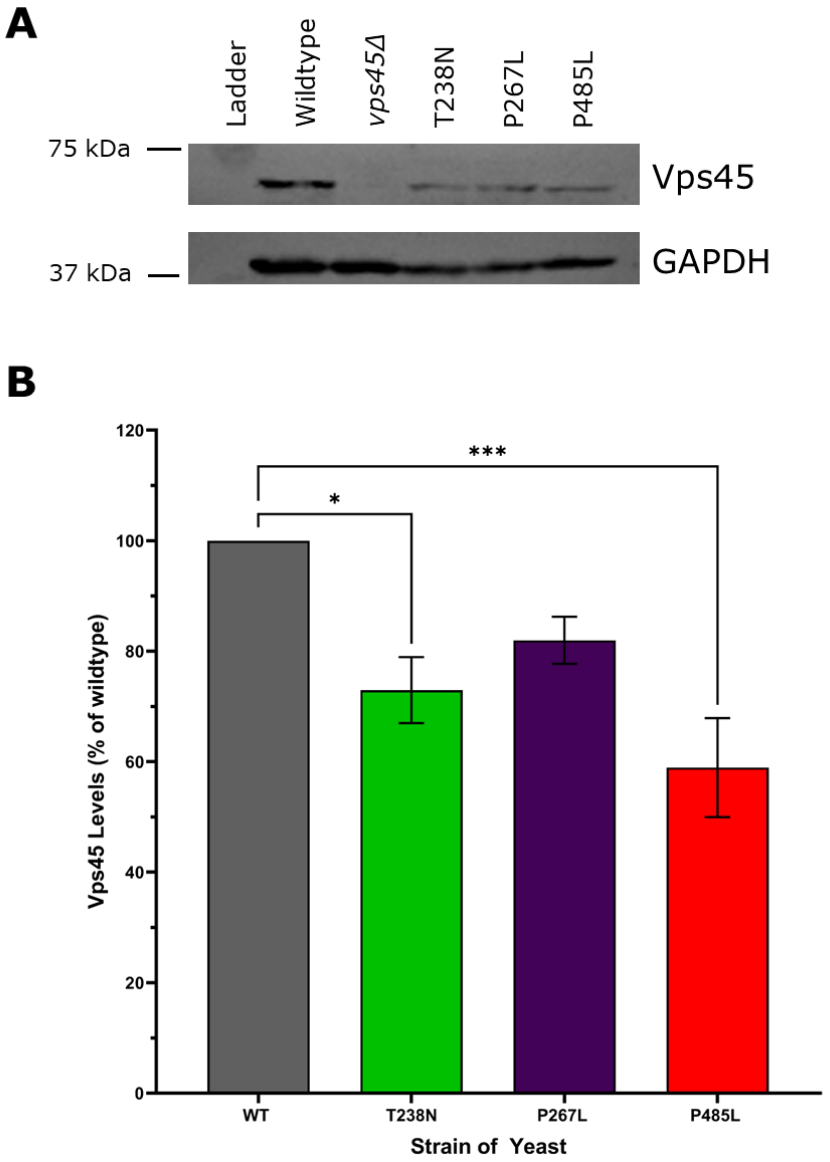

Figure 3.4 *-Vps45 levels in the VPS45 SCN mutant yeast; (A) western blot of Vps45 levels in cell lysates; Vps45 (67 kDa) can be seen in the wildtype, T238N, P267L and P485L yeast strains although at varying levels. GAPDH (37 kDa) is used as a loading control in this instance. (B) Quantification of SCN mutant Vps45 levels via western blot; a bar chart with the mean signal normalise to loading control and wildtype (+/-SEM) N=4. VPS45-T238N and VPS45-P485L displayed a statistically significant decrease in Vps45 levels (P<0.05(*), P<0.001(***)) by one-way ANOVA.*

3.3.4 SCN mutant yeast secrete wildtype levels of CPY.

Prior to the mutations found in SCN Vps45's studied role was through trafficking in the endosomal system. Yeast cells lacking Vps45 missort vacuolar hydrolases (Cowles *et al*., 1994; Piper *et al*., 1994) including CPY. CPY does not reach the vacuole in these cells and therefore is not cleaved into its enzymatically mature

form, this is demonstrated in **Figure 3.5A.** Therefore, in *vps45Δ* mutant yeast CPY is missorted and secreted from the cell (**Figure 3.5B**)**.** Whereas *VPS45*-T238N, *VPS45*-P267L and *VPS45*-P485L mutant yeast do not secrete CPY as the *vps45Δ* mutant does (**Figure 3.5B**). Cells lacking Tlg2, Vps45's cognate SNARE syntaxin, are known to secrete ~20% of CPY (Abeliovich *et al*., 1998) and this data shows that the *tlg2Δ* is secreting more CPY than the SCN mutants. Quantification of the CPY secretion as a percentage of wildtype secretion shows that *vps45Δ* yeast secretes ~80% more CPY than wildtype yeast, which is concurrent with the literature (Bryant *et al*., 1998a). However, the SCN mutant yeast secrete similar levels of CPY as the wildtype yeast (**Figure 3.5C**). These data demonstrate that these disease-causing mutations don't have any observable effect on Vps45's ability to traffic CPY through the endosomal system despite having reduced levels of the protein. This implies that the location of these residue changes is not important for the role of Vps45 in CPY traffic.

3.3.5 VPS45-T238N and VPS45-P485L have increased sensitivity to H_2O_2.

After discovering that despite causing SCN in patients, the mutant yeast did not display the same CPY missorting phenotype as *vps45Δ* yeast, a H_2O_2 sensitivity assay was developed by the lab to analyse the mutant yeasts susceptibility to apoptosis. H_2O_2 sensitivity is a wildly used method of establishing sensitivity to apoptosis in multiple organisms, due to its ability to be used to low doses to prevent necrosis (Xiang et al., 2016). The Vps45 SCN mutants T224N (T238N in yeast) demonstrated increased levels of apoptosis in neutrophils (Stepensky *et al*., 2013) using this assay we aimed to establish whether the yeast with the three SCN mutations would demonstrate a similar H_2O_2 sensitivity phenotype directly relating to the cells inability to rescue from apoptosis. The increase of H_2O_2 sensitivity of *vps45Δ* as raw data is shown in **Figure 3.6A**, quantification of this data is described in methods 2.8.2. The sensitivity of the yeast strains to H_2O_2 is quantified as a percentage of the wildtype (**Figure 3.6B**), a larger 'halo' indicates an increase in susceptibility and therefore a higher percentage of the wildtype 'halo' controls. The *vps45Δ*, *VPS45*-T238N and *VPS45*-P485L mutant yeast have a significant increase in their H_2O_2 sensitivity compared to the wildtype yeast ($P<0.0001$). The *VPS45*-P267L does not display an increased H_2O_2 sensitivity in these data. H_2O_2 induces apoptosis in yeast via increasing reactive oxygen species (ROS) in the cell which triggers apoptosis (Farrugia and

Balzan, 2012) and thus the increased sensitivity of cells lacking *VPS45* to H_2O_2 indicates that Vps45 has a protective role against this form of cell death. These data therefore indicate that two of the SCN mutant yeast are defective in protection from apoptosis. These data complement the observed acceleration in blood cell apoptosis seen in patients with the corresponding SCN disease causing mutations (Furutani *et al*., 2019).

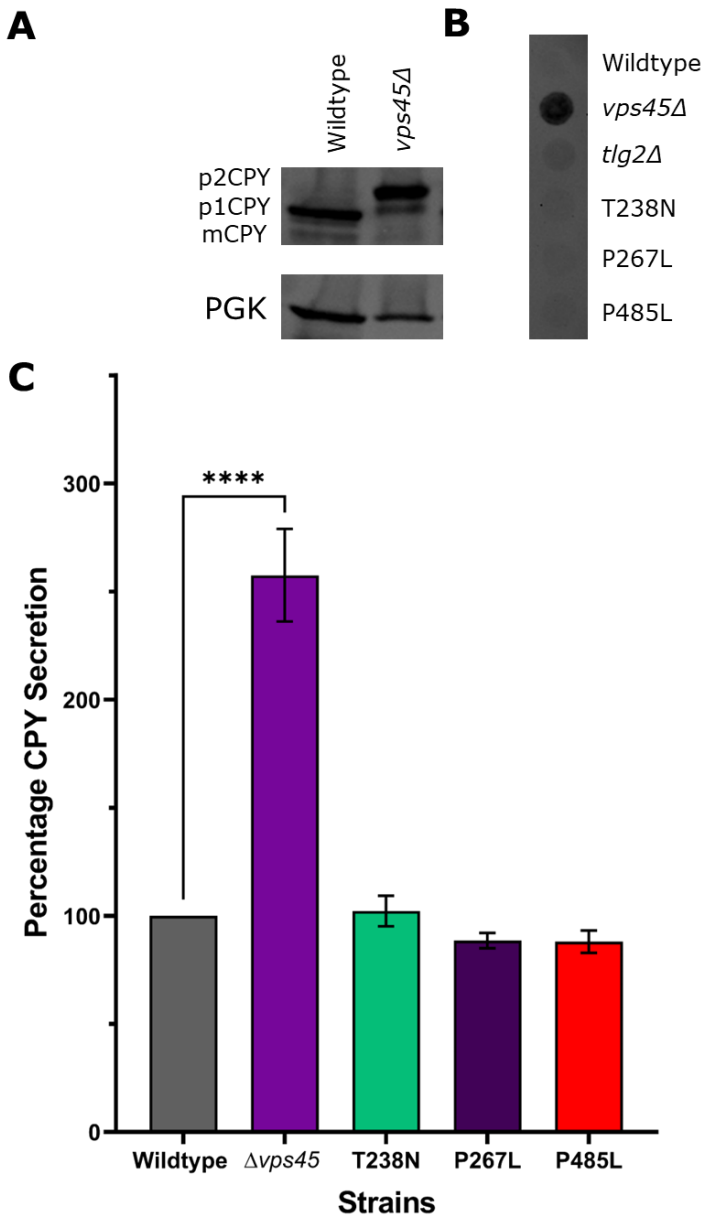

Figure 3.5 *-CPY secretion in vps45Δ and the SCN mutant yeast. (A) CPY travels through the cell into the vacuole where it is cleaved forming mature CPY. This western blot shows that the mCPY in the wildtype cell lysate is much higher than it is in the vps45Δ cell lysate. While the pro CPY which has not been cleaved and*

therefore not arrived at the vacuole is much higher in the vps45Δ cell lysate. (B) vps45Δ yeast is known to secrete CPY from the cell as it is not trafficked to the vacuole to be cleaved and therefore secreted (Bryant et al., 1998a). In cells lacking Tlg2, Vps45's cognate SNARE syntaxin, it is known to secrete ~20% of CPY (Abeliovich et al., 1998) but does not have as high a secretion as vps45Δ yeast. Here we see that the SCN mutant yeast display a similar CPY secretion phenotype to the wildtype yeast and not the tlg2Δ or vps45Δ yeast strains. (C) Quantification of the CPY secretion assay shows mean +/-SEM of CPY secretion assay (N=10). Only vps45Δ yeast has a statistically significant increase in CPY secretion (P<0.0001(****)) by one-way ANOVA.

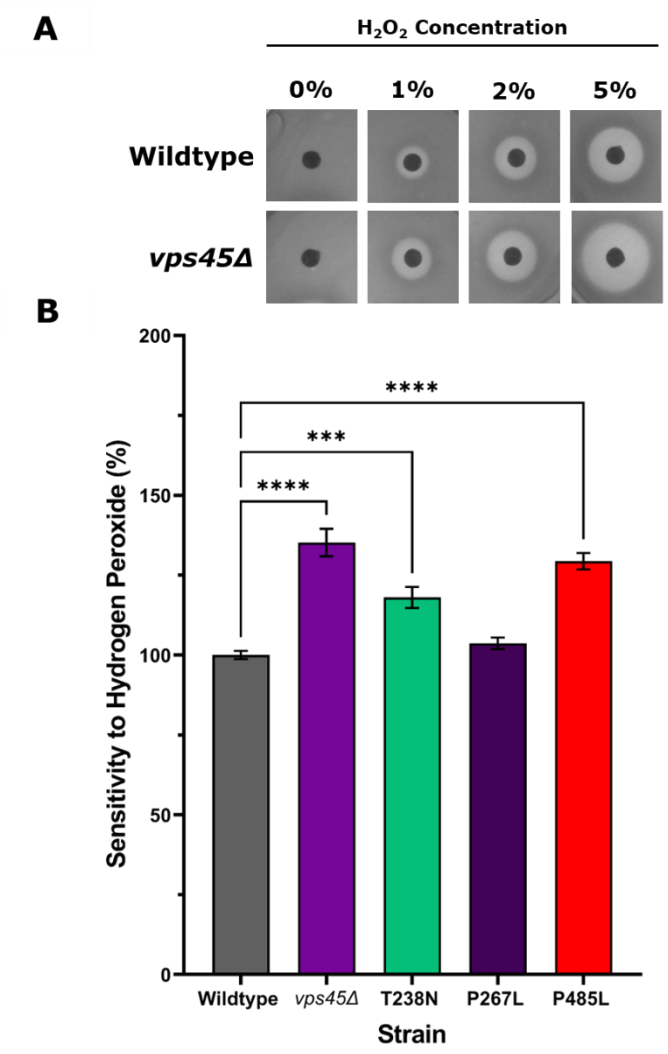

Figure 3.6 *- Assessment of susceptibility to apoptosis in SCN mutant yeast through the sensitivity to H_2O_2 assay; (A) Raw data displaying the 'halo' around the H_2O_2 soaked discs of the hydrogen peroxide sensitivity assay, the differences in area of no growth become clearer as the H_2O_2 percentage increases. I incorporate all four data points in the assay to quantify the data as described in Methods 2.8.2.(B) Percentage hydrogen peroxide sensitivity in BY4742 yeast mutant strains; quantified change in H_2O_2 sensitivity vps45Δ, T238N, P267L and P485L mutant yeast as a percentage of the mean of the BY4742 wildtype yeast control. mean +/- SEM compared to mutant strains using the H_2O_2 sensitivity*

assay, one-way ANOVA was applied to assess significance (P>0.05 (ns), P<0.001 (***), P<0.0001 (****)) N=5.

3.3.6 VPS45-T238N, VPS45-P267L and VPS45-P485L mutant yeast recover after nitrogen starvation.

Recovery following autophagy induced by nitrogen starvation can be monitored by cell viability (percentage survival). Wildtype cells recover after nitrogen starvation, shown in **Figure 3.7A**, with approximately ~50% of viable cells after 3 days of starvation. In the mutant *atg8Δ* strain, which is defective in autophagy, recovery was greatly diminished, with almost no viable cells at 3 days. only ~30% of the *vps45Δ* yeast were able to recover after 1 day of nitrogen starvation, whereas ~90% of *atg8Δ* yeast recovered after 1 day and ~60% after 2 days. Although both genotypes were defective in recovery, *vps45Δ* cells exhibited a more pronounced defect than *atg8Δ.* The severity of this phenotype led me to introduce a second autophagy control, *atg1Δ*, in order to ensure that it was not a problem with the *atg8Δ* control. The inability of *atg1Δ* cells to recover from autophagy induction after day 3~4 is consistent with the literature (Zhou *et al*., 2017). Atg1 and Atg8 function at different stages of autophagy (Wang and Klionsky, 2003) and therefore differing pathways will lead to the differences in their own recovery. In comparison to the mutants, ~30% of the wildtype yeast are still able to recover after 5 days of nitrogen starvation and the wildtype yeast even displays a ~10% increase in colonies formed after 1 day of nitrogen starvation compared to 0 days indicated by the peak on the line graph **Figure 3.7**. As the yeast are introduced to the nitrogen free medium at log phase this may be cells that were in later stages of replication and are budding.

As per my hypothesis I then repeated the data collection using the three SCN mutant strains, similarly, collecting the recovery from starvation data over 5 days. I predicted that the *VPS45*-P267L strain would have a similar phenotype to the wildtype and the *VPS45*-T238N and *VPS45*-P485L strains would have a similar phenotype to the *vps45Δ* due to the lower sensitivity to H_2O_2 and the location of the residue change on the 3D structure of the protein (**Figure 3.1**). However, the mutant yeast all displayed recovery curves like the wildtype yeast. The graph in **Figure 3.7B** displays the area under the curve (AUC) for all the

yeast strains after 5 days of nitrogen starvation. All three mutant yeast strains had a higher AUC than the wildtype yeast, *vps45Δ* yeast and the *atg8Δ* control. When calculating the area under the curve the mutant yeast all had AUC's that were statistically significantly increased from the *atg8Δ* control.

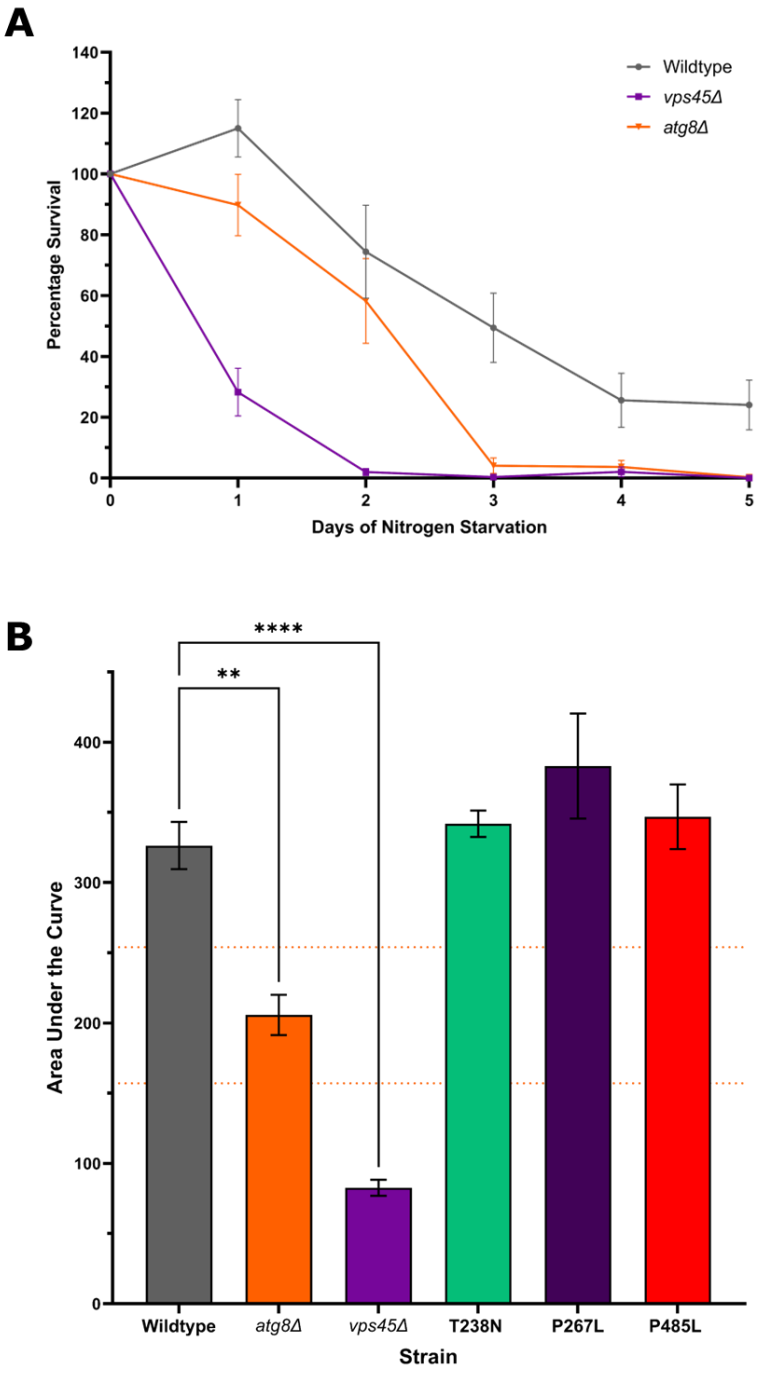

Figure 3.7 *- Quantification of recovery after nitrogen starvation data; (A) vps45Δ yeast does not recover after nitrogen starvation. Colonies of yeast were counted after yeast strains were exposed to nitrogen starvation for the indicated number of days. The number of colonies is recorded as a percentage of the number of colonies that formed after no nitrogen starvation on day 0 as described in methods 2.9.3. The assay was repeated four times and displays the*

mean +/-SEM of these repeats. vps45Δ cells have a clear defect in recovery after nitrogen starvation indicated by no colonies forming from day 2. This was even more so than the atg8Δ autophagy control which would lose ability to recover after day 3 or 4. Wildtype yeast display an increase in recovery after nitrogen starvation on day 1. (B) Area under the curve after 5 days of nitrogen starvation for the VPS45 mutant yeast; a bar chart displaying the mean and +/- SEM of the four areas under the curve calculated from four repeats. Dunnett's ANOVA was calculated to determine the statistical significance between wildtype and the other yeast strains. (P>0.05 (ns), P< 0.05 (*) P<0.01 (**), P<0.0001 (****)). The orange dotted lines represent the 95% confidence limits for atg8Δ yeast.

3.3.7 GFP-Ape1 traffic is unaffected by the introduction of the VPS45-T238N mutation in log phase and nitrogen starvation.

Ape1, like CPY, is a vacuolar hydrolase which requires movement across the cell in its precursor dodecamer form selectively through a CVT vesicle which uses autophagic machinery to target it to the vacuole. During starvation similar autophagic machinery allows for Ape1 to travel to the vacuole through non-selective autophagy (Su *et al*., 2015; Suzuki *et al*., 2002). Mis-localisation or loss of Ape1 in *vps45Δ* yeast and effector strains will expand on the autophagy recovery assay and allow us to visualise what happens inside the cell during autophagy induction and confirm normal autophagy function in the SCN mutant strains.

Using GFP-Ape1 in microscopy we observe the puncta representing Ape1 in the CVT vesicle during log phase whereas puncta in images after nitrogen starvation indicates Ape1 traveling via the autophagosome to the vacuole through non-selective autophagy. Using CMAC we can visualise the location of the vacuole in the cell. After arrival of GFP-Ape1 at the vacuole Ape1 is cleaved to become enzymatically active and GFP is visible in the vacuole. Pep4 is a vacuolar aspartyl protease required for maturation of vacuolar proteinases in the vacuole (Ammerer *et al*., 1986). Without Pep4 autophagosomal bodies accumulate inside the vacuole as they are unable to be degraded (Chen *et al*., 2014) we therefore used *pep4Δ* as a control for the cleavage of GFP-Ape1 in the vacuole. The second control was *atg8Δ*, Atg8 is a key autophagy player which is required for expansion of the autophagosome and involved in CVT traffic (Nair and Klionsky, 2011; Xie *et al*., 2008).

The micrographs in **Figure 3.8** show log phase cells and in wildtype cells where GFP-Ape1 is diffuse in the vacuole and in puncta in the CVT vesicle. *pep4Δ* shows multiple puncta inside and at the surface of the vacuole whereas the autophagy control *atg8Δ* shows puncta at the edge of the vacuole, both have no GFP signal inside the vacuole.

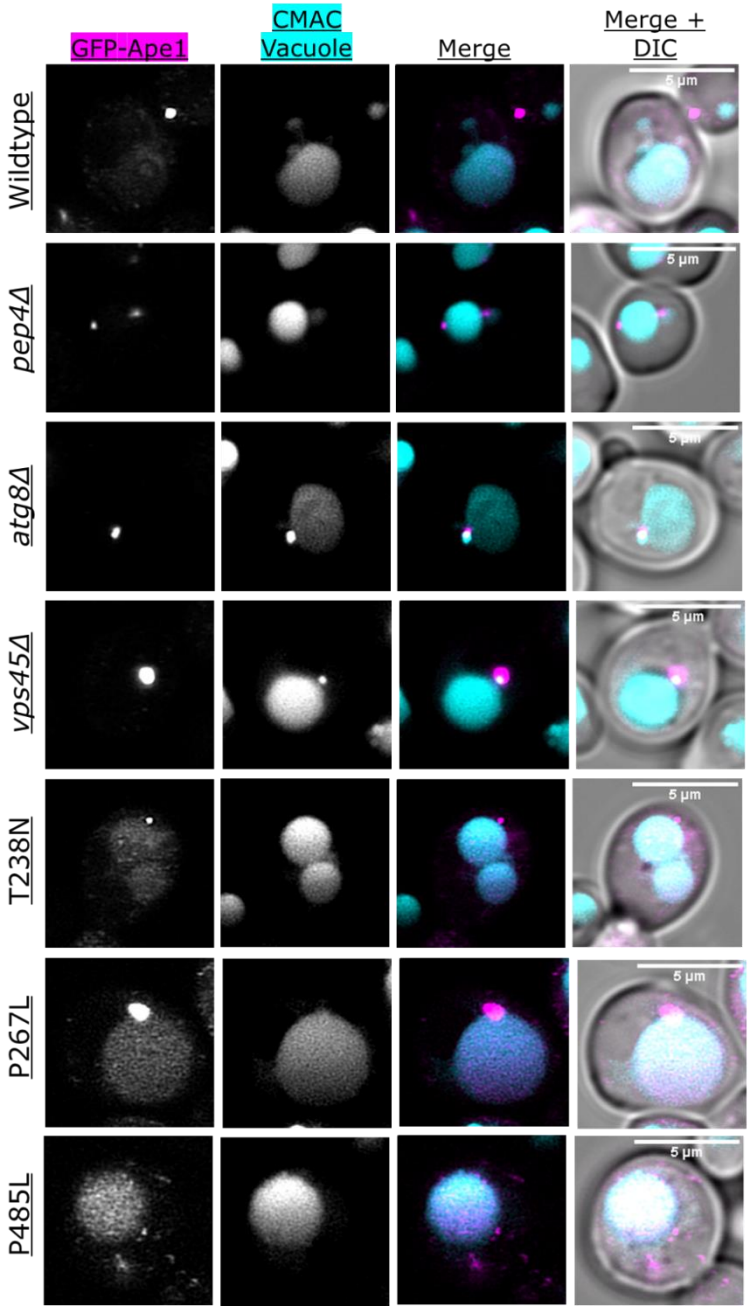

Figure 3.8 *– During log phase the SCN mutant strains displays an Ape1 trafficking phenotype similar to that of wildtype yeast; Micrographs displaying the localisation of GFP-Ape1 in mid-log phase Ape1 moves throughout the cell and is an indicator of autophagy function. Movement of Ape1 to the vacuole through the CVT pathway shows a pre-vacuolar compartment (PVC) shown as*

bright puncta, once Ape1 is degraded in the vacuole GFP displays a diffuse pattern.

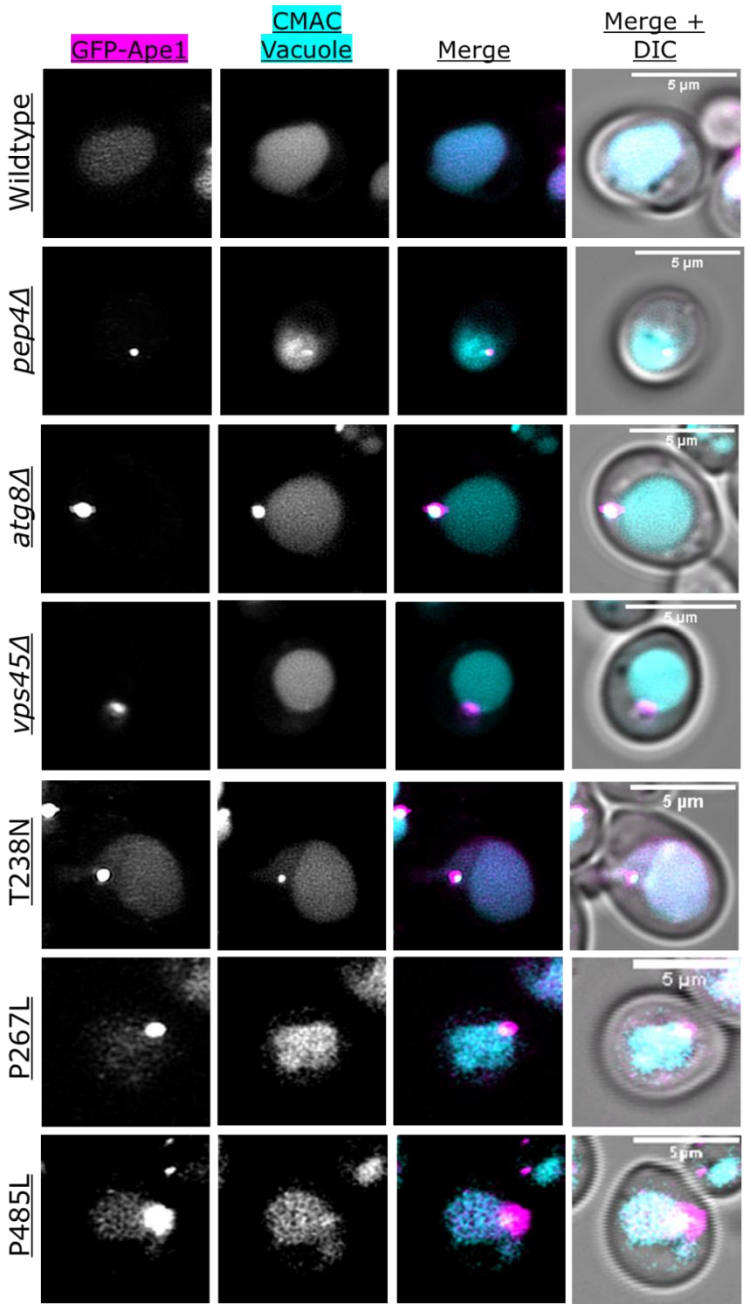

Figure 3.9 *– After autophagy induction SCN mutant yeast display conflicting GFP-Ape1 trafficking; Micrographs displaying the localisation of GFP-Ape1 after 4 hours of starvation from nitrogen (SD-N media). Ape1 moves throughout the cell and is an indicator of autophagy function. Movement of Ape1 to the vacuole through the CVT pathway shows a pre-vacuolar compartment (PVC) shown as bright puncta, once Ape1 is degraded in the vacuole GFP displays a diffuse pattern.*

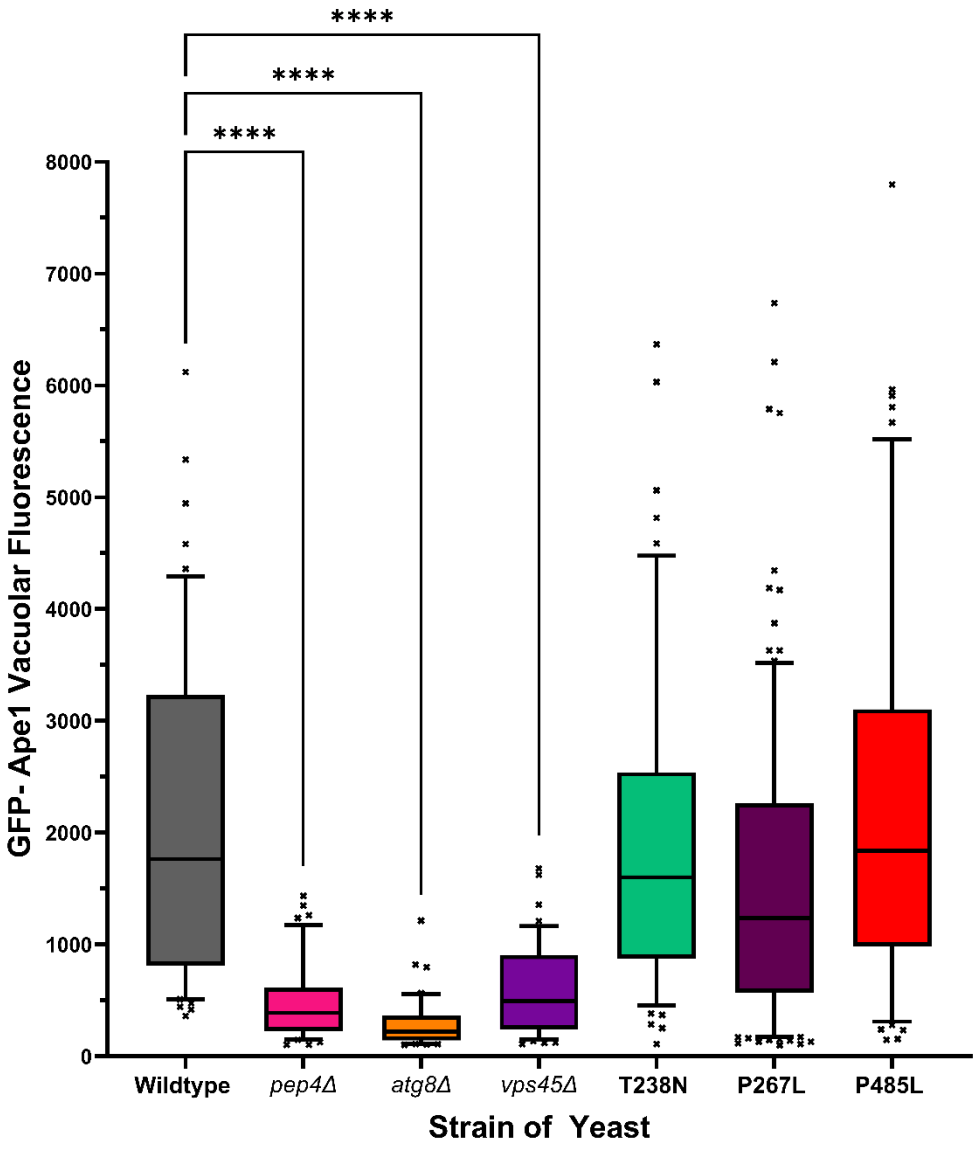

Figure 3.10 *- SCN mutant yeast show no defect in Ape1 traffic; Quantification of the micrographs shown in* ***Figure 3.9*** *show that after autophagy induction by nitrogen starvation the movement of Ape1 through the cell and to the vacuole is not perturbed as in autophagy mutants and vps45Δ cells.*

Here we determined the location of GFP in cells after 4 hours of nitrogen starvation wildtype GFP was found in the vacuole, of note, the *pep4Δ* strain had a reduction in puncta after nitrogen starvation although all were inside the vacuole (**Figure 3.9**). Both before and after nitrogen starvation large and singular GFP-Ape1 puncta are seen in the *atg8Δ* yeast at the periphery of the vacuole and statistically significantly less GFP-Ape1 was found in the vacuole in both instances. In *vps45Δ* yeast GFP-Ape1 presents in distinct singular puncta at the edge of the vacuole in each cell both before and after autophagy induction, although after nitrogen starvation the percentage of GFP-Ape1 in the

vacuole rose. This indicates that although required for the CVT pathway, other autophagic machinery recover some of transport of Ape1 to the vacuole under induction of autophagy in the *vps45Δ* strain. In contrast SCN mutant yeast have very bright singular puncta at the vacuole membrane and diffuse GFP can be observed throughout the cells, mainly in the vacuole. These data correspond with the nitrogen starvation data, in that the SCN mutant yeast strains do not show the same autophagic phenotype as the *atg8Δ* autophagy control. Through quantification of the micrographs (**Figure 3.10**) the quantity of Ape1 that was found free in the vacuole after autophagy induction was not significantly reduced in the SCN mutant yeast as in the *vps45Δ* and the *atg8Δ* and *pep4Δ* controls. This data shows that Ape1 trafficking after autophagy induction through nitrogen starvation is unaffected by the presence of the SCN mutations observed in patients.

3.3.8 E252K and L422P mutations have differing CPY and hydrogen peroxide phenotypes.

Throughout the entirety of this project the ongoing aim has been to characterise all 5 of the SCN mutations as yeast strains. Towards the end of the project, we developed the missing two mutations (E252K and L422P) as centromeric and 2μ plasmids in order to attempt to complete the story for these mutations as a group of 5. I transformed *vps45Δ* strains with the centromeric and 2μ plasmids to characterise their CPY and H_2O_2 sensitivity phenotypes as previously completed with the integrated mutant strains (*VPS45*-T238N, *VPS45*-P267L and *VPS45*-P485L). Using centromeric plasmids, the Vps45 levels show that overall, the plasmids only recover approximately 50% of the lost Vps45 and this is reduced in the T238N, P485L and E252K transformants (**Figure 3.11**). The P267L and the L422P mutant yeast have a slight increase in Vps45 levels. The E252K transformant has a huge reduction in Vps45 levels, in fact close to 0. This is reflected in **Figure 3.11C** as the CPY secretion of the E252K transformant is similar to that of the *vps45Δ* phenotype, which we did not see in any of the other *VPS45*-mutant strains or transformants. E252K also showed a H_2O_2 sensitivity phenotype like *vps45Δ* (**Figure 3.11D**). None of the other SCN *VPS45* transformants displayed this phenotype, however N=1 so statistical significance could not be assessed. The recovery of the *vps45Δ* H_2O_2 sensitivity phenotype had been observed prior in the project, by the T238N, P267L and P485L 2μ plasmids. I suspected that the addition of the uracil gene may be

improving the yeasts' ability to survive apoptosis due to great variation week by week in the halo area that something so minor could affect the results, however this data displayed similar results but the centromeric plasmids contained a leucine gene. I theorise that this particular assay is not sensitive enough to show variation and that only the most severe phenotypes are observed. Therefore, the *vps45Δ* H_2O_2 sensitivity phenotype can be restored by any addition of any variation of the Vps45 protein. However, this is not the case for the E252K Vps45 protein, indicating that the protein is produced but non-functional and therefore degraded.

In addition to the centromeric plasmid transformations I overexpressed SCN-*VPS45* using 2μ plasmids. Overexpression of the *VPS45* plasmid showed a 9-fold increase in the amount of Vps45 present in the cell in comparison to wildtype Vps45 levels, shown in **Figure 3.12A/B**. These data also show that overexpression of these SCN-*VPS45* plasmids had a reduction in the mutant Vps45 levels. Indicating that there is a clearance of the mutated proteins. Overexpression of the E252K 2μ plasmid corrects the *vps45Δ* CPY secretion phenotype (**Figure 3.12C**), however this was not observed with the centromeric expression of the E252K Vps45 protein suggesting that the CPY secretion phenotype seen in **Figure 3.11C** is due to the lack of protein as opposed to the change in the amino acid sequence. Interestingly, we observed in **Figure 3.12D** that the E252K protein displayed an increased H_2O_2 sensitivity phenotype despite increased expression of the mutated protein (**Figure 3.12B**). This phenotype suggests that the severity of the E252K mutation affects Vps45's role in apoptosis regardless of the increase of levels.

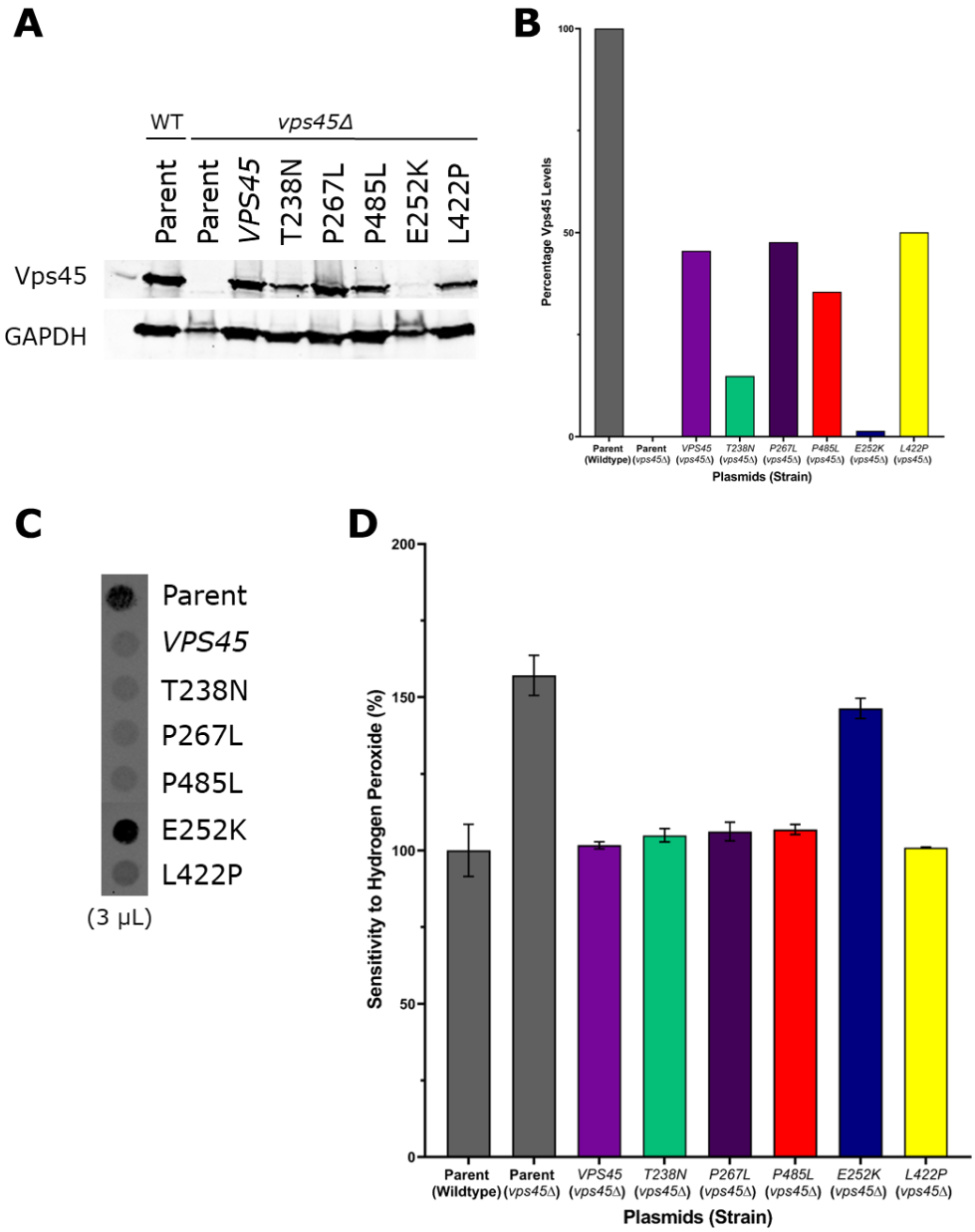

Figure 3.11 *– Dissecting the CPY and hydrogen peroxide sensitivity phenotypes of all SCN mutant Vps45 proteins. vps45Δ yeast was transformed with cen plasmids containing the VPS45 gene of all five identified SCN mutations (N=1). (A) Western Blot showing Vps45 levels from all transformations. (B) Quantification of figure 12A to compensate for loading inaccuracies. Vps45 levels were normalised to the band of wildtype yeast transformed with a parent plasmid. Analysis completed using Image J. (C) Raw western blot data of CPY secretion of all the mutant SCN overexpression transformants. (D) Percentage H_2O_2 sensitivity in BY4742 yeast wildtype and vps45Δ strains transformed with SCN mutant VPS45 plasmids; quantified change in H_2O_2 sensitivity mean +/- SEM of technical repeats (N=1).*

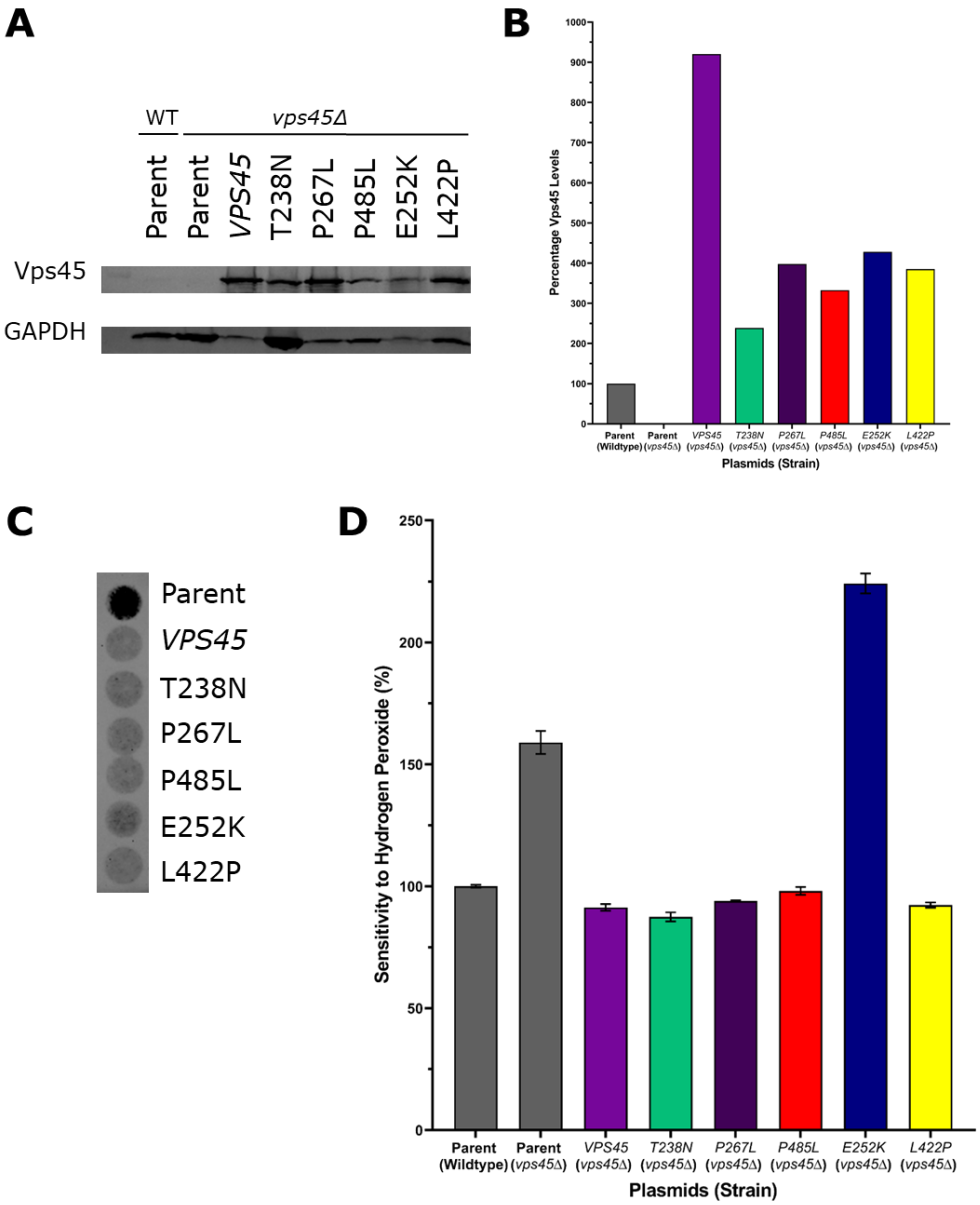

Figure 3.12 *- Dissecting the CPY and hydrogen peroxide sensitivity phenotypes of all SCN mutant Vps45 proteins. vps45Δ yeast was transformed with 2μ plasmids containing the VPS45 gene of all five identified SCN mutations. (N=1). (A) Western Blot showing Vps45 levels from all transformations. (B) Quantification of figure 12A to compensate for loading inaccuracies. Vps45 levels were normalised to the band of wildtype yeast transformed with a parent plasmid. Analysis completed using Image J. (C) Raw western blot data of CPY secretion of all the mutant SCN overexpression transformants. (D) Percentage H_2O_2 sensitivity in BY4742 yeast wildtype and vps45Δ strains transformed with SCN mutant VPS45 plasmids; quantified change in H_2O_2 sensitivity mean +/- SEM of technical repeats (N=1).*

3.4 Discussion

3.4.1 VPS45-T238N does not impair autophagy despite H_2O_2 sensitivity phenotype.

The relationship between autophagy and apoptosis is well researched but complicated and not particularly defined (Denton and Kumar, 2019). In this project we are investigating the role of Vps45 and SCN mutants in autophagy as it is thought that when autophagy is dysfunctional this can lead to apoptosis. A theory behind this is that the inability of the cell to traffic cargo from the TGN to the vacuole would lead to a 'backlog' and/or a reduction in retrograde transport from the endosome to the TGN and therefore, affecting trafficking to and from the ER. This leads to the belief that the dysfunction of Vps45 can induce apoptosis indirectly via ER stress (Stepensky *et al*., 2013). Through the introduction of tunicamycin the viability of Vps45 SCN mutants could be measured for ER stress response (Ishiwata-Kimata *et al*., 2022) though this was not within the scope of this thesis as our hypothesis involved investigating the SCN mutants' autophagy response.

The data shown demonstrates that *VPS45* mutant yeast can recover from induction of autophagy through nitrogen starvation as well as, if not better than, the wildtype yeast despite two of the three mutant yeast, *VPS45*-T238N and *VPS45*-P485L, having a sensitivity to H_2O_2 and therefore an increased susceptibility to apoptosis. The data shown in **Figure 3.7** supports this, as after inducing autophagy through nitrogen starvation *vps45Δ* has a severe phenotype. The phenotype is even more severe than the autophagy mutant control, after confirmation with the extra *atg1Δ* control I believe that this difference might be explained by the *vps45Δ* yeast being more susceptible to apoptosis than autophagy mutants and unable to recover from autophagy as well. This indicates that the role of Vps45 in autophagy is not intrinsic to the mechanism involving Vps45 in protection from apoptosis.

I believe that the peak in colonies at day 1 after reintroduction to rich media is due to the cells being grown to log phase and therefore cells that were close to replication undergo mitosis once out of SD-N media, which is seen in the SCN mutant yeast as well as the wildtype yeast. The *vps45Δ* yeast also did not

display the day 1 peak in recovery that all other strains displayed in one or more repeat, the large SEM and large difference in the *VPS45*-P267L mutant yeast AUC was largely due to a huge peak in recovery on day 1. In addition to this I observed that *vps45Δ* yeast also have a slower growth rate then the wildtype, taking longer to reach saturation in liquid media. This was not excluded from the quantification due to the mutant yeast also having this peak in growth and therefore we thought it was representative of the data. I also wanted to maintain the yeast strains being starved during log phase as I wanted to induce autophagy with the introduction of the SD-N media as opposed to cells already at saturation which induces changes in their metabolism (Leupold *et al*., 2019). Deletion of *VPS21,* a known effector of Vps45, shows the autophagosome outside of the vacuole from electron microscopy after starvation with nitrogen (Zhou *et al*., 2017), with *vps45Δ* displaying the same autophagosomal defect using GFP-Atg8 as a marker. The micrographs we collected reflect the phenotype that we hypothesised however the quantification analysis did not. I felt that the brightness of the puncta and the inability to determine a background baseline was skewing the quantification.

After adjusting the analysis parameters to represent distinct areas of the cytoplasm compared to vacuole instead of whole cytoplasm and whole vacuole (including puncta) it became clear that the variation from cell to cell included very low cytoplasmic GFP-Ape1 seen in wildtype and very high as seen in the *atg8Δ* but this did not incorporate the brightness of various or singular extremely bright puncta that appear to overlap the vacuolar membrane. Nor the skew that seemed a baseline level of GFP-Ape1 seemed to be at 50% in both cellular compartments. The random selection of the cytoplasm area of course, not only not fully random with human analysis but also does not account for the location of organelles other than the vacuole which we have stained for. In all the null mutants that have signal at the edge of the vacuole the clarity of whether this is inside or outside of the organelle is due to the brightness and scatter of the fluorophores (explained in **Figure 3.13**). 4D confocal analysis could be a good method of overcoming this as yeast are a good model to use due to the ease of staining whole organelles (Day *et al*., 2016). Or more simply taking multiple z-stacks instead of accounting for the cells total GFP immunofluorescence.

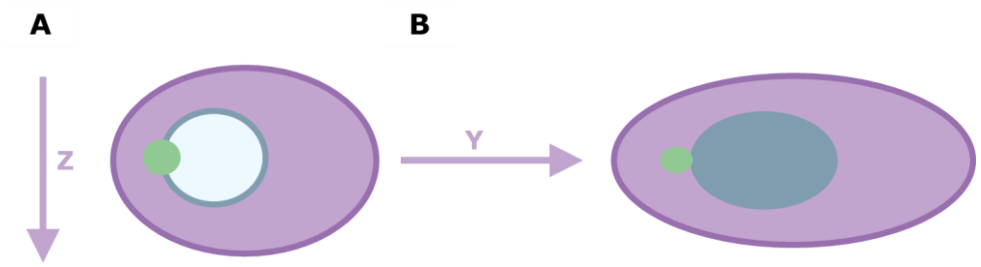

Figure 3.13 *– Graphic of the GFP-Ape1 in relation to the vacuole in yeast cells. (A) Graphic of the GFP-Ape1 puncta from above as we see through the microscope in* ***Figure 3.8*** *and* ***Figure 3.9.*** *(B) Theory of how we would see the GFP-Ape1 puncta were we to look at the yeast cells from the side from various z-stack images as opposed to from above.*

3.4.2 Location of SCN mutations in 3D Vps45 structure may determine effector binding power.

When mapped to the Vps45 3D structure three of the SCN mutations are found in the 'hinge' region of the protein (**Figure 3.1**). Physical interactions between these amino acids and their side chains could be altered with the introduction of an amino acid change in the sequence. Unpublished bioinformatic data from the Bryant lab described chemical changes of the *VPS45*-E252K mutation and how this could introduce chemical bonds effecting the action of the hinge region though the change of a negatively charged aspartic acid (E) to a positively charged lysine (K) molecule (Daniel Newsome, 2021). This data was supported by the data seen in **Figure 3.11** and **Figure 3.12**, as the E252K centromeric expression levels gave CPY and apoptotic phenotypes similar to that of the *vps45Δ* strain, but overexpression of E252K demonstrated a recovery of the CPY phenotype and maintained increased sensitivity to H_2O_2. So severe in fact, that any plasmid substitution of the 4 remaining *VPS45* mutated proteins shows no apoptotic phenotype. The *VPS45*-E238K mutation in humans has a syndromic effect, leading to developmental regression as well as causing SCN (Meerschaut *et al*., 2015). Whereas the *VPS45*-P253L (P267L in yeast) mutation which is not in the hinge region is described as a 'mild case' of SCN in the report describing the mutation (Newburger, 2018). This also means that we cannot confirm the nature of the *VPS45*-L422P H_2O_2 sensitivity assay through plasmid expression as we have seen this does not correspond to the phenotypes observed in the genetically *VPS45* mutated yeast. Though I would hypothesise that it would be

similar to the *VPS45*-P267L mutation due to the location of the amino acid change in the 3D structure and the presentation of the patients in clinic. The severity of the disease is unclear due to the patients presenting with recurrent oral infections (Alotaibi and Albarkheel, 2020) for example, the potential syndromic nature of the disease in these patients is not known.

My initial hypothesis that SCN mutations would lead to apoptosis due to perturbed autophagy was proven incorrect through the data described in this chapter The SCN causing mutations do not influence Vps45's ability to traffic CPY or recover from autophagy. Work in *C. elegans* has shown similar data showing complementation with SCN pathogenic Vps45 recovers the functionality of Vps45 loss in growth and endocytic function (Gengyo-Ando *et al*., 2024). Future bioinformatics work into this will need to investigate the localisation SCN mutations in Vps45's 3D structure to determine whether these mutations disrupt the localisation of Vps45 to target membranes or it's binding partners.

3.4.3 Vps45 is implicated in iron uptake, investigating the distinct roles of Vps45 in apoptosis versus autophagy.

Recently there has been an identified relationship between iron uptake, Vps45 and the mitochondria (Caza *et al*., 2018) amplifying importance of mitochondria in the regulation of apoptosis. This suggests that Vps45 may be involved in regulation of apoptosis through membrane traffic involving mitochondria as opposed to through the endosomal system in autophagy. Dysfunction in mitochondrial recycling through autophagy is thought to be a cause of transition from autophagy to apoptosis (Abeliovich and Klionsky, 2001) which was an influential factor in my original hypothesis that Vps45's role in autophagy was linked to a susceptibility to apoptosis. Neutrophils have few mitochondria and obtain their energy through glycolysis as opposed to oxidative phosphorylation (Borregaard and Herlin, 1982). The few mitochondria neutrophils have instead use their membrane potential in apoptotic signalling (Fossati *et al*., 2003) rather than for respiration, the importance of mitochondria in neutrophils and their short life span influenced the idea of neutrophils being highly susceptible to compromised Vps45 mediated mitochondrial traffic leading to premature cell death. Neutrophils also lack Bcl-2 (Iwai *et al*., 1994) which prevents the release of mitochondrial apoptotic factors such as cytochrome c (Kale *et al*., 2018). Yeast also lack the apoptotic factor Bcl-2 (Polĉic *et al.,* 2015) which makes it a

good model organism for understanding the increased sensitivity to apoptosis seen in patients' neutrophils. Multiple factors lead to the suggestion that neutrophils are more susceptible to the potential effects loss of Vps45 has on mitochondrial induced apoptosis.

The SCN patients described with *VPS45* mutations are unresponsive to granulocyte colony-stimulating factor (G-CSF) treatment (Stepensky *et al*., 2013) which ordinarily would promote the myeloid progenitor to produce more cells or to respond to infections (Mehta *et al*., 2015) via promoting the movement of the progenitor away from the bone marrow niche (King and Goodell, 2011). This naturally would occur via the increase in inflammatory cytokines during infection due to being part of the immune system the neutrophils' ability to process inflammatory cytokines correctly. In zebrafish Vps45 is required for transporting cargo required in progenitor cell differentiation (Mochizuki *et al*., 2018) suggesting that perhaps Vps45 could be required for differentiation of cells in the bone marrow niche with patients of Vps45 induced SCN displaying bone marrow fibrosis (Frey *et al*., 2021).

Autophagy is implicated in the pathogenesis of major neurodegenerative diseases, such as Alzheimer's (Nixon and Yang, 2012). A cause of this is thought to be that neurons are particularly vulnerable if there is an inability to clear lysosomal bodies from the cell (Nixon and Yang, 2012). Increased apoptosis seen in neutrophils in SCN is an obvious first point at patient contact. Although SCN presentation is clear in clinic the impairments seen in older SCN patients described by Meerschaut *et al*., who displayed developmental defects such as delayed neuromotor development (Meerschaut *et al*., 2015) could potentially be described by the multiple facets of the Vps45 protein.

3.5 Conclusions

Yeast lacking *VPS45* display multiple phenotypes in addition to missorting CPY, these include a temperature sensitive growth defect and increased sensitivity to high salt and oxidative stress (Piper *et al*., 1994). Here we show that two disease-causing mutants of *VPS45* seen in SCN display increased H_2O_2 sensitivity phenotypes despite the ability to sort CPY and recover from

autophagy induction. This suggests that the location of these residue changes inhibits Vps45's role in protection from apoptosis, and that this same location is not required for binding cognate partners required in CPY traffic or autophagy. The development of this data reveals the importance of the location of the residue changes in Vps45's protein functionality in protection from apoptosis.

4 Characterisation of phenotypes of Vps45 effectors.

4.1 Introduction

4.1.1 Identification of effectors of focus.

To assess the mechanism for Vps45 in apoptosis and how the SCN mutations play a role in the protein's dysfunction, I wanted to evaluate the role of Vps45 effectors in the 3 roles we identified for Vps45 in Chapter 3. Firstly, previous work from the Bryant lab identified two effectors of Vps45 that display an increased susceptibility to oxidative stress (**Figure 4.1**). This BioGRID and STRING analysis completed by Dimi Kioumourtzoglou identified Pep12 and Vac1 (Pep7) as physical interactors of Vps45 that also have oxidative stress sensitivity. In addition to the two proteins identified, I included Tlg2 as the cognate SNARE protein of Vps45 (Bryant and James, 2001) as well as Vps21 which binds to Vac1 aiding Vps45 and Pep12 in the docking of vesicles in endosomal traffic (Peterson *et al*., 1999).

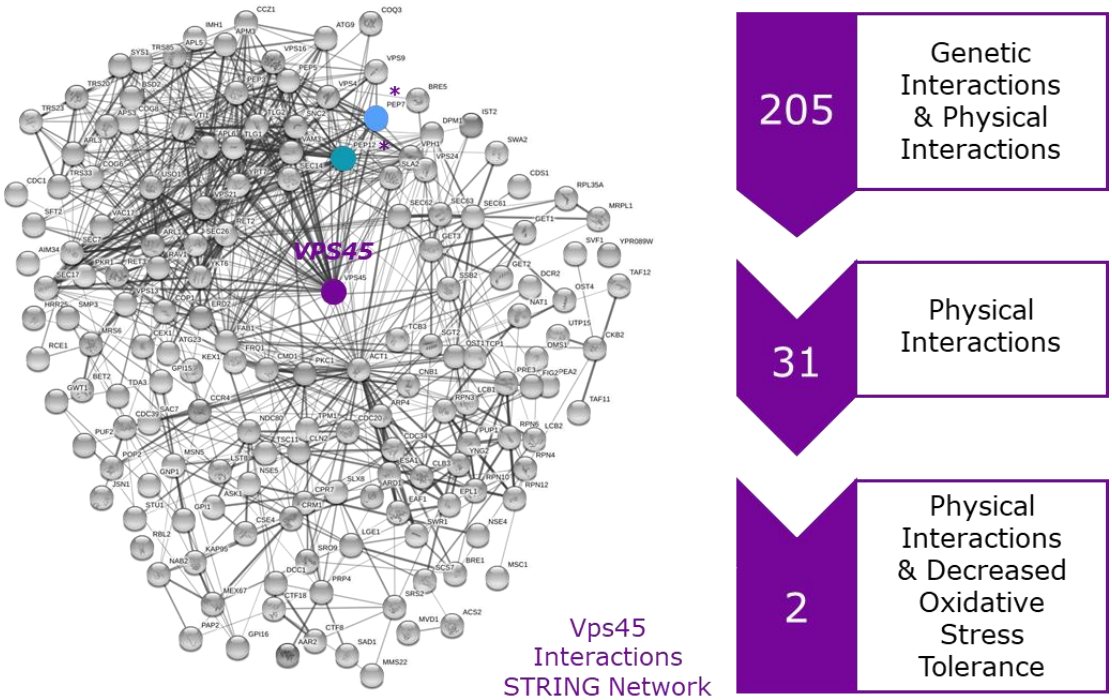

Figure 4.1 *- Dissection of Vps45 interactions Vps45's STRING network (STRING CONSORTIUM ©, 2024). 205 physical and genetic interactions documented (shown in STRING visualisation), 31 physical interactions of which 2 effectors had physical and decreased oxidative stress tolerance, PEP12 and PEP7 (VAC1)*

*are indicated by *. Adapted from Dr. Dimi Kioumourtzoglou and Dr. Katherine Paine's work from Dr.Paine's integrated masters project (2018) BioGRID (BioGRID, Biological General Repository for Interaction Datasets, TylersLab.com).*

4.1.2 Vps45 acts as an SM protein with cognate binding partner Tlg2

Central to Vps45's role in regulating vesicle fusion, is its interaction with Tlg2, the syntaxin requires Vps45 to form functional SNARE complexes. Through its role as an SM protein, Vps45 regulates SNARE complex formation through physical interactions with SNARE proteins (Misura *et al.*, 2000). Vps45 is involved in regulating SNARE complexes by binding of Tlg2 and Pep12 to aid formation of their cognate SNARE complexes and hence direct fusion of vesicles with organelles, allowing specificity of targeted vesicle contents (Bethani *et al*., 2007). One mechanism by which Vps45 aids SNARE complex formation is by holding t-SNARE Tlg2 in an open conformation (Eisemann *et al*., 2020) allowing Tlg2 to form a functional SNARE complex with v-SNARE Snc2 (Furgason *et al*., 2009). In mammalian cells Vps45 binds to syntaxin 16, the mammalian Tlg2 orthologue (Struthers *et al*., 2009) (**Figure 4.2A/B**), to allow for binding to v-SNARE VAMP4 (Kreykenbohm *et al*., 2002). Furthermore, Vps45 has two modes of interaction with Tlg2, one at the N-peptide of Tlg2 and the second after this section of the syntaxin, while the syntaxin is in a closed conformation (Burkhardt *et al*., 2008). Different modes of binding to syntaxins by Vps45 highlights the importance of different mutations in the protein that may disrupt one method of binding and not others (**Figure 4.3A/B**).

4.1.3 Pep12, Vac1 and Vps21 are involved in function of Vps45

In this chapter, I will characterise the phenotypes of functional effectors of Vps45 identified in section 4.1.1, in order to further understand their roles in Vps45 function. *VPS21*, *VPS45*, *VAC1* and *PEP12* are class D *vps* genes and therefore have larger vacuoles that do not fragment upon salt stress and have abnormal vacuolar inheritance (Weisman *et al*., 1990). They are located at the endosome and work independently from the class C core vacuole/endosome tethering (CORVET) complex (Peplowska *et al*., 2007). Activated GTPase Vps21 recruits the CORVET complex, Vac1, SNARE protein Pep12 and SM protein Vps45 for endocytosis. The CORVET complex is required for endosomal maturation and

is homologous to the vacuolar homotypic fusion and vacuole protein sorting (HOPS) complex (Shvarev *et al*., 2024) that aids endo-lysosomal vesicle fusion (Wagner *et al*., 2006). The CORVET complex localises to endosomes in the absence of Vac1 but not Vps21 (Cabrera *et al*., 2013). Vac1 physically binds to Vps21, signals from Vps21 aid Pep12 and Vps45 in docking of targeted Golgi-derived vesicles to the prevacuolar endosome (Peterson *et al*., 1999) (**Figure 4.3C**). Pep12 and Vps21 have been shown to co-localise to the pre-vacuolar compartment (Gerrard *et al*., 2000) with Pep12 being a t-SNARE protein that acts as an identifier for the late endosomal membrane (Pawelec *et al*., 2010).

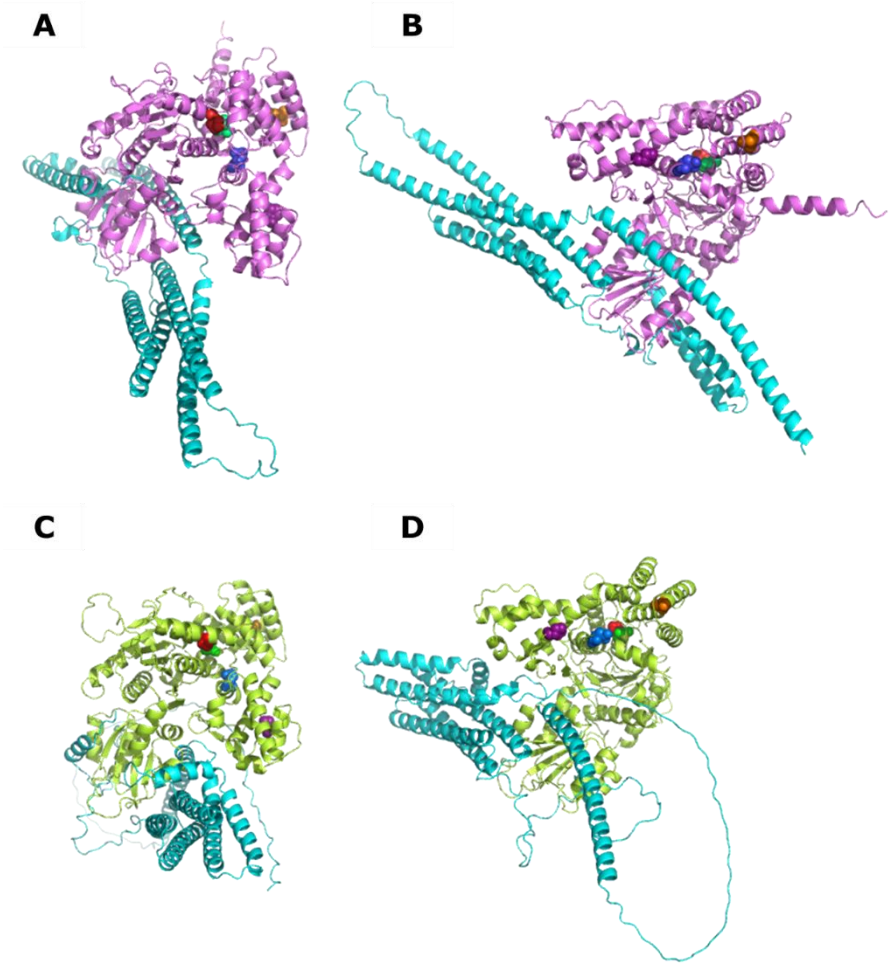

Figure 4.2 *- Binding of Vps45 and it's cognate syntaxin in Homo sapiens and Saccharomyces cerevisiae; (A+B) 3D PyMOL models of human Vps45 and Syntaxin 16 in two orientations and (C+D) showing yeast Vps45 and Tlg2 in two orientations, each image shows the five Vps45 SCN disease causing mutations and the amino acid position in the 3D model using PyMOL (PyMOL Molecular Graphics System, V 2.0, Schrödinger, LLC) FASTA sequences from UniProt were input into PyMOL and then aligned with the crystal structure of Vps45 bound to Tlg2 from C. thermophilum (Eisemann et al., 2020) using the RCSB Protein Data Bank, and database identifier 6XM1.*

Loss of Vps21 results in accumulation of vesicles, abnormal vacuolar morphology and missorting of vacuolar proteins (Horazdovsky *et al*., 1994). Rab GTPases are a large family of small GTPases that coordinate vesicular traffic through acting as switches for recruiting effector molecules (Stenmark, 2009). As a Rab GTPase, Vps21 aids vesicle trafficking and deletion of the Rab5 ortholog *YPT52* exacerbates *vps21Δ* phenotypes (Nickerson *et al*., 2012) indicating that other Rab5 proteins can compensate for the loss of Vps21. Through understanding the phenotypes of Vps21 this will suggest whether the protein is required for recruiting effectors in the pathways that involve Vps45.

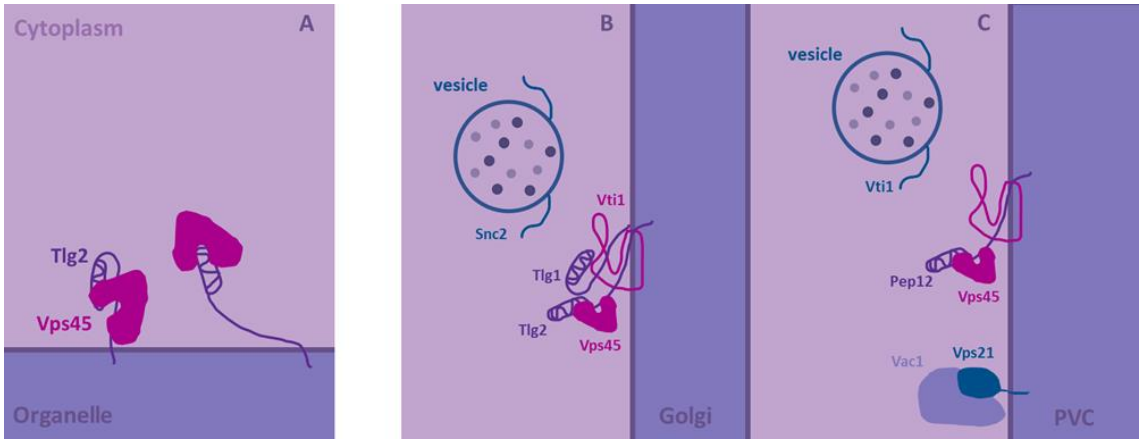

Figure 4.3 *- The binding modes of Vps45 and Tlg2 and the role of Vps45 and its effectors; (A) a cartoon depiction of the closed (left) and open (right) conformations of Tlg2 and the binding modes with Vps45. (B) At the late-Golgi membrane, Vps45 holds Tlg2 in an open conformation to aid SNARE complex binding with Vti1 and Tlg1. Endosome derived vesicles with v-SNARE Snc2 can fuse with the membrane. (C) At the pre-vacuolar compartment (PVC) or late endosome, Pep12 aids SNARE complex formation with Pep12 and Vti1. Activated Vps21 recruits Vac1 and Vps45 to the membrane.*

4.1.4 Vps45, Vps21, Vac1 and Pep12 act in autophagy

Under conditions of nutrient deprivation eukaryotic cells recycle non-essential components to promote cell survival. This process of macroautophagy is also triggered in response to cellular stresses (Anding and Baehrecke, 2017). Autophagosomes are double membraned vesicles containing material to be recycled and are indicators of autophagy. They are targeted to the vacuole where their contents are degraded to recycle constituent components (Kim and Klionsky, 2000). Vps45 interacts with Pep12 to traffic cellular material from the Golgi to the endosome (Burd *et al*., 1997) and *pep12Δ* cells displays an autophagic mutant phenotype described as an inability to traffic the vacuolar hydrolase aminopeptidase I (Ape1) to the vacuole under stress conditions (Chen

et al., 2014). Although, Pep12 is not required for Ape1 transport through the CVT pathway in normal conditions, Tlg2 and Vps45 are (Abeliovich *et al*., 1999). Vps45 is essential for the delivery of Ape1 to the vacuole through the CVT vesicle (Kirisako *et al*., 2000). The CVT pathway is considered to be a type of selective autophagy (Lynch-Day and Klionsky, 2010) in yeast. In addition, Pep12 also interacts with Vps21 at both the autophagosome and the early endosome, which further links these proteins to autophagic processes.

In *vps21Δ* cells autophagosomes accumulate outside of the vacuole when observed by electron microscopy. Vps21 recruits the factors in autophagy as well as at the early endosome (Chen *et al*., 2014). Non-specific autophagy is only partially blocked in the absence of Vps21, but specific autophagy is blocked (Chen *et al*., 2014), suggesting that Vps21 has multiple roles in autophagy and vesicle specificity. Vps21 is involved in the double membrane closure of the autophagosome in preparation for delivery to the vacuole (Zhou *et al*., 2017), and *pep12Δ*, *vac1Δ* and *vps45Δ* all also show an unclosed autophagosome phenotype, represented by a crescent-like Atg8 formation as opposed to a single puncta through fluorescent microscopy (Chen *et al*., 2014). Vps45's interactions with these effectors implicate that Vps45 has a significant role in autophagy, how they interact may influence selective as opposed to macroautophagy.

4.1.5 Vps45 effectors in Homo sapiens

In *Homo sapiens* Rabenosyn 5 (Vac1) and Vps45 are part of the endosomal recycling and Rab interactor (FERARI) complex which is involved in coordinating cargo through sorting endosomes which are required for the trafficking of proteins to determine whether they need to be recycled, secreted or degraded (Solinger *et al*., 2020). Rabenosyn 5 and Vps45 in human cells are effectors of the GTPase Rab5 (Vps21) on phodphatidylinositol-3-phosphate (PI3P)-positive endosomes (Nielsen *et al*., 2000). PI3K, a lipid kinase, is associated with endosomal membranes and the autophagosome preassembly machinery (Nascimbeni *et al*., 2017). Loss of Vps45 in humans leads to a reduction of β1-integrin recycling, as does loss of Rabenosyn 5 (Rahajeng *et al*., 2010). Loss of Vps45 leads to reduced Rabenosyn 5 and Syntaxin 16 (Tlg2) levels. Golgi condensation implicates Rabenosyn 5 and Vps45 are involved in bi-directional transport required for Golgi to early endosome recycling (Scheidel *et al*., 2018).

Vps45 is a highly conserved protein and interactions with the yeast effector homologs provides evidence that the roles of Vps45 and its corresponding effectors are crucial in trafficking throughout species.

4.2 Aims and Hypothesis

4.2.1 Aims for Chapter 4

In Chapter 3, I discussed data that indicates that the role of Vps45 in apoptosis that is associated with neutropenia in SCN patients is through a mechanism that is functionally distinct from endosomal trafficking and autophagy. The aims of this chapter are to use the previously described assays to identify any potential regulatory factors that collaborate with Vps45 in this novel role of protecting cells from apoptosis. For these studies previous bioinformatic data established effector proteins of Vps45 that are susceptible to oxidative stress. Pep12 and Vac1 are functionally involved with Vps21 identifying it as a third candidate to study. In addition, Vps45's binding partner Tlg2 was included as the fourth protein in these studies.

4.2.2 Objectives

My objectives in this chapter were to use the three assays described in Chapter 3, the CPY secretion assay (trafficking), H_2O_2 sensitivity assay (sensitivity to oxidative stress) and the recovery from nitrogen starvation assay (macroautophagy) to establish if Vps45 effector proteins regulate Vps45 function in these distinct roles. I considered whether deletion of effector genes would phenocopy mutations of *VPS45,* but also whether overexpression of any of these effectors in *vps45Δ* could recover the cellular phenotypes observed previously.

4.2.3 Hypothesis

I hypothesise that some Vps45 regulators will be involved in only certain functional roles. By assessing the consequences of deleting and overexpressing Vps45 effectors using different functional assays I hope to identify new factors that have a role in with Vps45 in protection from apoptosis.

4.3 Results

4.3.1 Vps45 effectors are defective in CPY trafficking.

Previously, it has been detailed that *tlg2Δ* yeast strains secrete approximately 20% of its total CPY (Abeliovich *et al*., 1998). In our quantification of the CPY secretion assay we see that the *tlg2Δ* strain secrete ~100% more CPY than wildtype and though this is not statistically significant (**Figure 4.4**) the difference in secretion is observable in the raw data (**Figure 3.5**). The remaining effector mutant yeast (*pep12Δ*, *vac1Δ* and *vps21Δ*) all have statistically significant increases in their CPY secretion (**Figure 4.4**). This is indicative of the nature of these proteins due to their role in the endosomal system.

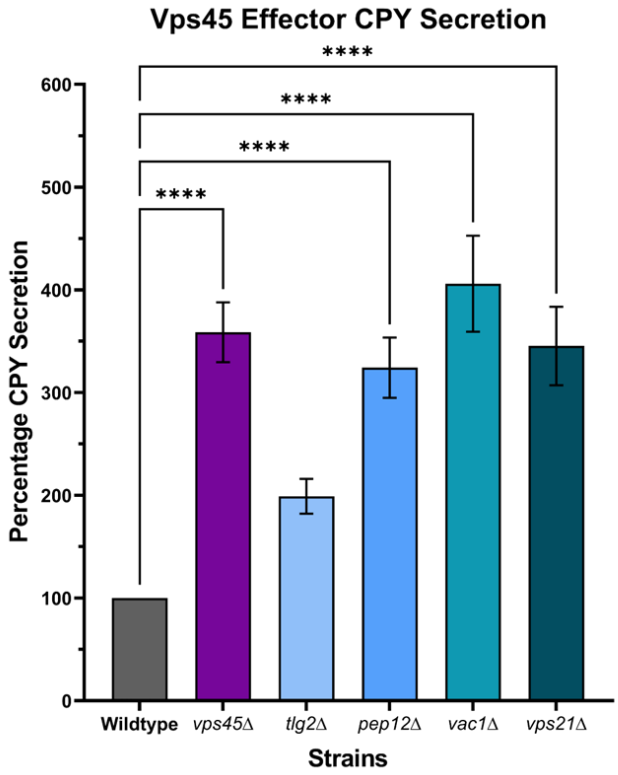

Figure 4.4 *- CPY secretion in the in the Vps45 effector mutant yeast; Quantification of the CPY secretion assay shows mean +/-SEM of CPY secretion (N=4). vps45Δ, pep12Δ, vac1Δ and vps21Δ yeast have a statistically significant increase in CPY secretion (P<0.0001(****)) by one-way ANOVA.*

4.3.2 pep12Δ and vac1Δ are sensitive to hydrogen peroxide.

In Chapter 3 we investigated *vps45Δ* and the *VPS45* SCN related mutants to understand the effect of these mutations on apoptosis in patients. Therefore,

we next investigated the H_2O_2 sensitivity of the effectors known to interact with Vps45. Here, we show that *pep12Δ* and *vac1Δ* have a statistically significant increased sensitivity to H_2O_2 (**Figure 4.5**). Although increased in *tlg2Δ* strain this is not significant as seen with the CPY assay. The *vps21Δ* strain had no increase in H_2O_2 sensitivity in comparison to the wildtype strain, despite large scale studies indicating an increased susceptibility to oxidative stress we did not observe this here (Brown *et al.*, 2006). Though of note, the previous studies were carried out at 3 mM H_2O_2 and our experimental data points (0%, 1%, 2% and 5% H_2O_2) equate to approximately 0 mM, 0.3 mM, 0.5 mM and 1.5 mM respectively.

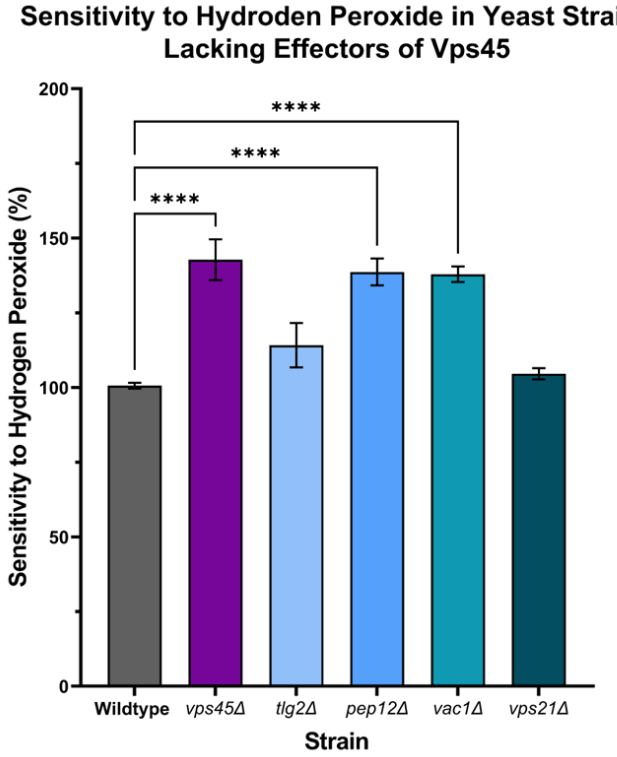

Figure 4.5 *- Percentage change in hydrogen peroxide sensitivity in the Vps45 effector mutant strains; Quantification of the hydrogen peroxide sensitivity assay shows mean +/-SEM (N=3). vps45Δ, pep12Δ and vac1Δ yeast has a statistically significant increase in hydrogen peroxide sensitivity (P<0.0001(****)) by one-way ANOVA.*

4.3.3 Only vps21Δ can recover after autophagy induction by nitrogen starvation.

The data indicates that of the strains tested, only *vps21Δ* demonstrates a robust recovery after nitrogen starvation. Conversely, the remaining strains (*vps45Δ*, *tlg2Δ*, *pep12Δ* and *vac1Δ*) display significantly lower area under the curve

compared to the wildtype strain (**Figure 4.6**). In addition, the AUC values of the strains do not fall into the confidence intervals of the *atg8Δ* strain (orange dotted line), indicating an even more severe phenotype than the autophagy control. All four strains had almost no recovery after day 4 of the assay in comparison to wildtype and *vps21Δ* which both had close to 80% recovery at day 5.

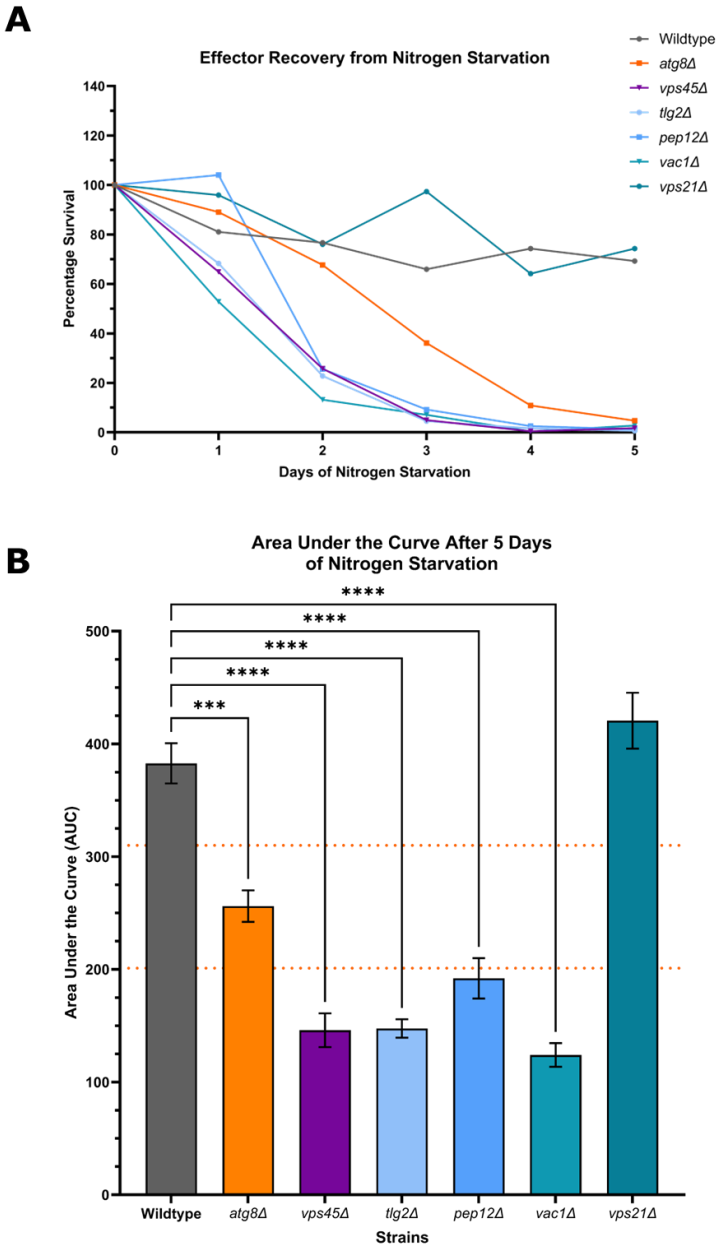

Figure 4.6 *– Effectors after autophagy induction by nitrogen starvation; (A) Vps45 and its effectors do not recover after nitrogen starvation. Colonies of yeast were counted after yeast strains were exposed to nitrogen starvation for 5 days. The number of colonies is recorded as a percentage of the number of colonies that formed after no nitrogen starvation on day 0. The assay was*

repeated four times and displays the mean of these repeats. (B) Area under the curve after 5 days of nitrogen starvation for the effector mutant yeast; Bar chart displaying the mean and +/-SEM of the four areas under the curve calculated from four repeats. One-way ANOVA was calculated to determine the statistical significance between atg8Δ and the other yeast strains. (P>0.05 (ns), P< 0.05 (*) P<0.01 (**), P<0.0001 (****) N=3. Orange dotted lines represent the 95% confidence limits for atg8Δ yeast.

4.3.4 Overexpression of TLG2 and VPS21 increases CPY secretion in wildtype yeast.

In order to test the efficacy of the plasmids and to have an understanding of how overexpression of these proteins affected the wildtype strains I transformed the BY4742 wildtype strain with plasmids containing each of the 5 genes (*VPS45*, *TLG2*, *PEP12*, *VAC1* and *VPS21*) and then a parental plasmid with no gene just the *URA3* auxotroph (**Figure 4.7A**). Interestingly, overexpression of *TLG2* and *VPS21* increased the CPY secretion of these wildtype cells. Although not conducted in the same experiment *TLG2* overexpression appeared to be at the higher levels than the *tlg2Δ* CPY secretion (**Figure 4.4**). The overexpression of *VPS21* also increased the CPY secretion of the wildtype cells. The increase in CPY secretion observed in wildtype cells when *TLG2* and *VPS21* were overexpressed was taken into consideration when analysing the CPY secretion of the effector null mutants overexpressing *TLG2* and *VPS21*.

4.3.5 CPY secretion phenotype and hydrogen peroxide sensitivity cannot be recovered by overexpression of effectors of Vps45.

Building on our previous observations I measured CPY secretion and H_2O_2 sensitivity in *vps45Δ* yeast transformed with Vps45 effectors (*TLG2*, *PEP12*, *VAC1* and *VPS21*). When *TLG2*, *VAC1* and *VPS21* were overexpressed CPY secretion was statistically significantly different from the wildtype with parent plasmid (**Figure 4.8A**). Though all statistically significantly different *TLG2* and *PEP12* overexpression partially recovered the CPY secretion phenotype (*PEP12* had P=0.08, one-way ANOVA). The overexpression of both of these had no effect on statistical significance in one-way ANOVA compared to the *vps45Δ* with parent plasmid either. The *vps45Δ* with parent plasmid was only statistically significantly different from wildtype with parent plasmid and *vps45Δ* with *VPS45* plasmid.

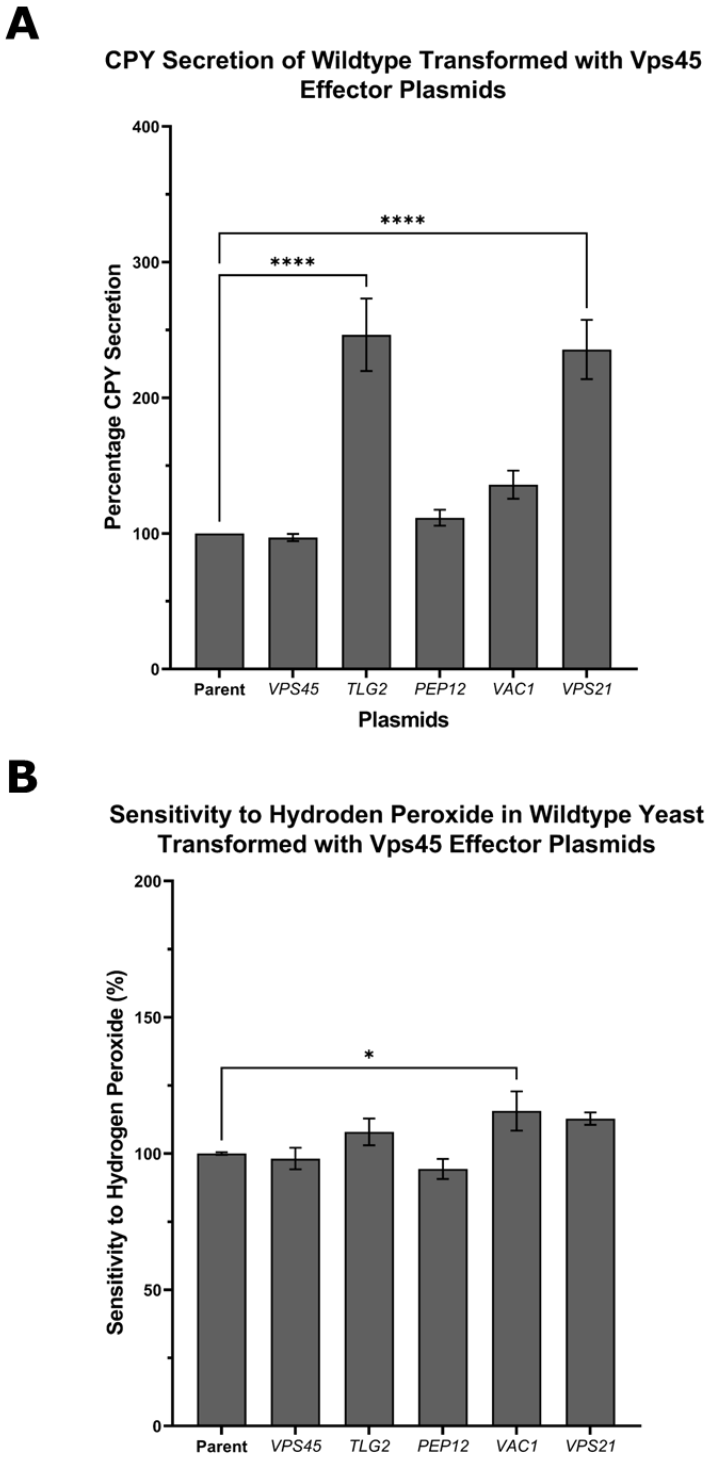

Figure 4.7 *- CPY secretion and H_2O_2 Sensitivity of Wildtype yeast transformed with effectors of Vps45; Quantification of CPY and H_2O_2 assays normalised to BY4742 Wildtype yeast transformed with parent plasmid with no gene. (A) CPY secretion: Quantification of the CPY secretion assay shows mean +/-SEM of CPY secretion (N=18). (P<0.0001(****)) by one-way ANOVA. (B) Percentage change in H_2O_2 sensitivity; Quantification of the hydrogen peroxide sensitivity assay shows mean +/-SEM (N=6). (P<0.05(*)) by one-way ANOVA.*

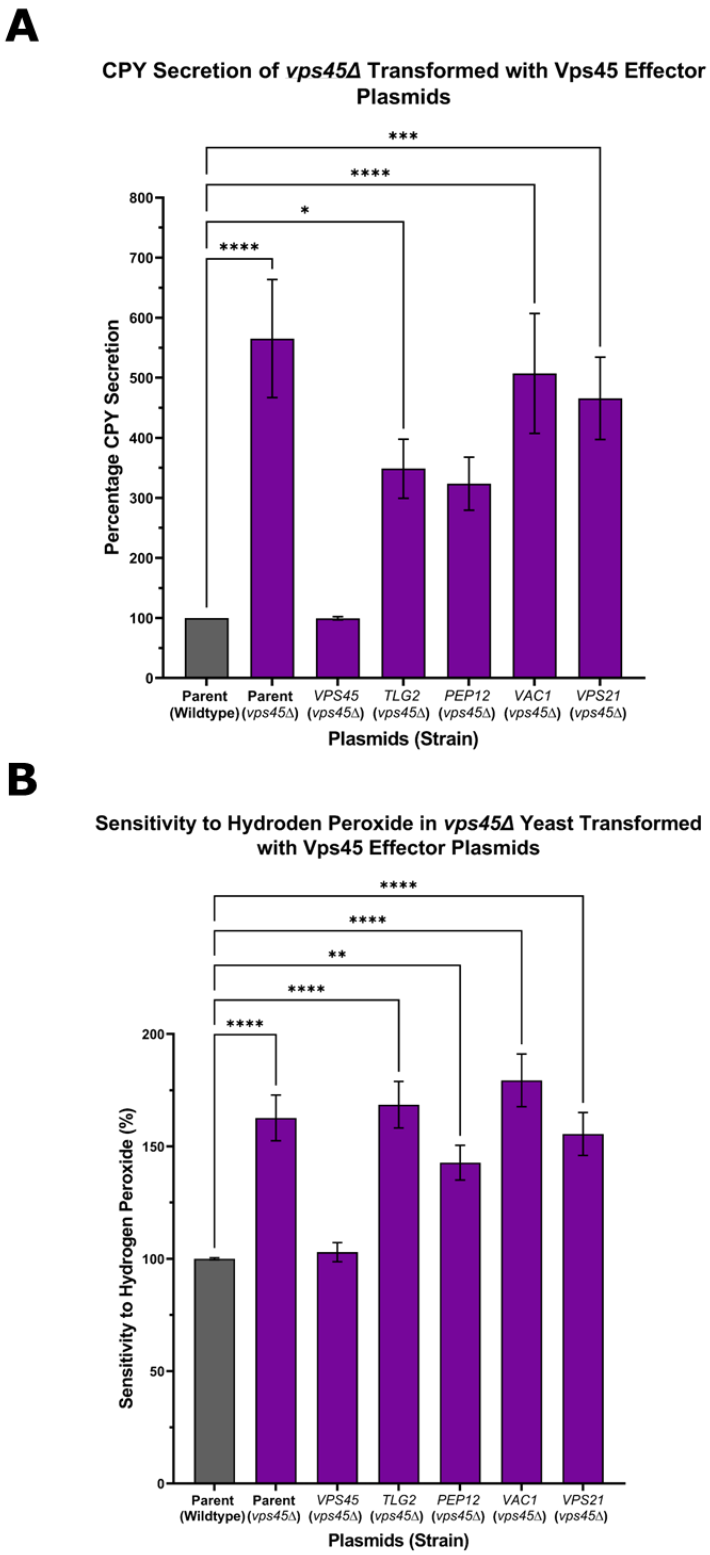

Figure 4.8 - *CPY secretion and H_2O_2 Sensitivity of vps45Δ yeast transformed with effectors of Vps45; Quantification of CPY and H_2O_2 assays normalised to BY4742 Wildtype yeast transformed with parent plasmid with no gene. (A) CPY secretion: Quantification of the CPY secretion assay shows mean +/-SEM of CPY secretion (N=17). (P<0.05(*), P<0.001(***)P<0.0001(****)) by one-way ANOVA. (B) Percentage change in H_2O_2 sensitivity; Quantification of the*

hydrogen peroxide sensitivity assay shows mean +/-SEM (N=6). (P<0.01(**),P<0.0001(****)) by one-way ANOVA.

In the H_2O_2 sensitivity data (**Figure 4.8B**), we observed similar results to the CPY secretion quantification. All *vps45Δ* transformed with overexpression effector plasmids were statistically significant from wildtype except *VPS45*, this shows that only the overexpression of *VPS45* has a complete rescue effect on the H_2O_2 sensitivity phenotype seen in *vps45Δ* yeast. No recovery by the Vps45 effector plasmids was observed, and this was reflected in the statistically significance of the one-way ANOVA completed comparing the *vps45Δ* with parent plasmid to the other transformants. Indicating that the severity of the Vps45 apoptotic phenotype cannot be recovered by overexpression of any of the effectors here.

4.3.6 Overexpression of PEP12 increases sensitivity to hydrogen peroxide in tlg2Δ yeast.

I then completed the same assays but using the Vps45 effector null strains transformed with Vps45 effector high copy plasmids to see whether any CPY secretion of H_2O_2 sensitivity phenotypes could be recovered by the overexpression of these Vps45 effectors. Previously, I have demonstrated that the *tlg2Δ* had a small non-significant CPY secretion phenotype (**Figure 4.4**). However, when transformed with any plasmid this phenotype was lost apart from the *TLG2* and *VPS21* overexpression plasmids (**Figure 4.9A**). This is consistent with the wildtype data in **Figure 4.7**, when the overexpression of *TLG2* and *VPS21* introduce a small CPY secretion phenotype.

In the *tlg2Δ* H_2O_2 sensitivity data we observed that only *PEP12* overexpression affected the sensitivity (**Figure 4.9B**). When the *tlg2Δ* strain was transformed with *PEP12* overexpression plasmid this was statistically significantly different from the wildtype parent and from the *tlg2Δ* with parent plasmid (P=**, one-way ANOVA).

4.3.7 pep12Δ hydrogen peroxide phenotype cannot be recovered by overexpression of Vps45 effector plasmids.

Building on our previous observation that CPY secretion in *pep12Δ* strains is elevated compared to wildtype (**Figure 4.4**), we next evaluated whether

overexpression Vps45 effector plasmids could rescue both the CPY secretion and H_2O_2 phenotypes observed in *pep12Δ* cells. When *pep12Δ* cells were transformed with Vps45 effector plasmids, CPY secretion became similar to wildtype — except for the transformant overexpressing *TLG2* (**Figure 4.10A**). Though none of these transformants were statistically significant from the *pep12Δ* with the parent plasmid, indicating that there was no significant recovery from the CPY secretion phenotype.

The H_2O_2 sensitivity phenotype of the *pep12Δ* transformed with the Vps45 effector plasmids showed no recovery of this sensitivity phenotype by the over expression plasmids (**Figure 4.10B**). Though on *TLG2* and *VAC1* overexpression was statistically significantly different from the wildtype data all four transformants showed similar percentage increases of H_2O_2 sensitivity in comparison to wildtype with parent plasmid. The *pep12Δ* with parent plasmid was statistically significantly different from the *pep12Δ* with *PEP12* transformant (P=**, one-way ANOVA) indicating that only overexpression of the protein lost could recover the H_2O_2 sensitivity phenotype observed by the *pep12Δ* strain.

4.3.8 TLG2 plasmid recovers vac1Δ CPY secretion phenotype.

CPY secretion of the *vac1Δ* strain is quantified in **Figure 4.4**, when transformed with the Vps45 effector plasmids *vac1Δ* had some recovery of this phenotype by overexpression of *VPS45* and *VPS21*, though not statistically significant from wildtype with parent plasmid (**Figure 4.11A**). *TLG2* overexpression in the *vac1Δ* almost fully recovers the *vac1Δ* CPY secretion phenotype.

The H_2O_2 sensitivity phenotype of the *vac1Δ* strain transformed with the Vps45 effector plasmids showed no recovery of this sensitivity phenotype by the over expression plasmids (**Figure 4.11B**). Here we see that the *vac1Δ* transformed with *VAC1* has a reduction in the sensitivity to H_2O_2 similar to wildtype with parent plasmid. However, the variance of the 3 repeats means that the one-way ANOVA cannot determine significance. In this instance time permitting at least two more sets of the assay would have been completed.

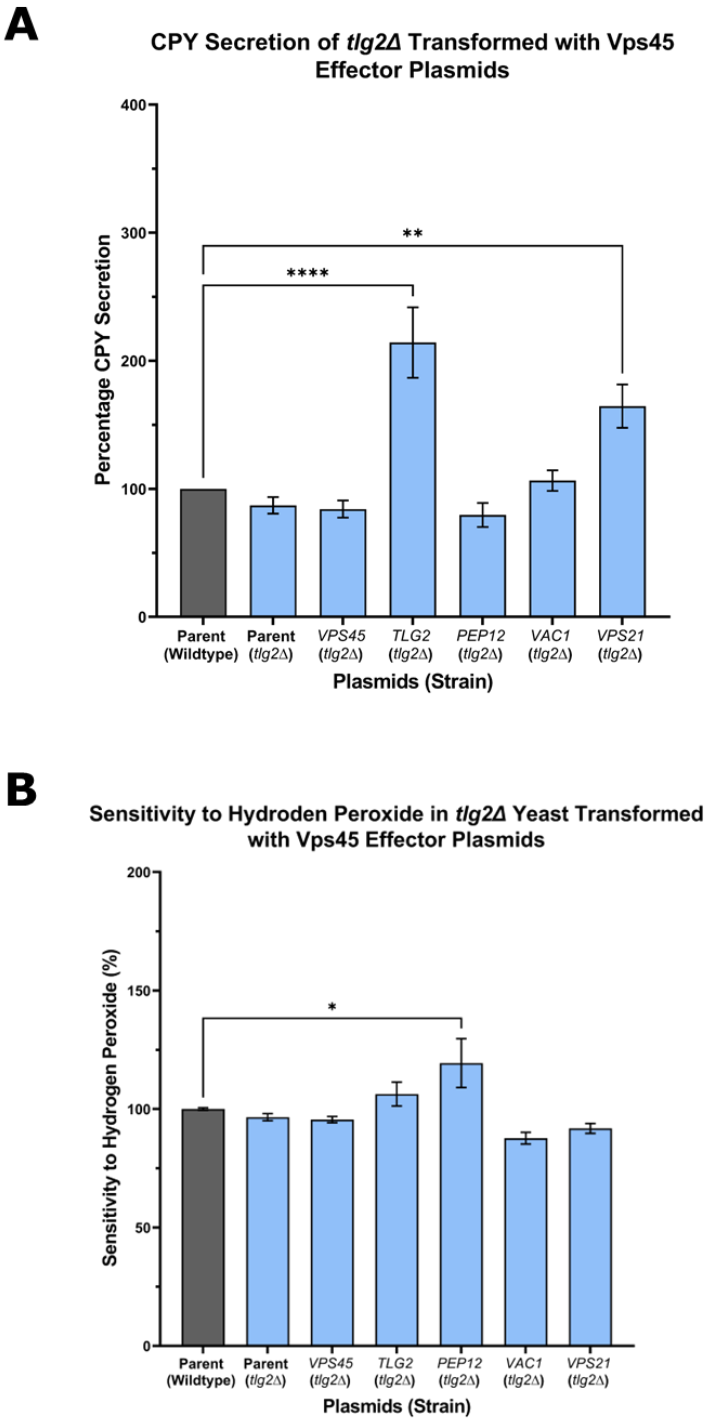

Figure 4.9 - *CPY secretion and H_2O_2 Sensitivity of tlg2Δ yeast transformed with effectors of Vps45; Quantification of CPY and H_2O_2 assays normalised to BY4742 Wildtype yeast transformed with parent plasmid with no gene. (A) CPY secretion: Quantification of the CPY secretion assay shows mean +/-SEM of CPY secretion (N=4). (P<0.01(**),P<0.0001(****)) by one-way ANOVA. (B) Percentage change in H_2O_2 sensitivity; Quantification of the hydrogen peroxide sensitivity assay shows mean +/-SEM (N=4). (P<0.05(*)) by one-way ANOVA.*

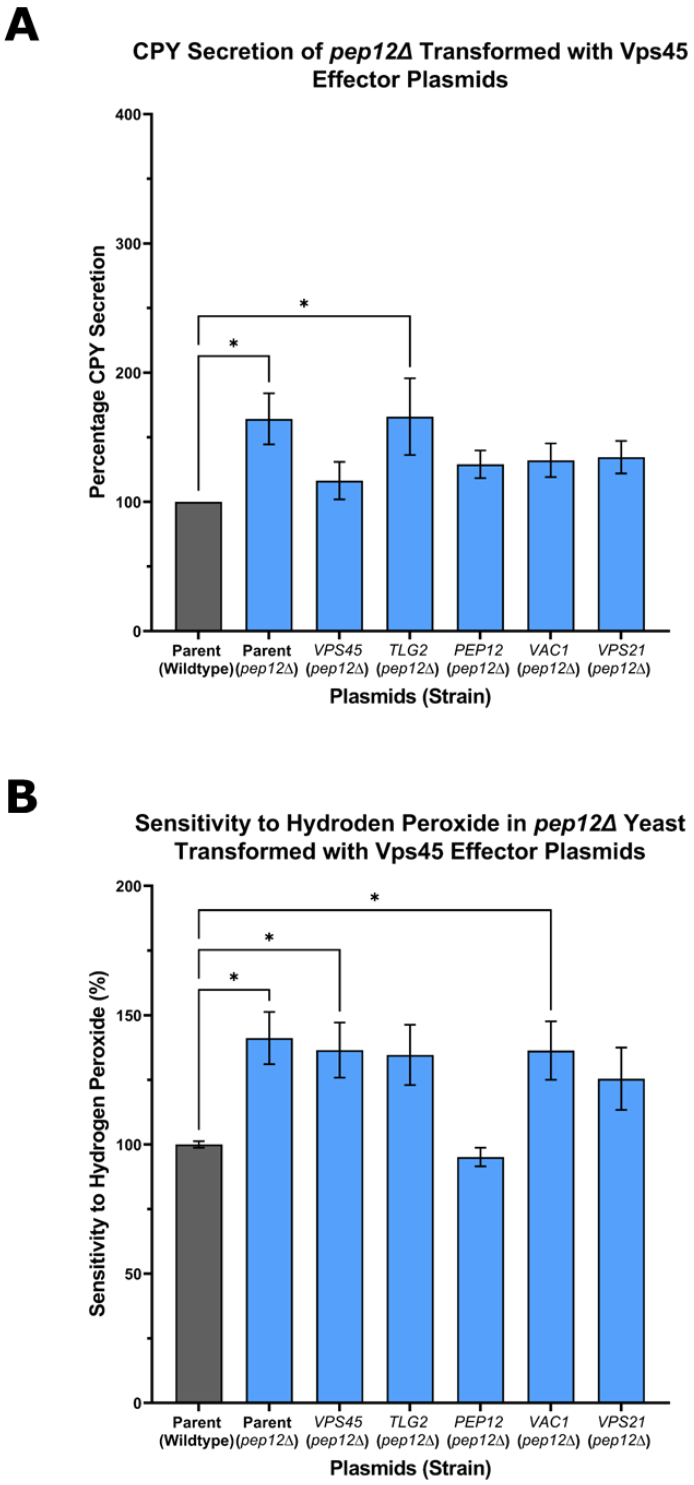

Figure 4.10 - *CPY secretion and H_2O_2 Sensitivity of pep12Δ yeast transformed with effectors of Vps45; Quantification of CPY and H_2O_2 assays normalised to BY4742 Wildtype yeast transformed with parent plasmid with no gene. (A) CPY secretion: Quantification of the CPY secretion assay shows mean +/-SEM of CPY secretion (N=9). (P<0.05(*)) by one-way ANOVA. (B) Percentage change in H_2O_2 sensitivity; Quantification of the hydrogen peroxide sensitivity assay shows mean +/-SEM (N=3). (P<0.05(*)) by one-way ANOVA.*

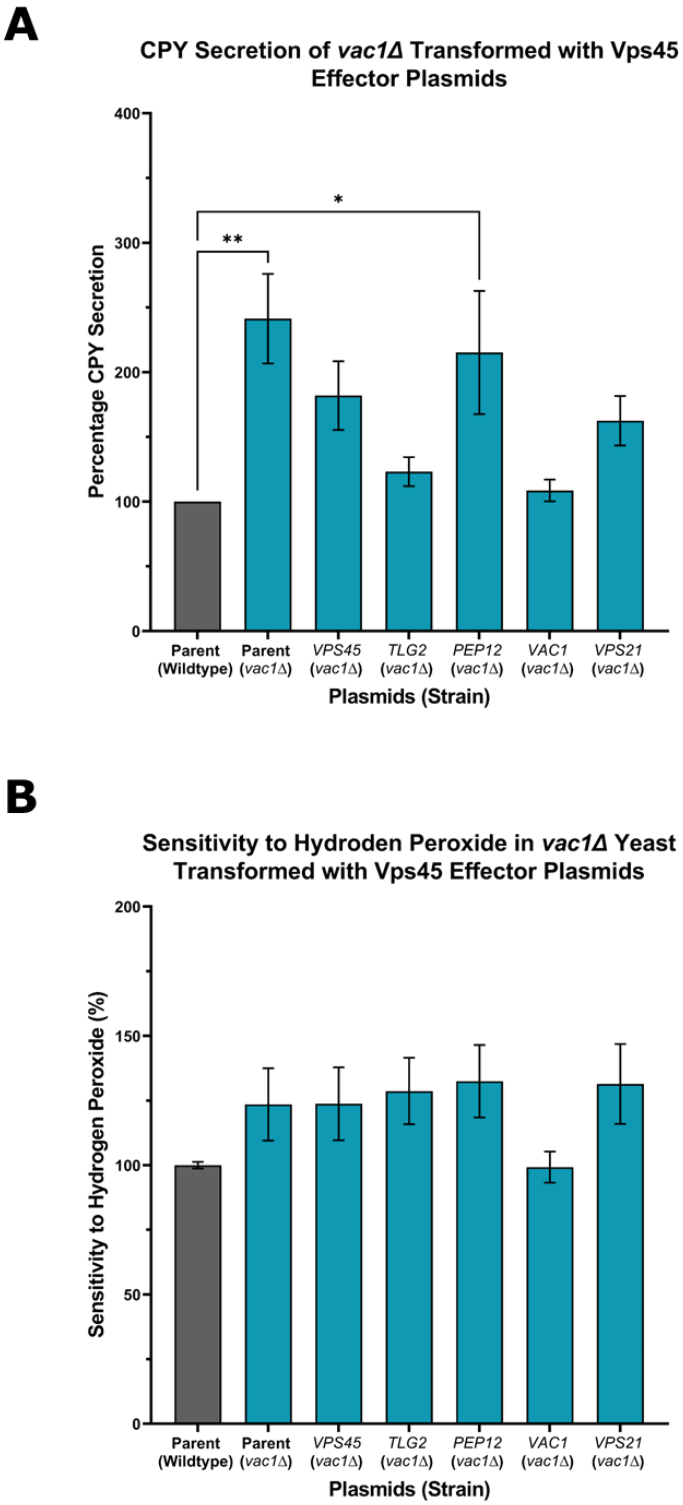

Figure 4.11 - *CPY secretion and H_2O_2 Sensitivity of vac1Δ yeast transformed with effectors of Vps45; Quantification of CPY and H_2O_2 assays normalised to BY4742 Wildtype yeast transformed with parent plasmid with no gene. (A) CPY secretion: Quantification of the CPY secretion assay shows mean +/-SEM of CPY secretion (N=8). (P<0.05(*), P<0.01(**)) by one-way ANOVA. (B) Percentage change in H_2O_2 sensitivity; Quantification of the hydrogen peroxide sensitivity assay shows mean +/-SEM (N=3) one-way ANOVA.*

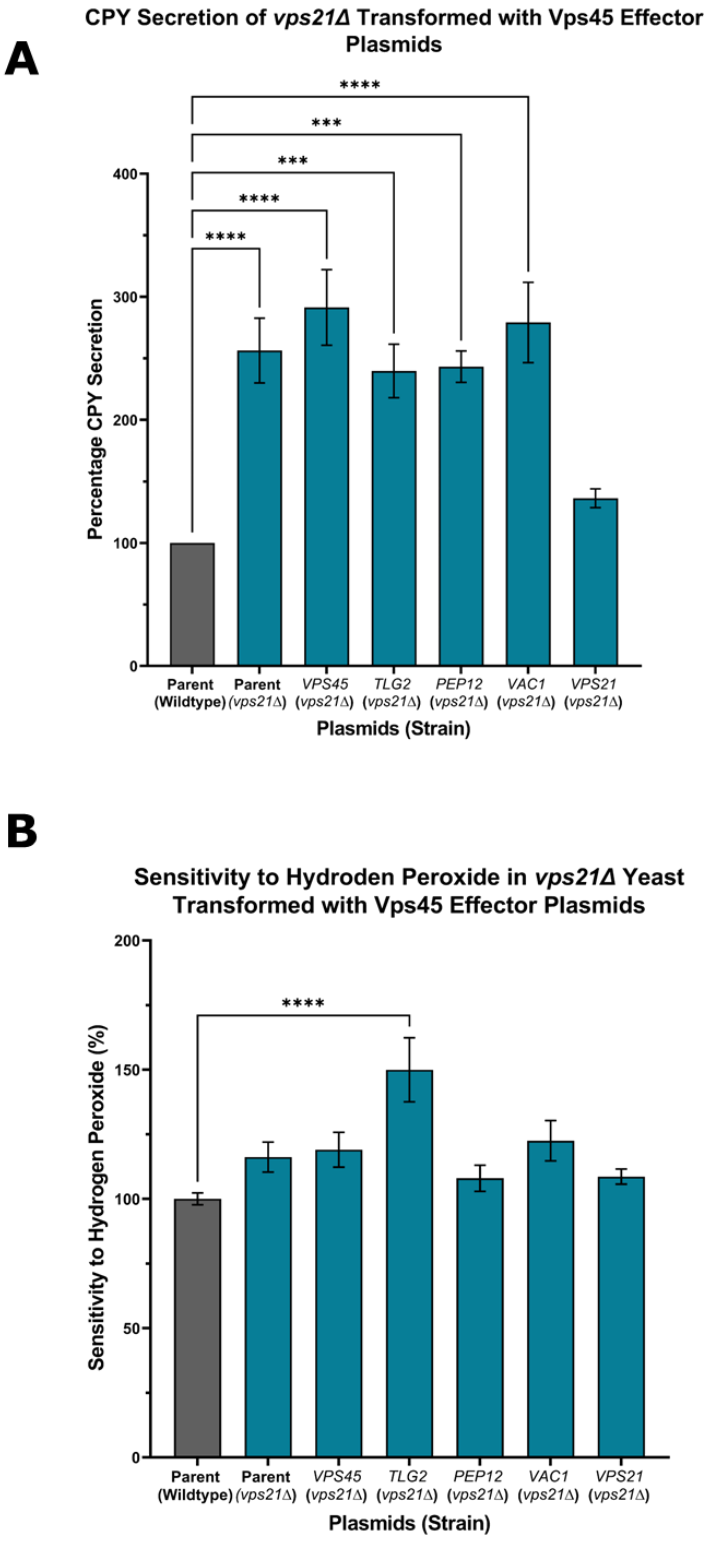

Figure 4.12 - *CPY secretion and H_2O_2 Sensitivity of vps21Δ yeast transformed with effectors of Vps45; Quantification of CPY and H_2O_2 assays normalised to BY4742 Wildtype yeast transformed with parent plasmid with no gene. (A) CPY secretion: Quantification of the CPY secretion assay shows mean +/-SEM of CPY secretion (N=12). (P<0.001(***), P<0.0001(****)) by one-way ANOVA. (B) Percentage change in H_2O_2 sensitivity; Quantification of the hydrogen peroxide*

sensitivity assay shows mean +/-SEM (N=3). (P<0.0001(****)) by one-way ANOVA.

4.3.9 TLG2 overexpression increases vps21Δ yeasts susceptibility to hydrogen peroxide.

vps21Δ yeast display a severe CPY phenotype (**Figure 4.4**). Overexpression of the Vps45 effectors had no effect on the CPY secretion phenotype with all transformants being statistically significantly different from wildtype with a parent plasmid (**Figure 4.12A**). Interestingly, overexpression of *TLG2* in *vps21Δ* introduces an H_2O_2 sensitivity phenotype not observed when the strain is transformed with the parent plasmid (**Figure 4.12B**). This suggest that Vps21's direct or indirect interaction with an effector of Tlg2 helps protect from apoptosis, and when overexpressed Tlg2 prevents this process from functioning as normal.

4.3.10 VPS45 overexpression does not correct effector recovery after autophagy induction phenotypes.

As with the CPY secretion assay and the H_2O_2 sensitivity assay I wanted to assess whether the overexpression of *VPS45* could recover the recovery from autophagy phenotype observed in *tlg2Δ*, *pep12Δ* and *vac1Δ* strains as seen in **Figure 4.6**. The assay was conducted over five days as before and one-way ANOVA used to determine the statistical significance of the recovery from nitrogen starvation area under the curve in comparison to wildtype transformed with *VPS45* (**Figure 4.13**). Here we saw that none of the strains with reduced area under the curve after nitrogen starvation was recovered by the *VPS45* overexpression plasmid, aside from the *vps45Δ*. Overexpression of *VPS45* in *vps21Δ* yeast had no effect on the recovery from nitrogen starvation which is slightly higher than the wildtype both with and without the *VPS45* plasmid.

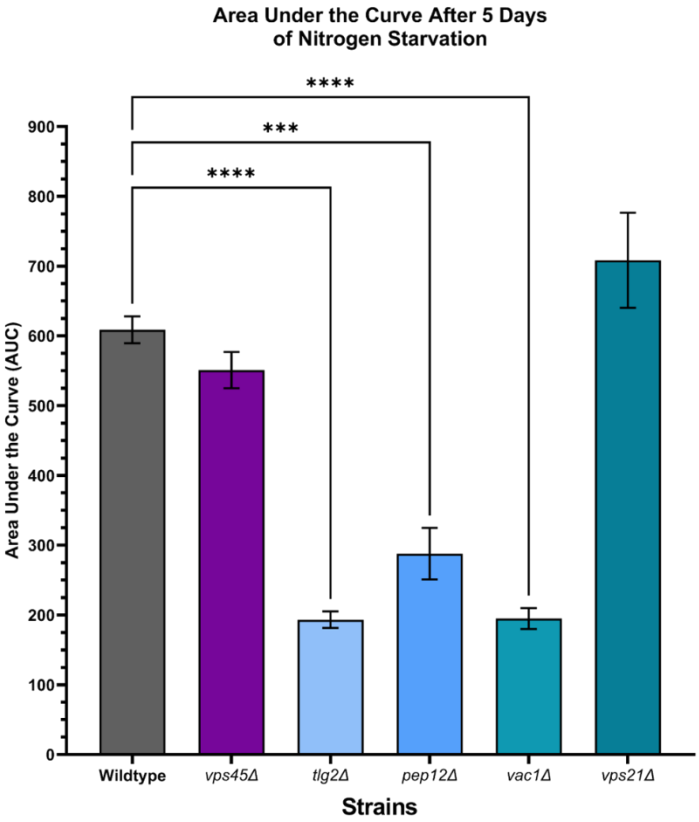

Figure 4.13 - *Overexpression of VPS45 plasmid cannot recover defects in autophagy in Vps45 effector null yeast; Recovery from nitrogen starvation assay; wildtype and mutant Vps45 effector yeast when transformed with VPS45 overexpression plasmids; all replicates were normalised to make them comparable to the wildtype with VPS45 plasmid which was observed in biological replicates in parallel with the data shown. One-way ANOVA assessed statistical significance of the data collected (P<0.001(***) and P<0.0001 (****)) mean +/- SEM (N=3) See* ***Figure 3.7*** *for reference to vps45Δ phenotype.*

4.3.11 Overexpression of effectors cannot recover vps45Δ recovery from autophagy phenotype.

Similarly to the CPY secretion and H_2O_2 sensitivity assays I was interested to see whether overexpression of any Vps45 effector proteins had an effect on the *vps45Δ* strains ability to recover from nitrogen starvation (**Figure 4.14**). Only the *VPS45* plasmid was able to recover the *vps45Δ*'s inability to recover after nitrogen starvation.

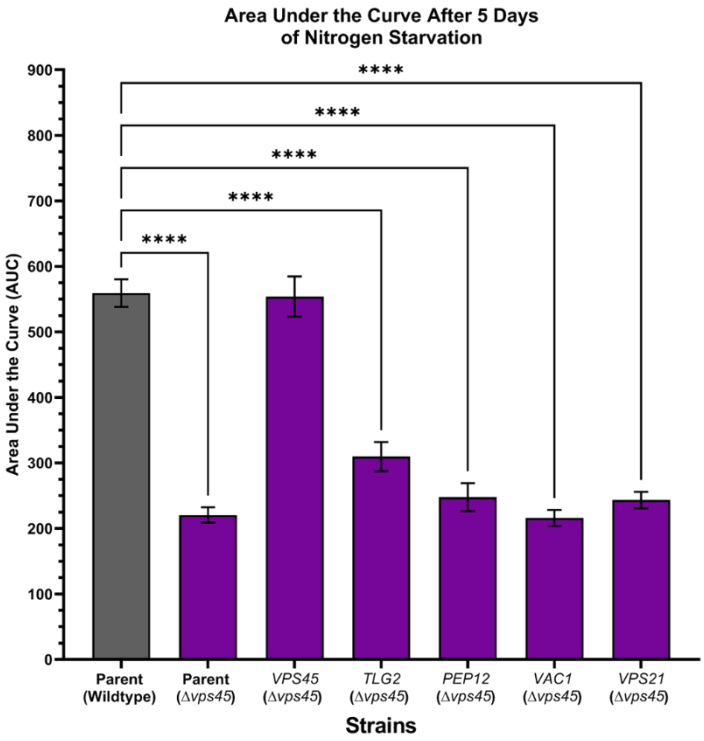

Figure 4.14 *- Overexpression of Vps45 effectors cannot recover defects in autophagy in vps45Δ recovery from nitrogen starvation assay; wildtype and mutant Vps45 effector yeast when transformed with overexpression plasmids; BY4742 yeast strains were transformed with 2μ plasmids containing effectors of Vps45. The parent plasmid with no gene, VPS45, TLG2, PEP12, VAC1 and VPS21. All replicates were normalised to make them comparable to the wildtype with parent plasmid which was observed in biological replicates in parallel with the data shown. One-way ANOVA assessed statistical significance of the data collected (P<0.05 (*), P<0.01(**) and P<0.0001 (****)) mean +/- SEM (N=3).*

4.4 Discussion

4.4.1 Overexpression of Vps45 effectors in CPY secretion

All effector null strains tested including *vps45Δ* had an increase in CPY secretion compared to wildtype (**Figure 4.4**), through overexpressing the Vps45 effector plasmids in all of these null strains we hoped to create a network that indicated any compensation of the overexpression for the missing proteins in the role of CPY traffic and therefore its mis-localisation and secretion (**Table 4.1**). *TLG2* overexpression and *VPS21* overexpression in wildtype cells introduced an increase in CPY secretion. This indicates that the overexpression of *TLG2* introduces problems in CPY traffic perhaps since Tlg2 is involved in multiple trafficking pathways that this overexpression leads to a prioritisation of the other pathways. Through Vps21's role as a GTPase and regulation of energy transfer

through the conversion of GTP to GDP the levels of these proteins are crucial in the regulation of the pathways that requires them. Due to this I think that the overexpression of *VPS21* leads to an imbalance which introduces the CPY secretion phenotype in the wildtype as the absence of the protein also has a severe CPY secretion phenotype.

Table 4.1 *- Statistical significance of CPY secretion in Vps45 effector strains in comparison to wildtype yeast.*

		Yeast Strain					
		Wildtype	*vps45Δ*	*tlg2Δ*	*pep12Δ*	*vac1Δ*	*vps21Δ*
			****		****	****	****
Plasmid	Parent	n/s	****	n/s	*	**	****
	VPS45	n/s	n/s	n/s	n/s	n/s	****
	TLG2	****	*	****	*	n/s	***
	PEP12	n/s	n/s	n/s	n/s	*	***
	VAC1	n/s	****	n/s	n/s	n/s	****
	VPS21	****	***	**	n/s	n/s	n/s

In the absence of *VPS45*, overexpression of *TLG2* and *PEP12* slightly recovers the CPY secretion phenotype though not significant. The role of these proteins as binding partners of Vps45 suggests that the processing of CPY can be redirected in the absence of Vps45 in the pathways that require it. In the *pep12Δ* strain all effectors recover the CPY secretion phenotype, this suggests that other effectors can compensate through the loss of Pep12 and recover this phenotype potentially through other routes. Overexpression of *TLG2* recovers the *vac1Δ* CPY secretion phenotype suggesting that trafficking of CPY deficiencies can be compensated by another route involving Tlg2. Tlg2 is thought to promote the CVT pathway over macroautophagy in nutrient rich conditions (Abeliovich *et al*., 1999). Even though Vps45, Pep12 and Vac1 work together in Golgi to endosome vacuolar hydrolase traffic, it has been reported that overexpression of *PEP12* and *VPS45* do not supress *VAC1* mutant CPY phenotypes (Webb *et al*., 1997). This coincides with our data that *vac1Δ* yeast CPY secretion phenotypes cannot be supressed by *VPS45* and *PEP12* overexpression.

4.4.2 Hydrogen peroxide sensitivity in Vps45 effector mutants

Of the Vps45 effector null yeast strains *vps45Δ*, *pep12Δ* and *vac1Δ* had statistically significant increases in H_2O_2 sensitivity (**Table 4.2**). Overexpression of *PEP12* in the *tlg2Δ* mutant introduces an H_2O_2 sensitivity phenotype, this suggest that in the absence of Tlg2 binding with Pep12 is prioritised in a membrane trafficking route that is not involved in the protection of the cell from apoptosis.

Table 4.2 *- Statistical signification of H_2O_2 sensitivity in Vps45 effector strains in comparison to wildtype yeast.*

		Yeast Strain					
		Wildtype	*vps45Δ*	*tlg2Δ*	*pep12Δ*	*vac1Δ*	*vps21Δ*
			****	n/s	****	****	n/s
Plasmid	Parent	n/s	****	n/s	*	n/s	n/s
	VPS45	n/s	n/s	n/s	*	n/s	n/s
	TLG2	n/s	****	n/s	n/s	n/s	****
	PEP12	n/s	**	*	n/s	n/s	n/s
	VAC1	*	****	n/s	*	n/s	n/s
	VPS21	n/s	****	n/s	n/s	n/s	n/s

VAC1 overexpression increased the H_2O_2 sensitivity in wildtype yeast. Vac1 is one of the four original proteins identified as containing a FYVE (Fab1, YOTB, Vac1, EEA1) domain, a highly conserved domain whereby proteins containing them are recruited to membranes in a pH dependant manner. The FYVE domain of Vac1 is crucial in the binding of Vac1 and Vps45 (Tall *et al*., 1999). FYVE domain containing proteins can be required in mitochondrial mediated apoptosis and autophagy (Tang, Hasan and Capelluto, 2023) these results corroborate the literature suggesting that the FYVE domain of Vac1 also plays a role in apoptosis. The FYVE domain in Vac1 is also what makes it a crucial protein in the transport of CPY through the cell through PI3P binding (Burd and Emr, 1998). Vac1 is involved in the transport of CPY through the cell through the CPY pathway which uses autophagic machinery regulated by PI3P to traffic CPY to the vacuole as opposed to the CVT pathway like Vps45 (Wurmser and Emr, 2002).

In *vps21Δ* yeast the overexpression of *TLG2* introduces a H_2O_2 sensitivity phenotype, in the absence of Vps21 the overexpression of *TLG2* may promote

other pathways that reduce Vps45's efficiency at protecting from apoptosis. The emphasis in the literature that Tlg2 has two forms, open and closed (Furgason *et al*., 2009), suggests that the form that the protein binds to Vps45 in may indicate distinct roles. This is supported by the fact that Vps45 stabilises the Tlg2 protein and regulates its levels, when absent Tlg2 is degraded, when this is prevented Tlg2 is non-functional and cannot bind to its SNARE binding partners Vti1 and Tlg1 (Bryant and James, 2001). As *tlg2Δ* cells lack a H_2O_2 sensitivity phenotype, this indicates that it is not required for Vps45's role in apoptosis. Repeating the H_2O_2 sensitivity assay and overexpressing effector plasmids with a *vps45Δtlg2Δ* double mutant would elaborate on whether the presence of Vps45 in the *tlg2Δ* cells is what maintains protection from apoptosis.

4.4.3 Vps45 required in recovery from nitrogen starvation

VPS45 overexpression had no effect on the recovery from nitrogen starvation phenotype observed in **Figure 4.6**. Likewise, the overexpression of all the effectors had no impact on the reduction in recovery from nitrogen starvation in *vps45Δ* yeast suggesting that Vps45 plays a crucial role in autophagy. The severity of the *vps45Δ* recovery from nitrogen starvation has been shown to be more severe than the *atg8Δ*. Preliminary experiments were completed using the *VPS45*-T238N overexpression plasmid and provided the same results as wildtype due to the *VPS45* SCN mutants' ability to recover after nitrogen starvation.

Table 4.3 *- Statistical significance of recovery after nitrogen starvation in Vps45 effector strains in comparison to wildtype yeast.*

		Yeast Strain					
		Wildtype	*vps45Δ*	*tlg2Δ*	*pep12Δ*	*vac1Δ*	*vps21Δ*
			****	****	****	****	n/s
Plasmid	Parent		****				
	VPS45		n/s	****	***	****	n/s
	TLG2		****				
	PEP12		****				
	VAC1		****				
	VPS21		****				

The *vps21Δ* yeast had no recovery after nitrogen starvation phenotype indicating no autophagy defect (**Table 4.3**). Though the literature states that Vps21 seems to have a less severe autophagy phenotype than its downstream counterparts (Vps3, Vac1 and Pep12) in other autophagy studies (Chen *et al*., 2014). Other literature suggests that the more severe endocytic phenotypes of these counterparts implies that Vps21 is independent of the recruitment of Vac1 and Pep12 to the endosome and autophagosomes (Gerrard *et al*., 2000; Tall *et al*., 1999).

4.4.4 Vps21 has a role in apoptotic flux

Vps21 as well as localising to the late endosome (Prescianotto-Baschong and Riezman, 2002) also localises to the mitochondrion (Sickmann *et al*., 2003). Well documented as a Golgi to vacuole trafficking molecule, Vps21 under nutrient stress conditions also prevents the accumulation of reactive oxygen species and mitochondrial respiration distress (Nakatsukasa *et al*., 2014). Vps21 and another Rab5 protein, Ypt53, are adaptable depending on the nutrient conditions, this could explain the difference in H_2O_2 sensitivity in our studies versus other literature (Brown *et al.,* 2006), where the presence of H_2O_2 at the concentrations used in our research (4.3.2) that lead to reactive oxygen species production can be compensated by other Rab5 proteins in protection from apoptosis.

4.4.5 Vps45 effectors are associated with iron trafficking and the mitochondrion

We have shown concurrent with the literature that Vps21 is not crucial for recovery from macroautophagy after induction with nitrogen starvation despite being involved in autophagosome closure (Zhou *et al*., 2017). This Vps21-dependent closure is thought to be through interactions with Vps21 and the Snf7-Atg11 subunit of the ESCRT complex, meanwhile Atg11-Atg32 interactions required for mitophagy progression is Vps21 independent (Wu *et al*., 2021). Loss of ECERT-III protein Snf7 or Vps4 leads to accumulation of mitochondrial markers and Atg32 on autophagosomes, Snf7 is recruited to Atg32 marked mitophagosomes through Atg11 and Atg32 binding (Wu *et al*., 2021). In addition to mitophagy related receptors Atg32 mitophagy can be regulated through PINK1/Parkin mediated ubiquitylation of mitochondria that have lost their membrane potential (Narendra *et al*., 2012).

Mitophagy in yeast is driven by Atg32 (Kanki *et al*., 2009; Okamoto *et al*., 2009) a mitochondrial surface protein that navigates selection of mitochondrion through mediating recognition by Atg11 for cargo in removal to the phagophore (Wang and Klionsky, 2011). As a highly energy consuming organelle the efficient removal of mitochondria during cell starvation is crucial in cell survival (Kanki *et al*., 2015). Atg8 is known to interact with Atg19 and Atg32 (Shintani *et al*., 2002), Atg19 is involved in the CVT pathway the selective autophagy pathway which traffics Ape1 through the cell to the vacuole. As discussed, the CVT pathway requires Tlg2 and Vps45 for maturation of the CVT vesicle (Abeliovich *et al*., 1999), indicating a link between the role of Tlg2 and Vps45 in mitophagy.

Mitochondrial involvement has been indicated, implicating that the role of these Vps45 effectors have a mitophagy clearance issue or a vesicular traffic of mitochondrial component. Also supported by the fact that transference of the vacuole to the daughter cell is inhibited in *VAC1* mutated yeast but not the mitochondrial or nuclear DNA (Weisman *et al*., 1990). The mitochondria as well as being crucial in energy production through oxidative phosphorylation are also a key regulator of apoptosis (Keeble and Gilmore, 2007). Daughter mitochondria with reduced membrane potential are quickly removed from the cell after cell fission through autophagy (Twig *et al*., 2008).

In the malaria parasite, *Plasmodium falciparum,* the absence of Rabenosyn 5 (Vac1), Vps45 and Rab 5 (Vps21) leads to the accumulation of haemoglobin filled vesicles in the cells (Sabitzki *et al*., 2024). The role of Vps45 in endocytic recycling should be further assessed in relation to these effectors in yeast. Though the role of Vps45 in iron recycling in pathogenic species (Caza *et al*., 2018) further prompts the assessment of Vps45 and its effectors in mitochondrial induced apoptosis with the *VPS45* SCN mutants in Chapter 6.

4.5 Conclusions

The multiple of roles of Vps45 lead to a complex network of interactions, in this instance the lack of full recovery in any of the three assays indicate that Vps45 is crucial for all three pathways: CPY pathway, apoptosis and autophagy. Potential overlap of these pathways, for instance, the ability of macroautophagy

to cover the CVT pathway during starvation and the interplay between autophagy and apoptosis make in difficult to make concrete conclusions other than infer roles. Also, the lack of compensatory action but introduction of phenotypes indicates that Vps45's roles in the cell are tightly controlled and reliant on balance of the corresponding protein effectors required in each membrane trafficking route.

5 Investigation into mitochondrial effects induced by SCN mutations.

5.1 Introduction

5.1.1 A novel function for Vps45.

Through Chapter 3 we observed the effects that the *VPS45* SCN mutants had on membrane trafficking, autophagy and apoptosis. We identified that these mutations had no effect on recovery from macroautophagy and CPY traffic in yeast strains, though they did have an effect on protection from apoptosis. In Chapter 4 we established that recovery from macroautophagy was not corrected by overexpression of Vps45 effectors in *vps45Δ* cells and therefore Vps45 is crucial in autophagy as well as protection from apoptosis despite the SCN effectors not affecting recovery from autophagy. This discouraged the hypothesis that the careful regulation of autophagy and apoptosis is tipped towards apoptosis in mutated or absent Vps45. In Chapter 4, we discussed how the Vps45 effector proteins may be linked to mitophagy indicating a link with dysregulated mitophagy that eventually leads to apoptosis in *VPS45* SCN mutant yeast. In this chapter, I will explore the possibility that the role of Vps45 in apoptosis is related to a yet undescribed regulatory role of the mitochondria.

5.1.2 Evolutionary Rate Covariation

Nathan Clark at the University of Pittsburgh has developed an algorithm named the evolutionary rate covariation (ERC) which analyses the relationship between proteins and how they have evolved over the evolutionary period of the organism (Clark *et al*., 2012). The data published has established a high evolutionary relationship between meiotic proteins under evolutionary pressure in yeast, and that genes that are involved in common pathways display a high ERC value and therefore we can use data with an ERC analysis to establish potentially undocumented relationships between genes (see 2.13). Nathan Clark kindly sent us his ERC profile for *VPS45* in yeast. I then analysed this data to explore proteins that had a high evolutionary correlation with Vps45 and explore novel relationships between Vps45 and other factors previously not-known to co-function.

5.2 Aims and Hypothesis

5.2.1 Aims for Chapter 5

The aim of this chapter was to investigate the role of Vps45 in apoptosis and what other mechanism Vps45 may be involved in, since the SCN mutants are not defective in macroautophagy.

5.2.2 Objectives

Use the ERC dataset provided by Nathan Clark to determine any proteins that may be involved with Vps45 that have been previously investigated. To also use this dataset as a starting point for any proteins that have a similar evolutionary growth pathway as Vps45 and what this may lead to.

5.2.3 Hypothesis

The route that Vps45 is required for in apoptosis may be identified through ERC data analysis, establishing this method as an indirect route of identifying effectors of proteins of interest.

5.3 Results

5.3.1 Understanding and dissecting the ERC dataset.

Using the *VPS45* ERC dataset I was able to identify genes that were likely to be related to Vps45. Since none of the known interactors were in the higher confidence intervals for the Vps45 dataset I decided to assess the properties of the proteins that did have a high ERC Fisher Transform value. Through a UniProt (UniProt the Universal Protein Knowledgebase, 2023) search of the top 1% and 5% of ERC-related proteins (**Figure 5.1**) I was able to establish the role of these proteins in the cell. Through the analysis of this data, the 35 proteins that had a Fisher Transform value of 3 or above (99% confidence) the largest proportion of the proteins were associated with the mitochondrion (orange) and the mitochondrial envelope (lilac) (**Figure 5.1A**). The next largest group was membrane, which was expected as Vps45 is a membrane trafficking protein. Of the proteins that had a Fisher Transform Value of 2 or above (95% confidence) the third largest organelle localisation was the mitochondrion and mitochondrial envelope, with chromosome (beige) and nucleus (pink) in first and second respectively (**Figure 5.1B**). To summarise, a large number of mitochondrial

proteins evolved at the same rate as Vps45, which suggests that there could be a regulatory link between Vps45 and mitochondria.

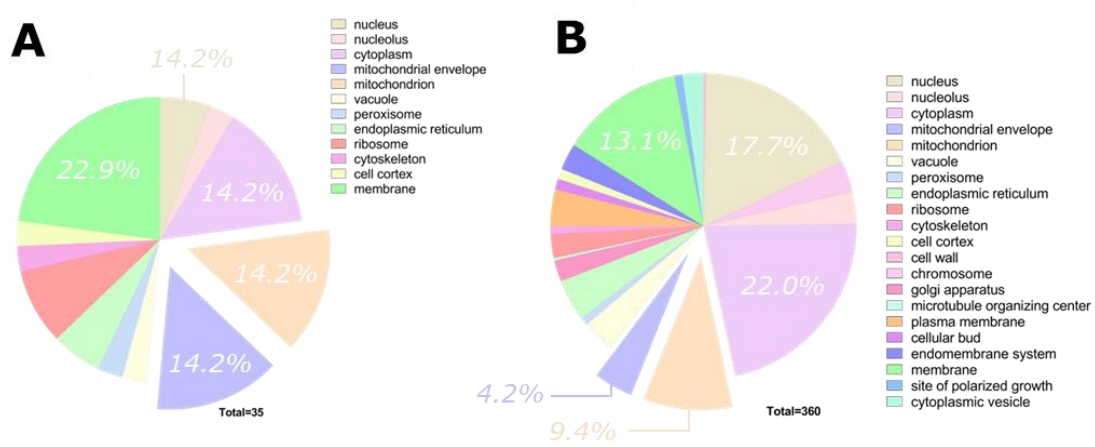

Figure 5.1 *- Quantification of UniProt data based on the ERC data; Organelle localisation of the proteins identified in the ERC dataset (A) proteins with a Fisher Transform value of greater than 3 (B) proteins with a Fisher Transform value of greater than 2. In the list of proteins quantified in (A) had the highest localisation at the mitochondria with 28.4% (lilac; mitochondrial envelope and orange; mitochondrion). This was a lesser proportion in the data shown in (B) but still third highest behind cytoplasm (pink) and nucleus (beige) at 13.6% of proteins.*

5.3.2 Identification of the PTM1 protein.

During my analysis of the ERC dataset and analysing the organelles that the proteins in the dataset were associated with, I found that *PTM1* has a high ERC value with the *VPS45* dataset. Ptm1 is a membrane bound protein of unknown function though is known to co-purify with late Golgi-derived vesicles that also contain Tlg2 (Inadome *et al*., 2005). *PTM1* also has a paralog, *YHL017W*, that was identified during whole genome duplication (Byrne and Wolfe, 2005). As Vps45 is known to regulate Tlg2 and is a binding partner of Tlg2 (Bryant and James, 2001), I wanted to test if these factors identified by the ECR dataset played a role in CPY trafficking or apoptosis. Therefore, I used the two null protein strains to assess the CPY secretion and hydrogen peroxide sensitivity of the proteins. I wanted to establish whether the copurification with Tlg2 established could be linked to these two known functions of Vps45. I found that *ptm1Δ* and *yhl017wΔ* have no CPY secretion phenotype in comparison to the *vps45Δ* and *tlg2Δ* and the phenotype is like that of wildtype (**Figure 5.2**). Indicating that the role of *PTM1* is not required for CPY trafficking (**Figure 5.2A**). We then investigated Ptm1 in protection from apoptosis by assessing

H_2O_2 sensitivity, this data showed slight increases in H_2O_2 sensitivity in the *PTM1* paralog but not the *ptm1Δ* neither was statistically significantly different from the wildtype yeast nor was the sensitivity as high as the *VPS45* SCN mutants (**Figure 5.2B**).

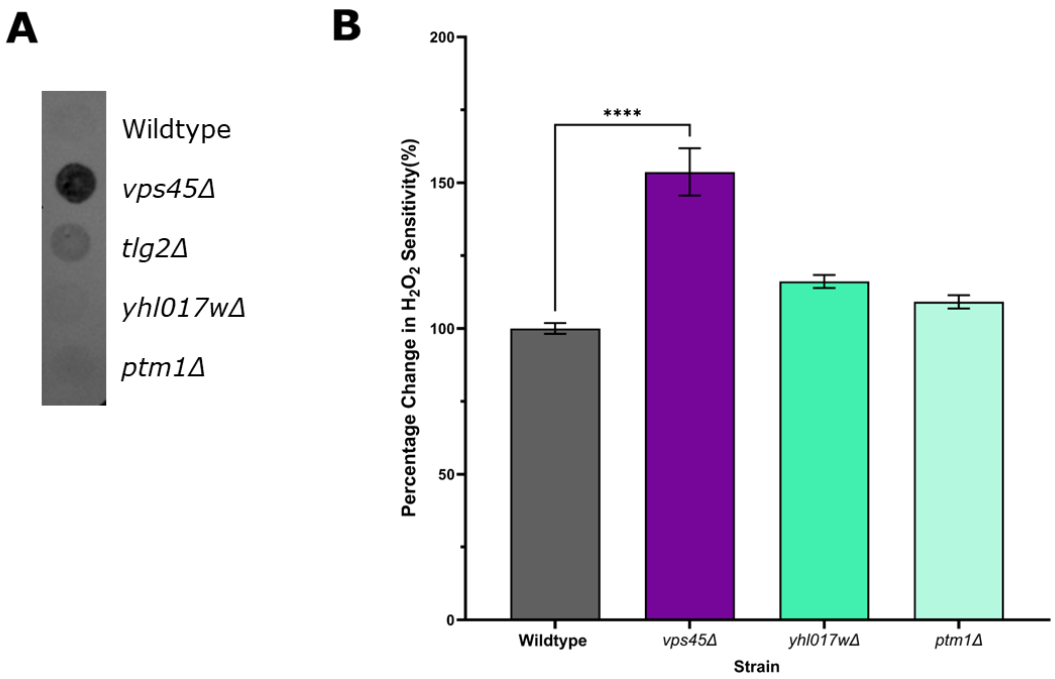

Figure 5.2 *- CPY secretion and H_2O_2 sensitivity of ptm1Δ and its genetic paralog; (A) Raw CPY Secretion of yhl017wΔ and ptm1Δ compared to wildtype, vps45Δ and tlg2Δ, N=1. (B) Percentage change in H_2O_2 sensitivity; Quantification of the hydrogen peroxide sensitivity assay shows mean +/-SEM (N=3). (P<0.0001(****)) by one-way ANOVA.*

5.3.3 Tlg2 is required for Atg9 cycling

Moving away from the ECR data temporarily, I decided to look at other effectors of Tlg2. The literature suggests that SNARE proteins play a role in fusion events that lead to Atg9 structures that serve as a precursor to the pre-autophagosome, and that Tlg2 acts as the t-SNARE required in this process (Nair and Klionsky, 2011). Atg9 is a lipid scramblase that is required for maturation of the autophagosome structure by expanding the edge of the membrane with Atg2 (Matoba *et al*., 2020). Atg9 localises to pools that cycle between the mitochondria and pre-autophagosome (He *et al*., 2006). Atg9 delivery to the autophagosome is dependent on the CVT pathway and autophagy induction in

starved cells, though Tlg2 is not required for delivery of Atg9 during autophagy. Atg9 delivery requires Golgi-endosome traffic as opposed to delivery from the mitochondria (Ohashi and Munro, 2010). Atg9 pools are frequently replenished to allow it to be recycled in multiple rounds of autophagosome formation (Reggiori *et al*., 2004). Atg9 travel to the autophagosome is dependent on Tlg2 and returning of Atg9 to the pool is dependent on Gos1 (Ohashi and Munro, 2010). The requirement of Tlg2 in the movement of Atg9 may induce a backlog of the protein in the absence of Vps45 due to a reduction in functional Tlg2 that interferes with Atg9's movement from the mitochondria inducing mitochondrial stress and eventually apoptosis.

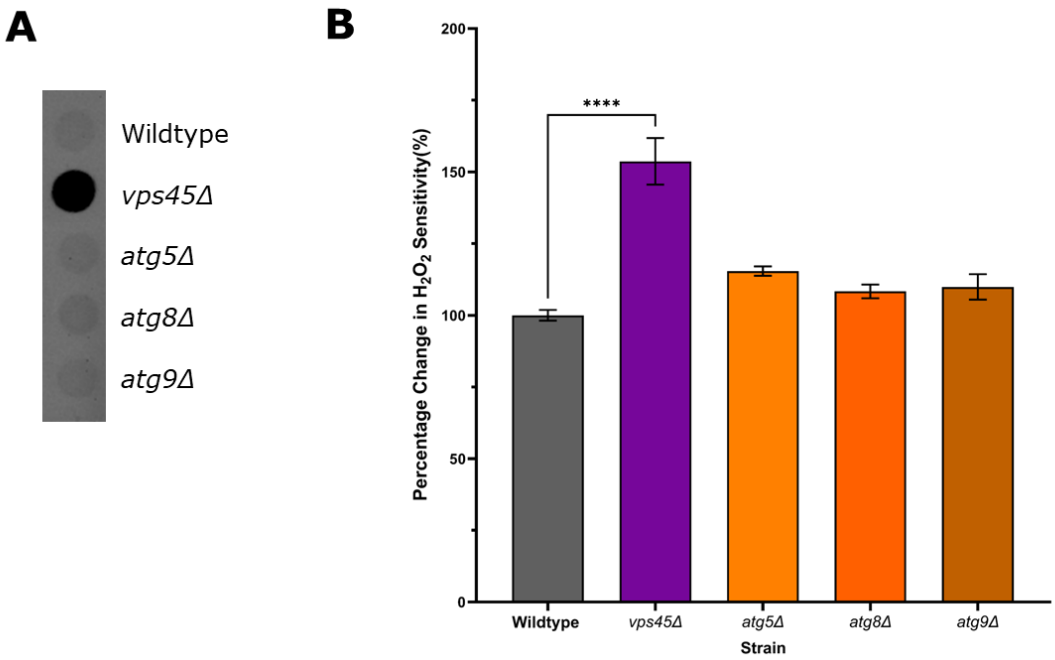

Figure 5.3 *- CPY secretion and H_2O_2 sensitivity of atg5Δ, atg8Δ and atg9Δ; (A) Raw CPY secretion of atg5Δ, atg8Δ and atg9Δ compared to wildtype and vps45Δ (N=1). (B) Percentage change in H_2O_2 sensitivity; Quantification of the hydrogen peroxide sensitivity assay shows mean +/-SEM (N=3). (P<0.0001(****)) by one-way ANOVA.*

While Atg9 is the only *ATG* protein that is required for the formation of the double membraned autophagosome (Noda *et al*., 2000), Atg5 is required for the expansion of the membrane (Mizushima *et al*., 2003). The Atg5-Atg12 complex is essential for autophagosome formation allowing for Atg8 binding (Romanov *et al*., 2012). Atg8 is a driver of autophagy with 3 human orthologs (LC3, GABARAP and GATE-16) (Shpilka *et al*., 2011) and is a major regulator of the

autophagosome through its role as a lipid conjugator (Nakatogawa *et al*., 2007). Atg5, Atg8 and Atg9 are in one of 5 separate functional groups in autophagy (Yorimitsu and Klionsky, 2005). Using this information, I decided to investigate whether loss of these autophagy proteins provided an apoptotic or CPY trafficking defect indicating a link to Vps45 and Tlg2. The data showed that none of the null *atg* strains (*atg5Δ*, *atg8Δ* or *atg9Δ*) showed a CPY secretion defect or a H_2O_2 sensitivity defect (**Figure 5.3**). More work into the relationship between Vps45 and Atg9 should be performed, time permitting a nitrogen starvation assay overexpressing *ATG9* in *vps45Δ* and *tlg2Δ* cells would be appropriate.

5.3.4 Growth assays indicate respiration problems in SCN mutants

Before progressing with the route of mitochondria based on the literature and the ERC data, I decided to use growth assays to determine whether this may be an appropriate strategy. I assessed the growth of wildtype, *vps45Δ*, *VPS45*-T238N, *VPS45*-P267L and *VPS45*-P485L on different media to provide indicators of what direction I should take my data collection (**Figure 5.4**). $CaCl_2$ media was used to determine whether *VPS45* mutant yeast had dysfunctional calcium homeostasis through ER or mitochondrial store dysregulation (Gogianu *et al*., 2024), *vps45Δ* yeast have been shown to be Ca^{2+} sensitive mutants (Hagihara *et al*., 2020). Here we observe the *vps45Δ* calcium sensitivity, but this is not observed in the *VPS45* SCN mutants, in fact they seem to have improved growth compared to wildtype under the high calcium growth conditions (**Figure 5.4B**). To understand the yeast strain's ability to switch from fermentation to respiration and therefore the efficiency of the mitochondria in the cell the strains were grown on a 3% ethanol/glycerol synthetic medium plate with no glucose (**Figure 5.4C**). The *vps45Δ* strain had a very severe growth phenotype on this media, and the *VPS45* SCN strains had a growth phenotype that was in between the *vps45Δ* and the wildtype with little growth after the second dilution in comparison to the wildtypes third dilution. Finally, the last treatment was with bathophenanthroline disulfonate (BPS) an iron chelator (Caza *et al*., 2018) that has shown to affect growth of *vps45Δ* in *Cryptococcus neoformans*. Here we observed the same defect in *vps45Δ* in *Saccharomyces cerevisiae* but the *VPS45* SCN mutants did not appear to have a growth defect when the iron chelator was present (**Figure 5.4D**).

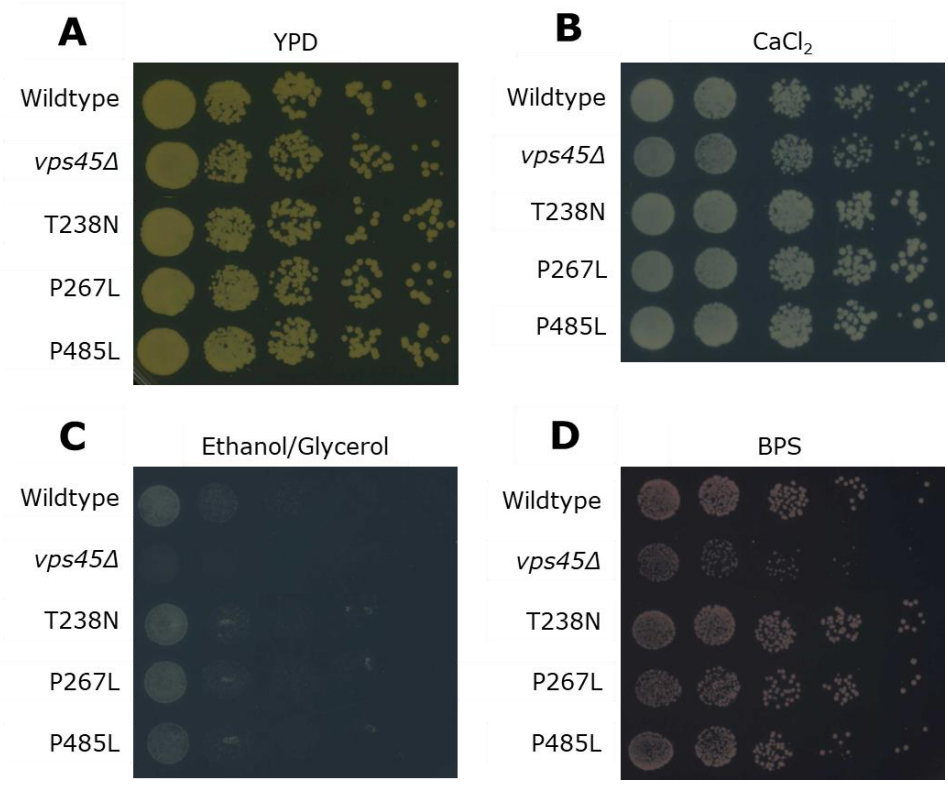

Figure 5.4 *- Growth assays for vps45Δ and VPS45 SCN mutants in different growth conditions; 5 µL of 0.6 OD_{600} log liquid culture at 1 in 5 dilutions on growth plates at 30°C for 48 hours. (A) YPD plate, (B) $CaCL_2$ plate, (C) Ethanol/Glycerol plate and (D) Iron chelation 150 µM BPS plate.*

5.3.5 Vps45 SCN mutant yeast have abnormal mitochondrial morphology

After determining that *vps45Δ* yeast was defective in iron metabolism and respiration I wanted to establish the mitochondrial morphology of these strains. Under normal log growth conditions with 4% glucose wildtype strains have long tubular structures when grown aerobically (Aung-Htut *et al*., 2013). The mitochondria of cells were labelled by expressing Cit1 tagged with mTurquiose2 from a plasmid (2.10.2). As described in the literature, Cit1 localises to the ribbon-shaped mitochondrial structures in wildtype cells (**Figure 5.5**) (Lee *et al*., 2007). The mitochondria in *vps45Δ* and the SCN mutant strains in comparison were different from wildtype, with fragmented puncta that were small and round were observed instead of ribbons. In the *VPS45*-T238N strain the mitochondria were clumped together. The brightness of Cit1 was also

reduced. Cit1 is a mitochondrial citrate synthase, a catalyst for the first reaction in the tricarboxylic acid (TCA) cycle (Lee *et al*., 2007) indicating a reduction of respiration in these mutant stains.

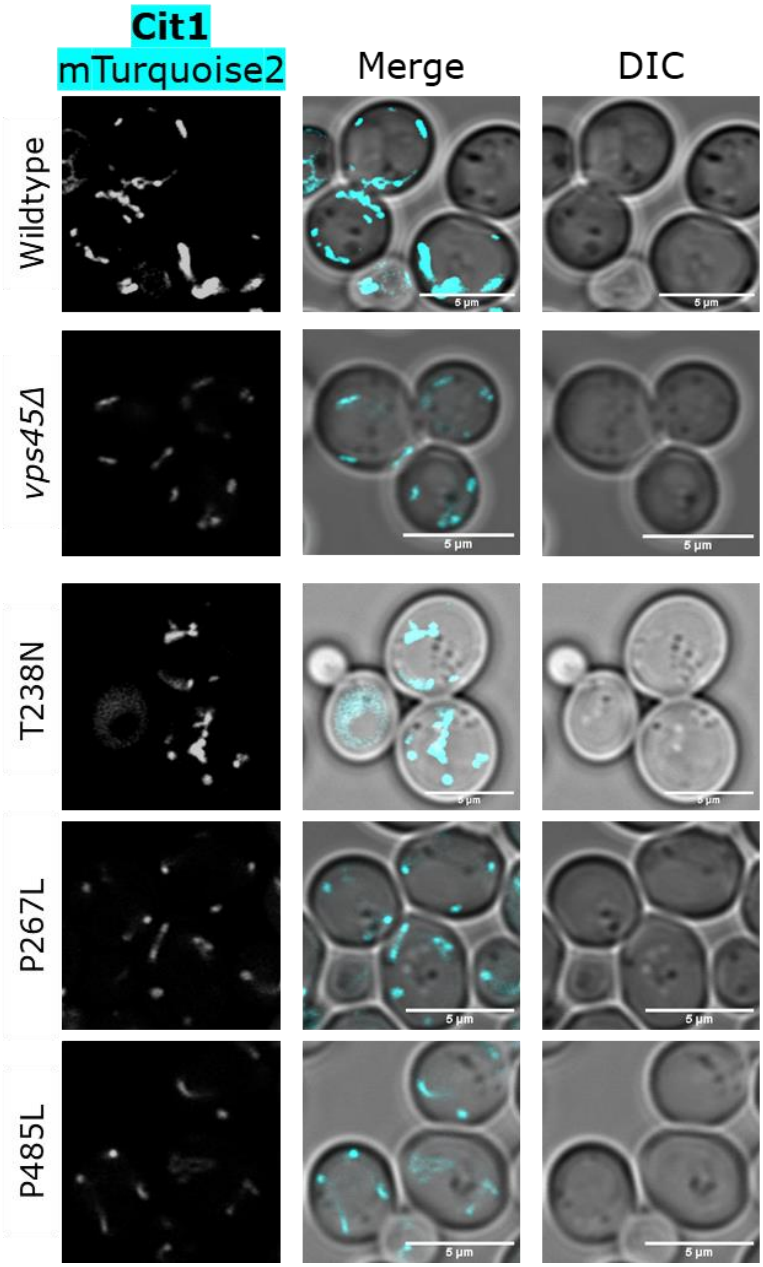

Figure 5.5 *- Mitochondrion morphology is disrupted in VPS45 SCN mutants; Micrographs displaying abnormal mitochondrial morphology through copper induced Cit1 mTurquoise2 fluorescence in vps45Δ and VPS45 SCN mutants, VPS45-T238N, VPS45-P267L and VPS45-P485L. VPS45 SCN mutants have smaller rounder Cit1 expression with reduced brightness.*

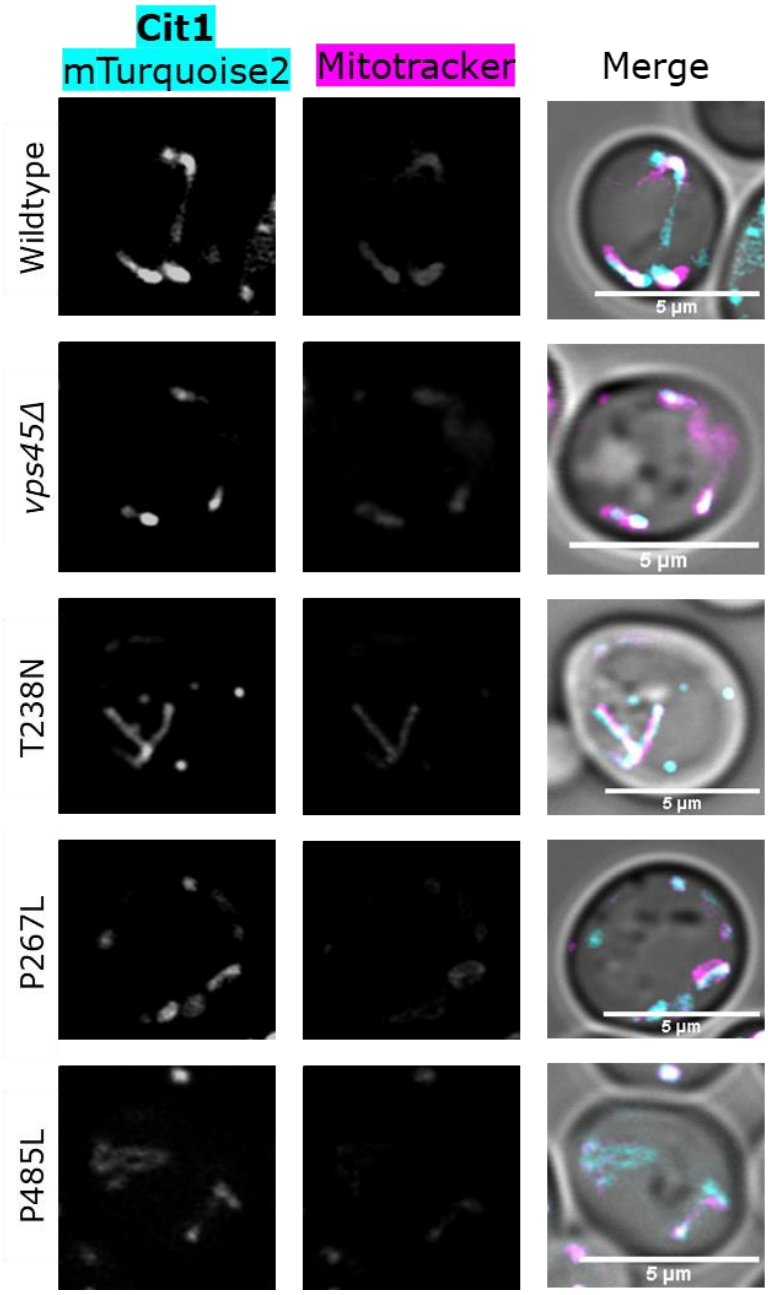

Figure 5.6 *- Mitochondrion membrane potential is reduced in VPS45 SCN mutants; Micrographs displaying abnormal mitochondrial mitotracker fluorescence through copper induced Cit1 mTurquoise2 fluorescence and CMXRos Mitotracker™ fluorescence in vps45Δ and VPS45 SCN mutants, VPS45-T238N, VPS45-P267L and VPS45-P485L. Abnormal morphology was observed and a reduction in the MitoTracker™ signal in the vps45Δ and VPS45 SCN mutant strains.*

5.3.6 Loss of Vps45 leads to reduced membrane potential in mitochondria.

After establishing that *VPS45* SCN mutants and *vps45Δ* have a defect in mitochondrial morphology I decided to investigate the functionality of the

mitochondria present by using CMXRos Red MitoTracker™ as an indicator of mitochondrial membrane potential (Callegari *et al*., 2012). Using Cit1 as a marker of the mitochondria the data shows the same small and round phenotype in the SCN *VPS45* mutants and the *vps45Δ* as was observed in **Figure 5.5** as well as a reduction in MitoTracker™ signal (**Figure 5.6**). This data was quantified by taking the Cit1 fluorescent signal and the MitoTracker™ fluorescent signal and taking a ratio of mitochondria:membrane potential to incorporate the difference of mitochondria sizes per cell (**Figure 5.7**). In the quantification of these micrographs, we observed a statistically significant reduction in *vps45Δ* and *VPS45*-P485L yeast MitoTracker™ signal. Though all *VPS45* SCN mutant yeast strains had a reduction in signal one-way ANOVA couldn't accurately determine significance due to the low number of *VPS45*-T238N cells examined (~10) in comparison to the other strains (~50). The large SEM values would have also been affected by the low number of cells analysed. Despite this the I believe this is strong evidence that can be confirmed with a higher population of cells analysed.

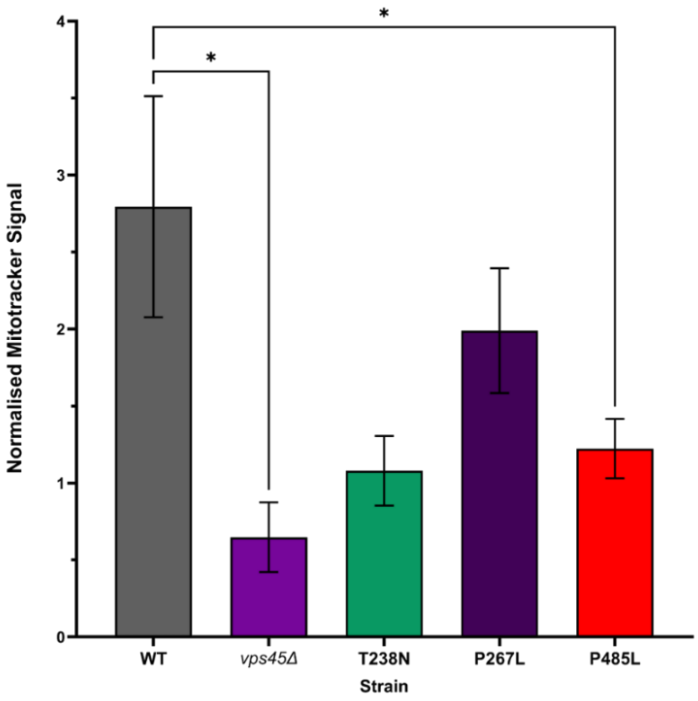

Figure 5.7 *– Quantification of Mitochondrial Mitotracker signal in log yeast strains. Quantification of mitochondrial Mitotracker fluorescence normalised to copper induced mTurquoise2-Cit1 fluorescence of the mitochondria in wildtype, vps45Δ and VPS45 SCN mutants (VPS45-T238N, VPS45-P267L and VPS45-P485L) N=1 (P<0.05, one-way ANOVA).*

5.3.7 Quantification of the Vps45 mitochondrial defect in SCN mutant yeast.

In order to compensate for the low number of cells analysed by micrograph I wanted to expand on this using a high-throughput method in order to confirm the loss of mitochondrial membrane potential in *vps45Δ* and *VPS45* SCN mutant yeast. Using flow cytometry I tried to assess this using *mef2Δ* as a negative control which is known to have a reduction in mitochondrial membrane potential using the CMXRos Red MitoTracker™ (**Figure 5.8**) (Callegari *et al*., 2012). Using three separate cell strain populations (pink, green and orange) compared to the unstained cells (red) we were able to determine that each population tended to have two distinct populations of mitochondrial membrane potential including the wildtype. The *mef2Δ* though only having one population was problematic in that the abnormal morphology of the cells made gating for the cells incredibly difficult. The ratio between the two populations is different between the wildtype and the *vps45Δ* and SCN mutants, though this is not uniform between the 4 strains. With *vps45Δ* (1.6:1) having two similar peaks but with less difference between the two than wildtype (2:1). Whereas the *VPS45*-T238N (1:5) and *VPS45*-P484L (1:1.4) SCN mutants all have variation between peaks which are not similar to wildtype or *vps45Δ* whereby the second peak of fluorescence is higher than the first. *VPS45*-P485L (1.8:1) has a ratio that is between *vps45Δ* and wildtype. In conclusion this data did not clarify any potential phenotypes, however the two distinct populations indicate that the data should have not been collected in log phase and should have been collected in an ethanol/glycerol media that shifts cells into respiration.

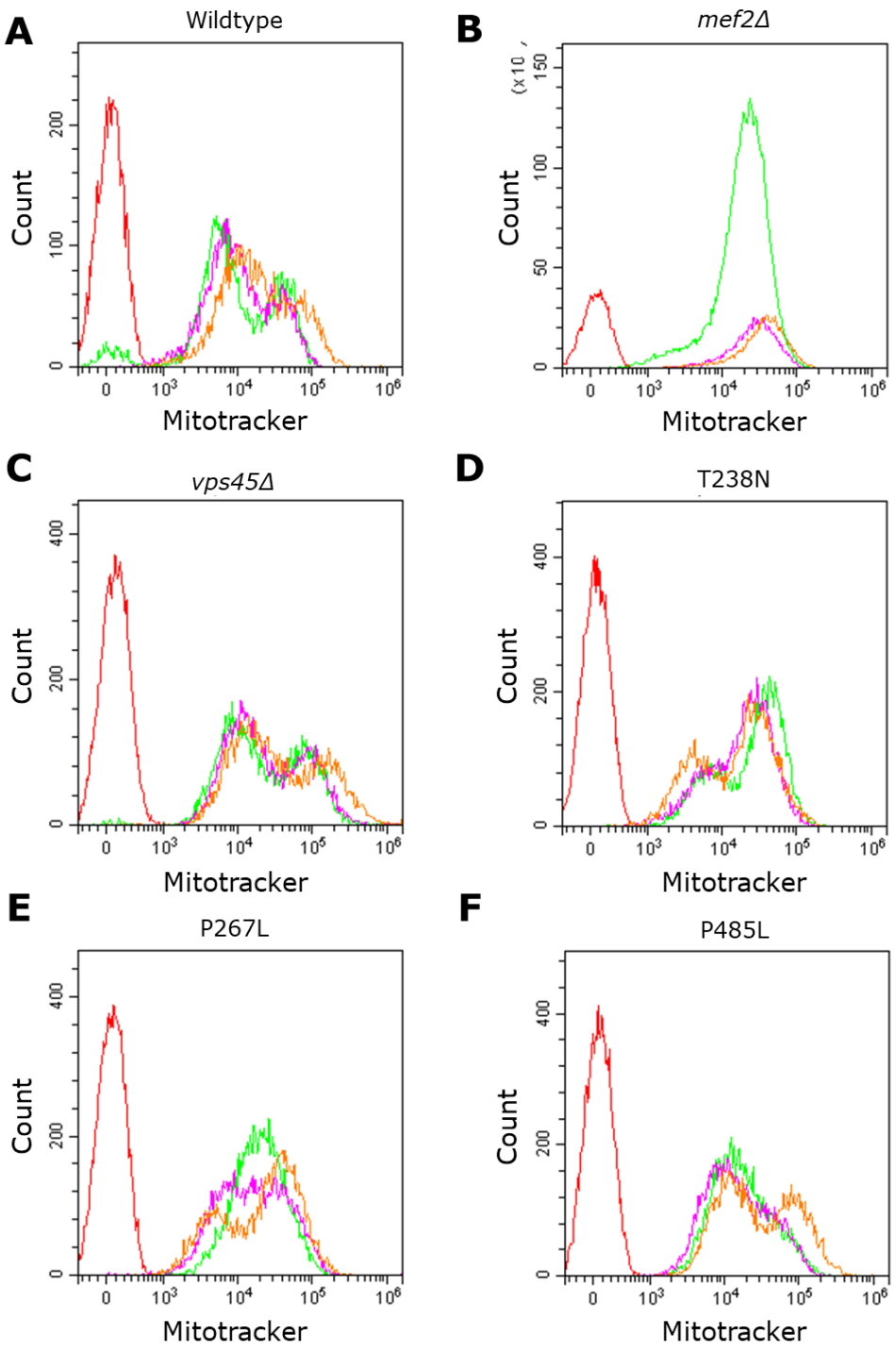

Figure 5.8 - *Flow Cytometry fluorescence of SCN mutant yeast; Y610 excitation laser, CMXRos fluorescence of mitochondria in 10,000 cells (N=3). Red = unstained cells, pink = data set 1, orange = data set 2 and green = data set 3. (A) wildtype, (B) mef2Δ, (C) vps45Δ, (D) VPS45-T238N, (E) VPS45-P267L and (F) VPS45-P485L. Data presentation by CytExpert (Beckman Coulter).*

5.4 Discussion

5.4.1 PTM1 and Atg9 investigations

Using the ERC data to establish newfound relationships of Vps45 proved useful in identification of *PTM1* and the link to mitochondrial proteins. In this instance the data showed no CPY secretion or H_2O_2 sensitivity defects which ruled out Ptm1 and the paralog, yhl017w, from further investigation in this chapter. However, the ability of the paralogs potentially compensating each other in this instance prompted the beginning of production of a double mutant to further investigate the H_2O_2 sensitivity phenotype. Time permitting the production and further testing would have been ideal, however the localisation of Atg9 to the mitochondria took priority over this. Unfortunately, this also provided no H_2O_2 sensitivity phenotype. With my focus being with the *VPS45* SCN mutants and the literature indicating a mitochondrial defect (Caza *et al*., 2018), combined with the ERC data the progression with this route took precedence. In future work I would hope that investigations into the role of Ptm1 would include western blotting to indicate any effects on Vps45 and Tlg2 levels in the absence of Ptm1 or microscopy investigating the localisation of Ptm1 in respect to Vps45. With Atg9 I would envisage an initial western blot to analyse the effect on Atg9 pools in *vps45Δ* and *tlg2Δ* cell lines before further work looking into the relationship (if any) between Atg9 and Vps45. Primarily because Vps45's role in autophagy is predicted to be in autophagosome closure and Atg9 is involved in the initial steps of autophagy (Yorimitsu and Klionsky, 2005). As it appearsVps45 has distinct roles in the cell Tlg2's role in endosomal trafficking of Atg9 may be independent of autophagy and strictly the CVT pathway. The role of Tlg2 in trafficking Atg9 in just nutrient rich conditions and not nitrogen starvation (Ohashi and Munro, 2010) may indicate that Vps45's role switches after autophagy induction.

5.4.2 Vps45 SCN mutants and mitochondrial defects

In this chapter we observed the mitochondrial morphology defects and a defect in mitochondrial membrane potential. The most interesting part of this data shown in **Figure 5.7** is that it correlates almost perfectly with the data shown in **Figure 3.6** whereby the *vps45Δ* yeast has the highest H_2O_2 sensitivity and yet the lowest mitochondrial membrane potential. Then the *VPS45*-T238N and *VPS45*-P485L have an increase in H_2O_2 sensitivity and have a reduction of

mitochondrial membrane potential but it is not as severe as the *vps45Δ* and then the *VPS45*-P267L has a slight increase in H_2O_2 sensitivity, but it is not significant and also has a reduction in membrane potential though not significant.

In mammalian cells mitophagy can be induced by CCCP and mitochondrial membrane potential shift can be monitored via flow cytometry (Mauro-Lizcano *et al*., 2015). In yeast mitophagy can be induced by culture with lactate as a sole carbon source and then shifted to amino acid starvation with glucose (Kanki and Klionsky, 2008). To get results that have a more definitive read-out from any flow cytometry experiments I believe that mitophagy would have to be induced in the yeast strains in this instance or if looking solely at the mitochondria health then in starvation phase of the yeast growth curve.

Vps45 in the pathogenic *Cryptococcus neoformans* is involved in the trafficking of the ferroxidase Cfo1, the *VPS45* mutant yeast showed sensitivity to inhibitors of electron transport complexes, changes in mitochondrial membrane potential and also calcium homeostasis impairments (Caza *et al*., 2018). In yeast we have shown evidence of calcium homeostasis problems as well as mitochondrial dysfunction in the *VPS45* SCN mutants. In human patients the *VPS45*-E238K mutation was associated with high ferritin accumulation (Karaatmaca *et al*., 2020) suggesting that iron was not being stored correctly. Interestingly, in human macrophage cell lines, high ferritin is associated with increased sensitivity to oxidative stress (Kurz *et al*., 2011) indicating that the reason these *VPS45* SCN mutants are susceptible to H_2O_2 as observed in Chapter 3 is due to their inability to traffic iron correctly leading to apoptosis as opposed to Vps45 playing a direct role in apoptosis protection.

Patients with SCN V caused by *VPS45* mutations cannot be treated by G-CSF injection which is usually the standard treatment in SCN patients. Vps45 has been shown to be involved in G-CSF receptor recycling (Frey *et al*., 2021), there are two types of ferritin H-ferritin and L-ferritin, H-ferritin interacts with the intracellular domain of G-CSFR. When G-CSF binds to the receptor, H-ferritin dissociates from the C-terminus of the receptor and leads to an increase in ROS in the cell (Yuan *et al*., 2004). G-CSFR being trapped in early endosomes in

vps45Δ cells (Frey *et al*., 2021) may lead to increases of H-ferritin leading to increased ROS and mitochondrial damage. β1 integrin was reduced on the cell surface of SCN mutant patients (Vilboux *et al*., 2013) loss of Rabenosyn 5 (Vac1) and Vps45 in humans leads to internalisation of β1 integrin (Rahajeng *et al*., 2010). β1 integrin expression is also decreased by increased iron in the cell in human cells (Sponsel *et al*., 1996) but also increases in G-CSF lead to upregulation of β1 integrin in cancer cells which promotes cell migration (Chakraborty *et al*., 2006; Furmento *et al*., 2016). Low levels of G-CSFR caused by faulty iron stores from dysfunctional mitochondria in *VPS45* SCN patients may lead to decreased cell surface β1 integrin as well as apoptosis.

5.5 Conclusions

Through the analysis of the *VPS45* SCN mutants in mitochondrial morphology and mitochondrial membrane potential we observed a significant defect in both. Through further analysis with higher populations and biological repeats I think that this fulfils a good standing for future work into the area. This combined with the literature indicating a role in mitochondrial function and iron uptake in *Cryptococcus neoformans* (Caza *et al*., 2018) is indicative of the value of future work. The role of the SCN mutants in the role of iron turnover in yeast would be a three-part study at least, determining whether the role of Vps45 is directly involved with the mitochondria, whether Vps45 is involved in mitophagy or whether Vps45 protein trafficking promotes healthy mitochondria.

6 Discussion

6.1 Thesis Discussion

6.1.1 The characterisation of Vps45 roles.

This thesis has fundamentally explored the function of Vps45 in three distinct roles: CPY trafficking, protection from apoptosis and recovery from autophagy induction. Here I have shown that Vps45 is required for membrane trafficking, autophagy and apoptosis. In contrast we have established that the SCN-*VPS45* mutant yeast function properly in membrane trafficking and autophagy and are only defective in protection from apoptosis. This argues against my original hypothesis that susceptibility of *VPS45* mutants to apoptosis observed in SCN patients was explained through defective control of autophagy. In addition to this, we have identified that the role of Vps45 in apoptosis may be through an unidentified mitochondrial mechanism, due to *VPS45* SCN mutant yeast exhibiting defects in mitochondrial morphology and reduction of membrane potential. In further support for the role of Vps45 in apoptosis protection being distinct from its well characterised roles in trafficking and autophagy, mutants lacking the cognate SNARE Tlg2 do not exhibit a hypersensitivity to H_2O_2 phenotype and its inability to recover the apoptotic phenotype when Vps45 is absent.

6.1.2 Considering SCN mutations in the context of Vps45 structure.

Yeast lacking *VPS45* display multiple phenotypes in addition to missorting CPY, these include a temperature sensitive growth defect and increased sensitivity to high salt and oxidative stress (Piper *et al*., 1994). In Chapter 3, we show that the disease-causing mutations in *VPS45* identified in SCN patients display different H_2O_2 sensitivity phenotypes despite the ability to sort CPY to the vacuole and recover from autophagy induction. The ability of these mutants to exert an increase in apoptosis while maintaining other Vps45 functions indicates value in the location of the residue changes induced by the mutations.

The development of this data reveals the importance of the location of the residue changes in the apoptotic pathway Vps45 is required for. When mapped to the Vps45 structure *VPS45*-T238N, *VPS45*-E252K and *VPS45*-P485L

homologous to the SCN residue changes are in found in the 'hinge' region of the protein (**Figure 3.1**). Unpublished bioinformatic data by the Bryant lab (Daniel Newsome, 2021) described chemical changes of the *VPS45*-E252K mutation and how this could introduce chemical bonds effecting the action of the hinge region though the change of a negatively charged aspartic acid (E) to a positively charged lysine (K) molecule. Physical interactions between these amino acids and their side chains could be altered with the introduction of an amino acid change in the sequence affecting the hinge capabilities required for Vps45 binding.

As shown by the preliminary data in Chapter 3 and that the integration of the *VPS45*-E252K mutation into yeast via homologous recombination has proven much more difficult than the other mutations. This may align with the observation that the *VPS45*-E238K mutant has the most severe patient phenotype (Meerschaut *et al*., 2015). The expression of the *VPS45*-E252K using the single copy plasmid indicates that the mutant *VPS45*-E252K Vps45 is being degraded due to the lack of Vps45 protein observed in the western blot (**Figure 3.11**). This suggests that *VPS45*-E252K is a non-functional protein in yeast, supported by the fact that Tlg2 is degraded in the absence of Vps45 (Bryant and James, 2001) we can conclude that these proteins are susceptible to degradation when non-functional. This is further supported by the countless efforts to create a viable strain in which all failed, I designed an approach to incorporate a restriction enzyme site to screen integrations before sequencing but although positive colonies were identified, they too lacked the E252K associated mutation despite harbouring the *VPS45-his5*$^{+}$ cassette.

This implies that the hinge region of the protein is crucial for all modes of binding to different syntaxins. The *VPS45*-E238K mutation in humans has a syndromic effect, leading to developmental regression as well as causing SCN (Meerschaut *et al*., 2015). This combined with our data implies that this mutation leads to residue changes that interferes with multiple modes of traffic that require Vps45 in humans. Though in murine models Vps45 knock outs prove to be embryonic lethal (Frey *et al*., 2021) therefore indicating that in higher eukaryotes mutations in the hinge region do not render the protein entirely non-functional. In addition to this the *VPS45*-P253L residue change which is not in the hinge

region is described as a 'mild case' of SCN in the report describing the mutation (Newburger, 2018) which not only explains the mutant yeasts lack of H_2O_2 sensitivity but also confirms that the two different binding modes of Vps45 as an SM protein is required for different trafficking pathways. It is also possible that the relatively small range of sensitivity measured by a halo zone of inhibition following exposure to H_2O_2 might not be sensitive enough to show a phenotype of a mutation with a milder disease presentation, but more sensitive approaches might reveal a difference. I tried to achieve this by developing a 96 well plate-based approach to measure growth in liquid media containing H_2O_2, but this did not provide consistent results for growth.

6.1.3 Apoptotic role of Vps45

The relationship between autophagy and apoptosis is complicated and not particularly well defined (Denton and Kumar, 2019). As dysfunction in autophagy can lead to apoptosis (Chang *et al*., 2022) we initially were investigating the role of Vps45 SCN mutants and the effectors' role in autophagy. Though in Chapter 3 we established that the apoptotic action of Vps45 was separate from its role in autophagy. In the literature it is theorised that Vps45's role in apoptosis explained by the perturbed trafficking of cargo from the Golgi to the vacuole leading to a reduction in retrograde transport from the endosome to the Golgi and in consequence affecting trafficking to and from the ER. This leads to the notion that the dysfunction of Vps45 can induce apoptosis indirectly via ER stress (Stepensky *et al*., 2013). From the data in this thesis, I hypothesise that Vps45's role in recycling mitochondrial proteins is involved in its role in apoptosis, and this is separate from Vps45's role in autophagy, CPY traffic and CVT trafficking. Through its role as an SM protein, I believe that it's most likely that Vps45 aids SNARE complex binding required for the trafficking of vesicles containing dysfunctional mitochondria. In addition to this Rab5 (Vps21) is recruited to the dysfunctional mitochondrial membranes downstream of PARKIN activation in mammalian cells (Hammerling *et al*., 2017, Yamano *et al*., 2018). Perhaps a Vps21 and Vps45 complex is required for the clearance of these dysfunctional mitochondria, which is hindered in the presence of the SCN mutations observed in patients.

It appears that the different binding methods of Vps45 to syntaxins affects the roles that it is required for in the cell and that this also represents the differing in the effectors apoptotic and autophagic phenotypes. To assess this, a mode of action would be to use electron microscopy to look at vesicle accumulation in the mutant strains under nitrogen stress for autophagy compared to lactate stress for mitophagy, as well as the traffic of different proteins in these strains by fluorescence microscopy. As mitophagy and autophagy are simultaneous in yeast the effect of stressors on the mutant strains would be crucial in differentiating between the pathways.

6.1.4 SM proteins in disease

Autophagy is implicated in the pathogenesis of major neurodegenerative diseases, such as Alzheimer's (Nixon and Yang, 2012). A cause of this is thought to be that neurons are particularly vulnerable if there is an inability to clear lysosomal bodies from the cell (Nixon and Yang, 2012). Although my project is based on SCN and the ability to compare Vps45 functionality in yeast to neutrophils, this is intriguing due to the neurological impairments of older SCN patients described in the literature. Described patients displayed developmental defects such as delayed neuromotor development (Meerschaut *et al*., 2015). These patients who present with a severe syndromic disease tend to have the *VPS45*-E238K mutation. As established, this has also been the most severe mutant we have seen in yeast. These data suggest that the severity of the *VPS45*-E234K mutation in patients may also be caused by a detrimental effect on autophagy, due to the residue change affecting the hinge movement of the Vps45 protein discussed above. This may mean that the severity of the disease and neurological implications are due to the location and type of residue change in patients, which is not seen in the *VPS45*-T224N patients. Further experiments into the effect of the *VPS45*-E252K mutation in yeast in autophagy would be interesting but not beneficial to the development of the data here.

Initial disease presentation is specific to the haematopoietic system due to the life-threatening urgency. Follow up of patients' post-bone marrow transplant indicates that the disease is not confined to the hematopoietic system and further symptoms such as neurological impairment present later in infant development. Vps45 is expressed in high quantities in the central nervous

system this is thought to be due to the mass vesicle transport required in the neurons of the brain (El-Husseini *et al*., 1997). In addition to this, the SM protein, Sec1, has been implicated in the exocytosis of neurotransmitters into the synapses of the brain (Halachmi and Lev, 1996). Neurological involvement in the SCN V patients may be due to the importance of SM proteins in the brain as they are required for the high vesicle turnover. Conversely, as we have established in this project, the involvement of Vps45 in the health of mitochondria may be important in the neurological development of SCN V patients, due to the brain being such a high energy consumer and the faulty clearance of dysfunctional mitochondria leading to poor neurological development.

6.1.5 Effectors of Vps45 and their proposed method of action

Vps21 is known to act in autophagosome double membrane closure (Chen *et al*., 2014; Zhou *et al*., 2017) and the t-SNARE Vti1 is involved in multiple pathways to the vacuole and interacts with Pep12 (Fischer von Mollard and Stevens, 1999). When the autophagosome enters the vacuole, the outer membrane is removed leaving a single membraned vesicle inside the vacuole (Mijaljica *et al*., 2007). Initially, I believed that Vps45 may be involved in the transport of a vacuolar lipase that is required in the vacuole and delivered by Vps45 similarly to how it is involved in the CPY pathway. The lack of this enzyme in the vacuole due to Vps45 loss or dysfunction would mean that the contents of the single membrane autophagosome cannot be released into the vacuole. However, in *vps45Δ* and *pep12Δ* cells the autophagosome associates, unclosed, at the vacuole membrane as in *vps21Δ* cells (Zhou *et al*., 2017). Combined with the recovery from nitrogen starvation data shown in Chapter 5, I now believe that Vps45's involvement in autophagy is due to its role as an SM protein in SNARE complex binding of vesicles being sequestered to the phagophore. Vps21 is involved in autophagosome closure (Zhou *et al.,* 2017) and is required for recruitment of a PI3K complex to the phagophore (Zhao et al., 2022), perhaps Vps45/Vps21 complex is required for phagophore expansion through sequestering of vesicles, without which the autophagosome double membrane closure is prevented. In the microscopy data shown in Chapter 3 I observed singular bright puncta of GFP-Ape1 indicating the autophagosome, perhaps indicative of vesicular docking to the phagophore but unable to progress through

autophagy. Interestingly, Vac8 acts as a tether of the autophagosome, docking it to the vacuole, loss of Vac8 leads to fewer autophagosomes that are free in the cytosol (Hollenstein *et al*., 2019). Vac8 is also involved in the CVT pathway and mitophagy (Park *et al*., 2019), therefore I think that investigating whether Vac8 is upregulated in loss of Vps45 would be indicative of whether Vps45 disturbs the phagophore expansion and therefore autophagosome closure and docking to the vacuole.

6.1.6 Mitochondrial action of Vps45

Dysfunction in mitochondrial recycling through autophagy is thought to be a cause of transition from autophagy to apoptosis (Abeliovich and Klionsky, 2001). Currently, the role of Vps45 in mitochondrial clearance appears to be what promotes apoptosis in *vps45Δ* and *VPS45* SCN mutant yeast. This suggests that Vps45 may be involved in regulation of apoptosis through membrane traffic involving mitochondria as opposed to through the endosomal system in autophagy. By analysing the Evolutionary Rate Co-variation (ERC) data collection acquired from Dr. Nathan Clark of the University of Utah (Clark *et al*., 2012) we established that there is a correlative evolutionary rate between the Vps45 protein and crucial mitochondrial proteins in yeast. Using this data and the identified relationship between iron uptake, Vps45 and the mitochondria (Caza *et al*., 2018), we established a link between the Vps45 and mitochondrial stress and mitochondrial induced apoptosis. Which we confirmed by demonstrating that *vps45Δ* and *VPS45* SCN mutants had abnormal mitochondrial morphology and reduced mitochondrial membrane potential.

Neutrophils have few mitochondria and obtain their energy through glycolysis as opposed to oxidative phosphorylation (Borregaard and Herlin, 1982). The few mitochondria neutrophils have instead use their membrane potential in apoptotic signalling (Fossati *et al*., 2003) rather than for respiration. Through measuring the cell death of yeast unable to produce energy through glycolysis and the biochemical levels of Vps45 in these cells we would determine whether Vps45 is required for the oxidative mitochondrial demands of the neutrophils. Conversely, mitochondrial ATP synthesis can be inhibited by antimycin A (Ye *et al*., 2015). Using mutant yeast strains lacking key genes in the respiratory pathway such as NADH dehydrogenase would allow for evaluating the role of

Vps45 in a eukaryotic cell which is forced to produce energy separately from the mitochondria. Thus, an important aspect in the progression of this question is to investigate a relationship between the *VPS45* mutant yeast and the potential inability to protect the cell from mitochondrial induced apoptosis.

6.1.7 Neutrophil susceptibility to apoptosis caused by Vps45 mutations

Neutrophils also lack Bcl-2 (Iwai *et al*., 1994), Bcl-2 prevents the release of mitochondrial apoptotic factors such as cytochrome c (Kale *et al*., 2018). Yeast does not express members of the Bcl-2 family or have corresponding homologues, which makes the translation of the data acquired in yeast specifically transferable to neutrophils. Bcl-2 can also induce apoptosis under ER stress which can be observed via ER release of its Ca^{2+} stores. Bcl-2 has also been implicated in the ER autophagy induction (Heath-Engel *et al*., 2008). Therefore, the lack of Bcl-2 in yeast and neutrophils is favourable towards the hypothesis these cells lacking Vps45 are more susceptible to cell death via mitochondrial stress as opposed to ER stress. This information indicates that using yeast as a model organism in SCN neutrophil studies is not limited by the complexity of apoptosis in human cells.

6.1.8 G-CSF Treatment and Vps45 involvement

The SCN patients described with *VPS45* mutations were unresponsive to granulocyte colony-stimulating factor (G-CSF) treatment (Stepensky *et al*., 2013) which ordinarily would promote the myeloid progenitor to produce more cells or to respond to infections (Mehta *et al*., 2015) via promoting the movement of the progenitor away from the bone marrow niche (King and Goodell, 2011). This naturally would occur via the increase in inflammatory cytokines during infection. Therefore, it is important to establish the role of Vps45 in the movement of cellular cargos in mammalian cells which have a high turnover and potentially the ability to differentiate into various cell types. Especially as Vps45 is required in cellular traffic from the Golgi which directs newly synthesized proteins to their different sub-cellular destination (Gu *et al*., 2001). In zebrafish Vps45 is required for transporting cargo required in progenitor cell differentiation (Mochizuki *et al*., 2018) suggesting that perhaps Vps45 could be required for differentiation of cells in the bone marrow niche

with patients of Vps45 induced SCN displaying bone marrow fibrosis (Frey *et al*., 2021).

6.2 Proposed model for Vps45 in protection from apoptosis

Considering all of the data collected and where it stands within the literature, I propose that Vps45's role in apoptosis is through perturbed clearance of the mitochondria in mitophagy. Due to this the increase of ROS and problematic iron storage in the cell leads to mitochondrial induced cell death through caspase release. Improper iron storage would also affect G-CSFR recycling in mammals due to the binding of the cytoplasmic region to H-ferritin stores. As Vps45 is primarily a trafficking protein I hypothesise that Vps45 is required for trafficking a crucial component required for mitochondrial health or is part of a network of machinery as in autophagy that aids mitochondrial clearance. Therefore, due to this the cells are susceptible to apoptosis particularly through H_2O_2 sensitivity due to the increased ROS this would cause. In the instance of the SCN patients, the neutrophils unconventional use of the mitochondria and short life span would make the cells more prone to apoptosis as opposed to ER stress from a backlog in retrograde traffic as suggested previously in the literature (Stepensky *et al*., 2013). In addition to this the mis-trafficking of G-CSFR and consequential decrease of β1 integrin on the cell surface would lead to perturbed migration of the cells leading to the dry bone marrow aspirations and nucleated red blood cells observed in patients.

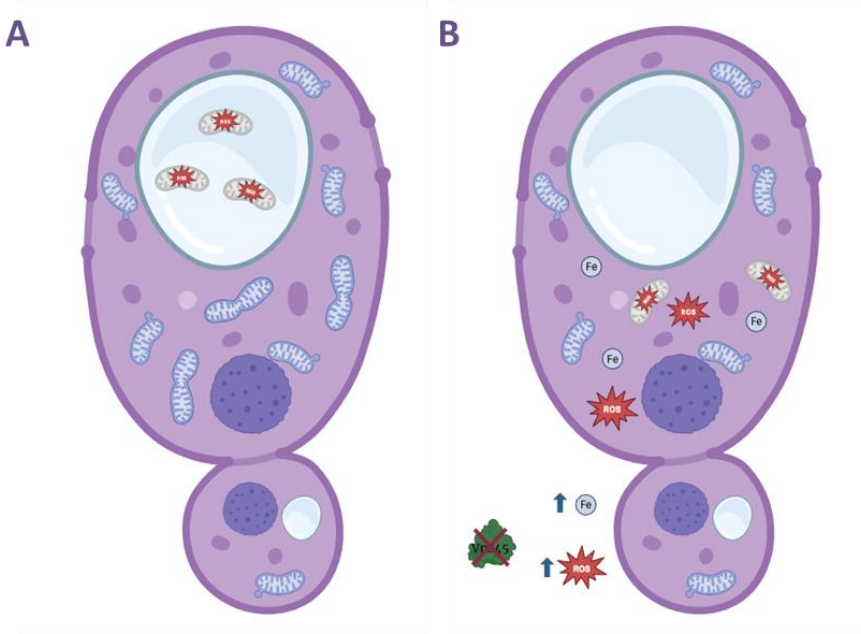

Figure 6.1 *- Proposed model for Vps45's role in protection from apoptosis; (A) in healthy cells when Vps45 is present, mitochondria are removed when dysfunctional through mitophagy, under stress excess mitochondria are removed as they are a large energy consumer. When Vps45 is missing or mutated as in the SCN mutant yeast (B) mitochondrial clearance is perturbed. The cells are unable to traffic mitochondria to the vacuole and so dysfunctional mitochondria release excess ROS into the cell and iron stores are released.*

6.3 Future Work

Throughout this discussion I have alluded to multiple next steps in analysis of Vps45's role in apoptosis. Time permitting my first step after corroborating all my thesis data would be to review levels of Pep12 in *VPS45* SCN mutant yeast western blotting. This would indicate whether the implied role of Pep12 in apoptosis in Chapter 5 is affected by Vps45 mutants that have increased susceptibility to apoptosis. Next, using electron microscopy I would assess the number of vesicles in *VPS45* SCN mutant yeast to confirm whether this is similar to the increase seen in the *vps45Δ* and the location of mitochondria after mitophagy induction.

Also, using fluorescence microscopy to assess the contents of these vesicles after inducing autophagy, mitophagy and apoptosis. I would also use fluorescence microscopy to track movement of key mitophagy player, Atg32, through the cell as well as western blot for Atg32 levels in *VPS45* SCN mutant

strains. Flow cytometry analysis of the *VPS45* SCN mutant yeast would act as a key tool assessing the role of Vps45 in apoptosis. Flow cytometry assessing mitochondrial membrane potential after induction of mitophagy, autophagy and apoptosis as described for the microscopy, but clearly not using *mef2Δ* for gating as I did here due to the size of the mutant cells.

6.4 Conclusions

This thesis has provided insight into the effect of mutations seen in SCN patients on the protein Vps45 in the model organism yeast. Here, we have established that Vps45 is involved in multiple trafficking pathways within the cell, some of which are translatable to mammals. We have shown that the SCN mutations do not affect Vps45's role in CPY trafficking or autophagy but do have an effect on the role(s) of Vps45 in protection from apoptosis and the mitochondria. This thesis has emphasised the importance of the position of these residue changes on the function of the protein and it is implied that this has different effects on the mode of binding Vps45 uses to different effectors which are required for different pathways.

7 References

Abeliovich, H., Darsow, T., Emr, S.D., 1999. Cytoplasm to vacuole trafficking of aminopeptidase I requires a t-SNARE-Sec1p complex composed of Tlg2p and Vps45p. EMBO J 18, 6005–6016. https://doi.org/10.1093/emboj/18.21.6005

Abeliovich, H., Grote, E., Novick, P., Ferro-Novick, S., 1998. Tlg2p, a Yeast Syntaxin Homolog That Resides on the Golgi and Endocytic Structures*. Journal of Biological Chemistry 273, 11719–11727. https://doi.org/10.1074/jbc.273.19.11719

Abeliovich, H., Klionsky, D.J., 2001. Autophagy in Yeast: Mechanistic Insights and Physiological Function. Microbiol. Mol. Biol. Rev. 65, 463–479. https://doi.org/10.1128/MMBR.65.3.463-479.2001

Alotaibi, F.A., Albarkheel, A.I., 2020. Periodontal Disease in Two Siblings with VPS45-associated Severe Congenital Neutropenia Type V: A Case Report. Int J Clin Pediatr Dent 13, 572–575. https://doi.org/10.5005/jp-journals-10005-1841

Ammerer, G., Hunter, C.P., Rothman, J.H., Saari, G.C., Valls, L.A., Stevens, T.H., 1986. PEP4 gene of Saccharomyces cerevisiae encodes proteinase A, a vacuolar enzyme required for processing of vacuolar precursors. Mol Cell Biol 6, 2490–2499. https://doi.org/10.1128/mcb.6.7.2490-2499.1986

Ancliff, P.J., Gale, R.E., Liesner, R., Hann, I.M., Linch, D.C., 2001. Mutations in the ELA2 gene encoding neutrophil elastase are present in most patients with sporadic severe congenital neutropenia but only in some patients with the familial form of the disease. Blood 98, 2645–2650. https://doi.org/10.1182/blood.V98.9.2645

Anding, A.L., Baehrecke, E.H., 2017. Cleaning House: Selective Autophagy of Organelles. Dev Cell 41, 10–22. https://doi.org/10.1016/j.devcel.2017.02.016

Antonin, W., Fasshauer, D., Becker, S., Jahn, R., Schneider, T.R., 2002. Crystal structure of the endosomal SNARE complex reveals common structural principles of all SNAREs. Nat Struct Biol 9, 107–111. https://doi.org/10.1038/nsb746

Aung-Htut, M.T., Lam, Y.T., Lim, Y.-L., Rinnerthaler, M., Gelling, C.L., Yang, H., Breitenbach, M., Dawes, I.W., 2013. Maintenance of Mitochondrial Morphology by Autophagy and Its Role in High Glucose Effects on Chronological Lifespan of Saccharomyces cerevisiae. Oxidative Medicine and Cellular Longevity 2013, 636287. https://doi.org/10.1155/2013/636287

Bankaitis, V.A., Johnson, L.M., Emr, S.D., 1986. Isolation of yeast mutants defective in protein targeting to the vacuole. Proc Natl Acad Sci U S A 83, 9075–9079. https://doi.org/10.1073/pnas.83.23.9075

Banta, L.M., Robinson, J.S., Klionsky, D.J., Emr, S.D., 1988. Organelle assembly in yeast: characterization of yeast mutants defective in vacuolar biogenesis and protein sorting. Journal of Cell Biology 107, 1369–1383. https://doi.org/10.1083/jcb.107.4.1369

Bethani, I., Lang, T., Geumann, U., Sieber, J., Jahn, R., Rizzoli, S., 2007. The specificity of SNARE pairing in biological membranes is mediated by both proof-reading and spatial segregation. The EMBO journal 26, 3981–92. https://doi.org/10.1038/sj.emboj.7601820

Bock, J.B., Klumperman, J., Davanger, S., Scheller, R.H., 1997. Syntaxin 6 functions in trans-Golgi network vesicle trafficking. Mol Biol Cell 8, 1261–1271. https://doi.org/10.1091/mbc.8.7.1261

Bock, J.B., Matern, H.T., Peden, A.A., Scheller, R.H., 2001. A genomic perspective on membrane compartment organization. Nature 409, 839–841. https://doi.org/10.1038/35057024

Borregaard, N., Herlin, T., 1982. Energy Metabolism of Human Neutrophils during Phagocytosis. J Clin Invest 70, 550–557. https://doi.org/10.1172/JCI110647

Boxer, L., Dale, D.C., 2002. Neutropenia: causes and consequences. Semin Hematol 39, 75–81. https://doi.org/10.1053/shem.2002.31911

Boxer, L.A., 2006. Severe Congenital Neutropenia: Genetics and Pathogenesis. Trans Am Clin Climatol Assoc 117, 13–32.

Brachmann, C.B., Davies, A., Cost, G.J., Caputo, E., Li, J., Hieter, P., Boeke, J.D., 1998. Designer deletion strains derived from Saccharomyces cerevisiae S288C: a useful set of strains and plasmids for PCR-mediated gene disruption and other applications. Yeast 14, 115–132. https://doi.org/10.1002/(SICI)1097-0061(19980130)14:2<115::AID-YEA204>3.0.CO;2-2

Brown, J.A., Sherlock, G., Myers, C.L., Burrows, N.M., Deng, C., Wu, H.I., McCann, K.E., Troyanskaya, O.G., Brown, J.M., 2006. Global analysis of gene function in yeast by quantitative phenotypic profiling. Mol Syst Biol 2, 2006.0001. https://doi.org/10.1038/msb4100043

Bryant, N.J., James, D.E., 2003. The Sec1p/Munc18 (SM) protein, Vps45p, cycles on and off membranes during vesicle transport. J Cell Biol 161, 691–696. https://doi.org/10.1083/jcb.200212078

Bryant, N.J., James, D.E., 2001. Vps45p stabilizes the syntaxin homologue Tlg2p and positively regulates SNARE complex formation. EMBO J 20, 3380–3388. https://doi.org/10.1093/emboj/20.13.3380

Bryant, N.J., Piper, R.C., Gerrard, S.R., Stevens, T.H., 1998a. Traffic into the prevacuolar/endosomal compartment of Saccharomyces cerevisiae: a VPS45-dependent intracellular route and a VPS45-independent, endocytic route. Eur J Cell Biol 76, 43–52. https://doi.org/10.1016/S0171-9335(98)80016-2

Bryant, N.J., Piper, R.C., Weisman, L.S., Stevens, T.H., 1998b. Retrograde traffic out of the yeast vacuole to the TGN occurs via the prevacuolar/endosomal compartment. The Journal of Cell Biology 142, 651–663. https://doi.org/10.1083/jcb.142.3.651

Burd, C.G., Emr, S.D., 1998. Phosphatidylinositol(3)-phosphate signaling mediated by specific binding to RING FYVE domains. Mol Cell 2, 157–162. https://doi.org/10.1016/s1097-2765(00)80125-2

Burd, C.G., Peterson, M., Cowles, C.R., Emr, S.D., 1997. A novel Sec18p/NSF-dependent complex required for Golgi-to-endosome transport in yeast. MBoC 8, 1089–1104. https://doi.org/10.1091/mbc.8.6.1089

Burkhardt, P., Hattendorf, D.A., Weis, W.I., Fasshauer, D., 2008. Munc18a controls SNARE assembly through its interaction with the syntaxin N-peptide. EMBO J 27, 923–933. https://doi.org/10.1038/emboj.2008.37

Burman, C., Ktistakis, N.T., 2010. Regulation of autophagy by phosphatidylinositol 3-phosphate. FEBS Letters 584, 1302–1312. https://doi.org/10.1016/j.febslet.2010.01.011

Byrne, K.P., Wolfe, K.H., 2005. The Yeast Gene Order Browser: combining curated homology and syntenic context reveals gene fate in polyploid species. Genome Res 15, 1456–1461. https://doi.org/10.1101/gr.3672305

Cabrera, M., Arlt, H., Epp, N., Lachmann, J., Griffith, J., Perz, A., Reggiori, F., Ungermann, C., 2013. Functional Separation of Endosomal Fusion Factors and the Class C Core Vacuole/Endosome Tethering (CORVET) Complex in Endosome Biogenesis. J Biol Chem 288, 5166–5175. https://doi.org/10.1074/jbc.M112.431536

Callegari, S., Gregory, P.A., Sykes, M.J., Bellon, J., Andrews, S., McKinnon, R.A., Lopes, M.A. de B., 2012. Polymorphisms in the Mitochondrial Ribosome Recycling Factor EF-G2mt/MEF2 Compromise Cell Respiratory Function and Increase Atorvastatin Toxicity. PLOS Genetics 8, e1002755. https://doi.org/10.1371/journal.pgen.1002755

Carpp, L.N., Ciufo, L.F., Shanks, S.G., Boyd, A., Bryant, N.J., 2006. The Sec1p/Munc18 protein Vps45p binds its cognate SNARE proteins via two distinct modes. J Cell Biol 173, 927–936. https://doi.org/10.1083/jcb.200512024

Carpp, L.N., Shanks, S.G., Struthers, M.S., Bryant, N.J., 2007. Cellular levels of the syntaxin Tlg2p are regulated by a single mode of binding to Vps45p. Biochem Biophys Res Commun 363, 857–860. https://doi.org/10.1016/j.bbrc.2007.09.067

Carr, C.M., Rizo, J., 2010. At the junction of SNARE and SM protein function. Curr Opin Cell Biol 22, 488–495. https://doi.org/10.1016/j.ceb.2010.04.006

Caza, M., Hu, G., Nielson, E.D., Cho, M., Jung, W.H., Kronstad, J.W., 2018. The Sec1/Munc18 (SM) protein Vps45 is involved in iron uptake, mitochondrial function and virulence in the pathogenic fungus Cryptococcus neoformans. PLOS Pathogens 14, e1007220. https://doi.org/10.1371/journal.ppat.1007220

Chakraborty, A., White, S.M., Guha, S., 2006. Granulocyte colony-stimulating receptor promotes β1-integrin-mediated adhesion and invasion of bladder cancer cells. Urology 68, 208–213. https://doi.org/10.1016/j.urology.2006.01.046

Chang, K.-C., Liu, P.-F., Chang, C.-H., Lin, Y.-C., Chen, Y.-J., Shu, C.-W., 2022. The interplay of autophagy and oxidative stress in the pathogenesis and therapy of retinal degenerative diseases. Cell & Bioscience 12, 1. https://doi.org/10.1186/s13578-021-00736-9

Chen, Y., Zhou, F., Zou, S., Yu, S., Li, S., Li, D., Song, J., Li, H., He, Z., Hu, B., Björn, L.O., Lipatova, Z., Liang, Y., Xie, Z., Segev, N., 2014. A Vps21 endocytic module regulates autophagy. Molecular Biology of the Cell 25, 3166–3177. https://doi.org/10.1091/mbc.E14-04-0917

Chen, Y.A., Scheller, R.H., 2001. SNARE-mediated membrane fusion. Nat Rev Mol Cell Biol 2, 98–106. https://doi.org/10.1038/35052017

Cilenti, L., Soundarapandian, M.M., Kyriazis, G.A., Stratico, V., Singh, S., Gupta, S., Bonventre, J.V., Alnemri, E.S., Zervos, A.S., 2004. Regulation of HAX-1 anti-apoptotic protein by Omi/HtrA2 protease during cell death. J Biol Chem 279, 50295–50301. https://doi.org/10.1074/jbc.M406006200

Clark, N.L., Alani, E., Aquadro, C.F., 2012. Evolutionary rate covariation reveals shared functionality and coexpression of genes. Genome Res. 22, 714–720. https://doi.org/10.1101/gr.132647.111

Conibear, E., Stevens, T.H., 1998. Multiple sorting pathways between the late Golgi and the vacuole in yeast. Biochimica et Biophysica Acta (BBA) - Molecular Cell Research 1404, 211–230. https://doi.org/10.1016/S0167-4889(98)00058-5

Coonrod, E.M., Stevens, T.H., 2010. The Yeast vps Class E Mutants: The Beginning of the Molecular Genetic Analysis of Multivesicular Body Biogenesis. MBoC 21, 4057–4060. https://doi.org/10.1091/mbc.e09-07-0603

Cooper, A.A., Stevens, T.H., 1996. Vps10p cycles between the late-Golgi and prevacuolar compartments in its function as the sorting receptor for multiple yeast vacuolar hydrolases. J Cell Biol 133, 529–541. https://doi.org/10.1083/jcb.133.3.529

Cowles, C.R., Emr, S.D., Horazdovsky, B.F., 1994. Mutations in the VPS45 gene, a SEC1 homologue, result in vacuolar protein sorting defects and accumulation of membrane vesicles. J Cell Sci 107 (Pt 12), 3449–3459.

Cowles, C.R., Snyder, W.B., Burd, C.G., Emr, S.D., 1997. Novel Golgi to vacuole delivery pathway in yeast: identification of a sorting determinant and required transport component. EMBO J 16, 2769–2782. https://doi.org/10.1093/emboj/16.10.2769

Cueva, R., García-Alvarez, N., Suárez-Rendueles, P., 1989. Yeast vacuolar aminopeptidase yscI. Isolation and regulation of the APE1 (LAP4) structural gene. FEBS Lett 259, 125–129. https://doi.org/10.1016/0014-5793(89)81510-8

Cutler, N.S., Heitman, J., Cardenas, M.E., 1999. TOR kinase homologs function in a signal transduction pathway that is conserved from yeast to mammals. Molecular and Cellular Endocrinology 155, 135–142. https://doi.org/10.1016/S0303-7207(99)00121-5

Dale, D.C., Bonilla, M.A., Davis, M.W., Nakanishi, A.M., Hammond, W.P., Kurtzberg, J., Wang, W., Jakubowski, A., Winton, E., Lalezari, P., Robinson, W., Glaspy, J.A., Emerson, S., Gabrilove, J., Vincent, M., Boxer, L.A., 1993. A Randomized Controlled Phase III Trial of Recombinant Human Granulocyte Colony-Stimulating Factor (Filgrastim) for Treatment of Severe Chronic Neutropenia. Blood 81, 2496–2502.

Dann, S.G., Thomas, G., 2006. The amino acid sensitive TOR pathway from yeast to mammals. FEBS Letters, Istanbul Special Issue 580, 2821–2829. https://doi.org/10.1016/j.febslet.2006.04.068

Day, K.J., Papanikou, E., Glick, B.S., 2016. 4D Confocal Imaging of Yeast Organelles. Methods Mol Biol 1496, 1–11. https://doi.org/10.1007/978-1-4939-6463-5_1

Denton, D., Kumar, S., 2019. Autophagy-dependent cell death. Cell Death Differ 26, 605–616. https://doi.org/10.1038/s41418-018-0252-y

Dröse, S., Brandt, U., 2008. The Mechanism of Mitochondrial Superoxide Production by the Cytochrome *bc*1 Complex*. Journal of Biological Chemistry 283, 21649–21654. https://doi.org/10.1074/jbc.M803236200

Dulubova, I., Sugita, S., Hill, S., Hosaka, M., Fernandez, I., Südhof, T.C., Rizo, J., 1999. A conformational switch in syntaxin during exocytosis: role of munc18. EMBO J 18, 4372–4382. https://doi.org/10.1093/emboj/18.16.4372

Dulubova, I., Yamaguchi, T., Gao, Y., Min, S.-W., Huryeva, I., Südhof, T.C., Rizo, J., 2002. How Tlg2p/syntaxin 16 'snares' Vps45. EMBO J 21, 3620–3631. https://doi.org/10.1093/emboj/cdf381

Dulubova, I., Yamaguchi, T., Wang, Y., Südhof, T.C., Rizo, J., 2001. Vam3p structure reveals conserved and divergent properties of syntaxins. Nat Struct Biol 8, 258–264. https://doi.org/10.1038/85012

Eisemann, T.J., Allen, F., Lau, K., Shimamura, G.R., Jeffrey, P.D., Hughson, F.M., 2020. The Sec1/Munc18 protein Vps45 holds the Qa-SNARE Tlg2 in an open conformation. eLife 9, e60724. https://doi.org/10.7554/eLife.60724

El-Husseini, A.E., Guthrie, H., Snutch, T.P., Vincent, S.R., 1997. Molecular cloning of a mammalian homologue of the yeast vesicular transport protein vps45. Biochim Biophys Acta 1325, 8–12. https://doi.org/10.1016/s0005-2736(97)00014-x

Falcone, C., Mazzoni, C., 2016. External and internal triggers of cell death in yeast. Cell. Mol. Life Sci. 73, 2237–2250. https://doi.org/10.1007/s00018-016-2197-y

Farré, J., Burkenroad, A., Burnett, S.F., Subramani, S., 2013. Phosphorylation of mitophagy and pexophagy receptors coordinates their interaction with Atg8 and Atg11. EMBO Reports 14, 441–449. https://doi.org/10.1038/embor.2013.40

Farrugia, G., Balzan, R., 2012. Oxidative Stress and Programmed Cell Death in Yeast. Frontiers in Oncology 2, 64. https://doi.org/10.3389/fonc.2012.00064

Feng, Y., Backues, S.K., Baba, M., Heo, J., Harper, J.W., Klionsky, D.J., 2016. Phosphorylation of Atg9 regulates movement to the phagophore assembly site and the rate of autophagosome formation. Autophagy 12, 648–658. https://doi.org/10.1080/15548627.2016.1157237

Feng, Y., Klionsky, D.J., 2017. Autophagic membrane delivery through ATG9. Cell Res 27, 161–162. https://doi.org/10.1038/cr.2017.4

Fischer von Mollard, G., Stevens, T.H., 1999. The Saccharomyces cerevisiae v-SNARE Vti1p is required for multiple membrane transport pathways to the vacuole. Mol Biol Cell 10, 1719–1732. https://doi.org/10.1091/mbc.10.6.1719

Fogel, A.I., Dlouhy, B.J., Wang, C., Ryu, S.-W., Neutzner, A., Hasson, S.A., Sideris, D.P., Abeliovich, H., Youle, R.J., 2013. Role of Membrane Association and Atg14-Dependent Phosphorylation in Beclin-1-Mediated Autophagy. Molecular and Cellular Biology 33, 3675–3688. https://doi.org/10.1128/MCB.00079-13

Fossati, G., Moulding, D.A., Spiller, D.G., Moots, R.J., White, M.R.H., Edwards, S.W., 2003. The Mitochondrial Network of Human Neutrophils: Role in Chemotaxis, Phagocytosis, Respiratory Burst Activation, and Commitment to Apoptosis. The Journal of Immunology 170, 1964–1972. https://doi.org/10.4049/jimmunol.170.4.1964

Frey, L., Ziętara, N., Łyszkiewicz, M., Marquardt, B., Mizoguchi, Y., Linder, M.I., Liu, Y., Giesert, F., Wurst, W., Dahlhoff, M., Schneider, M.R., Wolf, E., Somech, R., Klein, C., 2021. Mammalian VPS45 orchestrates trafficking through the endosomal system. Blood 137, 1932–1944. https://doi.org/10.1182/blood.2020006871

Fröhlich, K.U., Madeo, F., 2000. Apoptosis in yeast--a monocellular organism exhibits altruistic behaviour. FEBS Lett 473, 6–9. https://doi.org/10.1016/s0014-5793(00)01474-5

Furgason, M.L.M., MacDonald, C., Shanks, S.G., Ryder, S.P., Bryant, N.J., Munson, M., 2009. The N-terminal peptide of the syntaxin Tlg2p modulates binding of its closed conformation to Vps45p. Proc Natl Acad Sci U S A 106, 14303–14308. https://doi.org/10.1073/pnas.0902976106

Furmento, V.A., Marino, J., Blank, V.C., Cayrol, M.F., Cremaschi, G.A., Aguilar, R.C., Roguin, L.P., 2016. Granulocyte colony-stimulating factor (G-CSF) upregulates β1 integrin and increases migration of human trophoblast Swan 71 cells via PI3K and MAPK activation. Experimental Cell Research 342, 125–134. https://doi.org/10.1016/j.yexcr.2016.03.005

Furutani, E., Newburger, P.E., Shimamura, A., 2019. Neutropenia in the age of genetic testing: Advances and challenges. American Journal of Hematology 94, 384–393. https://doi.org/10.1002/ajh.25374

Ganley, I.G., Lam, D.H., Wang, J., Ding, X., Chen, S., Jiang, X., 2009. ULK1·ATG13·FIP200 Complex Mediates mTOR Signaling and Is Essential for Autophagy*. Journal of Biological Chemistry 284, 12297–12305. https://doi.org/10.1074/jbc.M900573200

Geng, J., Klionsky, D.J., 2008. Quantitative regulation of vesicle formation in yeast nonspecific autophagy. Autophagy 4, 955–957. https://doi.org/10.4161/auto.6791

Gengyo-Ando, K., Kumagai, M., Ando, H., Nakai, J., 2024. Domain 3a mutation of VPS33A suppresses larval arrest phenotype in the loss of VPS45 in Caenorhabditis elegans. MicroPubl Biol 2024. https://doi.org/10.17912/micropub.biology.001155

Gerrard, S.R., Bryant, N.J., Stevens, T.H., 2000. VPS21 controls entry of endocytosed and biosynthetic proteins into the yeast prevacuolar compartment. Mol Biol Cell 11, 613–626. https://doi.org/10.1091/mbc.11.2.613

Gogianu, L.I., Ruta, L.L., Farcasanu, I.C., 2024. Shedding Light on Calcium Dynamics in the Budding Yeast: A Review on Calcium Monitoring with Recombinant Aequorin. Molecules 29, 5627. https://doi.org/10.3390/molecules29235627

Gozuacik, D., Kimchi, A., 2004. Autophagy as a cell death and tumor suppressor mechanism. Oncogene 23, 2891–2906. https://doi.org/10.1038/sj.onc.1207521

Gu, F., Crump, C.M., Thomas, G., 2001. Trans-Golgi network sorting. Cell Mol Life Sci 58, 1067–1084.

Gueldener, U., Heinisch, J., Koehler, G.J., Voss, D., Hegemann, J.H., 2002. A second set of loxP marker cassettes for Cre-mediated multiple gene knockouts in budding yeast. Nucleic Acids Research 30, e23. https://doi.org/10.1093/nar/30.6.e23

Hagihara, K., Kanda, Y., Ishida, K., Satoh, R., Takasaki, T., Maeda, T., Sugiura, R., 2020. Chemical genetic analysis of FTY720- and Ca2+ -sensitive mutants reveals a functional connection between FTY720 and membrane trafficking. Genes Cells 25, 637–645. https://doi.org/10.1111/gtc.12800

Halachmi, N., Lev, Z., 1996. The Sec1 family: a novel family of proteins involved in synaptic transmission and general secretion. J Neurochem 66, 889–897. https://doi.org/10.1046/j.1471-4159.1996.66030889.x

Hammerling, B.C., Najor, R.H., Cortez, M.Q., Shires, S.E., Leon, L.J., Gonzalez, E.R., Boassa, D., Phan, S., Thor, A., Jimenez, R.E., Li, H., Kitsis, R.N., Dorn, G.W., Sadoshima, J., Ellisman, M.H., Gustafsson, Å.B., 2017. A Rab5 endosomal pathway mediates Parkin-dependent mitochondrial clearance. Nat Commun 8, 14050. https://doi.org/10.1038/ncomms14050

Hanson, P.I., Roth, R., Morisaki, H., Jahn, R., Heuser, J.E., 1997. Structure and conformational changes in NSF and its membrane receptor complexes visualized by quick-freeze/deep-etch electron microscopy. Cell 90, 523–535. https://doi.org/10.1016/s0092-8674(00)80512-7

He, C., Song, H., Yorimitsu, T., Monastyrska, I., Yen, W.-L., Legakis, J.E., Klionsky, D.J., 2006. Recruitment of Atg9 to the preautophagosomal structure by Atg11 is essential for selective autophagy in budding yeast. J Cell Biol 175, 925–935. https://doi.org/10.1083/jcb.200606084

Heath-Engel, H.M., Chang, N.C., Shore, G.C., 2008. The endoplasmic reticulum in apoptosis and autophagy: role of the BCL-2 protein family. Oncogene 27, 6419–6433. https://doi.org/10.1038/onc.2008.309

Heissig, B., Hattori, K., Dias, S., Friedrich, M., Ferris, B., Hackett, N.R., Crystal, R.G., Besmer, P., Lyden, D., Moore, M.A.S., Werb, Z., Rafii, S., 2002. Recruitment of stem and progenitor cells from the bone marrow niche requires MMP-9 mediated release of kit-ligand. Cell 109, 625–637. https://doi.org/10.1016/s0092-8674(02)00754-7

Helliwell, S.B., Wagner, P., Kunz, J., Deuter-Reinhard, M., Henriquez, R., Hall, M.N., 1994. TOR1 and TOR2 are structurally and functionally similar but not identical phosphatidylinositol kinase homologues in yeast. Mol Biol Cell 5, 105–118. https://doi.org/10.1091/mbc.5.1.105

Henson, P.M., Johnston, R.B., 1987. Tissue injury in inflammation. Oxidants, proteinases, and cationic proteins. J Clin Invest 79, 669–674. https://doi.org/10.1172/JCI112869

Ho, K.-H., Chang, H.-E., Huang, W.-P., 2009. Mutation at the cargo-receptor binding site of Atg8 also affects its general autophagy regulation function. Autophagy 5, 461–471. https://doi.org/10.4161/auto.5.4.7696

Hollenstein, D.M., Gómez-Sánchez, R., Ciftci, A., Kriegenburg, F., Mari, M., Torggler, R., Licheva, M., Reggiori, F., Kraft, C., 2019. Vac8 spatially confines autophagosome formation at the vacuole in S. cerevisiae. J Cell Sci 132, jcs235002. https://doi.org/10.1242/jcs.235002

Horazdovsky, B.F., Busch, G.R., Emr, S.D., 1994. VPS21 encodes a rab5-like GTP binding protein that is required for the sorting of yeast vacuolar proteins. The EMBO Journal 13, 1297–1309. https://doi.org/10.1002/j.1460-2075.1994.tb06382.x

Hou, S., Wang, X., Yu, Y., Ji, H., Dong, X., Li, J., Li, H., He, H., Li, Z., Yang, Z., Chen, W., Yao, G., Zhang, Y., Zhang, J., Bi, M., Niu, S., Zhao, G., Zhu, R., Liu, G., Jia, Y., Gao, Y., 2023. Invasive fungal infection is associated with antibiotic exposure in preterm infants: a multi-centre prospective case–control study. Journal of Hospital Infection 134, 43–49. https://doi.org/10.1016/j.jhin.2023.01.002

Ichimura, Y., Kirisako, T., Takao, T., Satomi, Y., Shimonishi, Y., Ishihara, N., Mizushima, N., Tanida, I., Kominami, E., Ohsumi, M., Noda, T., Ohsumi, Y., 2000. A ubiquitin-like system mediates protein lipidation. Nature 408, 488–492. https://doi.org/10.1038/35044114

Inadome, H., Noda, Y., Adachi, H., Yoda, K., 2005. Immunoisolaton of the yeast Golgi subcompartments and characterization of a novel membrane protein, Svp26, discovered in the Sed5-containing compartments. Mol Cell Biol 25, 7696–7710. https://doi.org/10.1128/MCB.25.17.7696-7710.2005

Ishiwata-Kimata, Y., Le, Q.G., Kimata, Y., 2022. Induction and Aggravation of the Endoplasmic-Reticulum Stress by Membrane-Lipid Metabolic Intermediate Phosphatidyl-N-Monomethylethanolamine. Front. Cell Dev. Biol. 9. https://doi.org/10.3389/fcell.2021.743018

Iwai, K., Miyawaki, T., Takizawa, T., Konno, A., Ohta, K., Yachie, A., Seki, H., Taniguchi, N., 1994. Differential expression of bcl-2 and susceptibility to anti-Fas-mediated cell death in peripheral blood lymphocytes, monocytes, and neutrophils. Blood 84, 1201–1208.

Jahn, R., Cafiso, D.C., Tamm, L.K., 2023. Mechanisms of SNARE proteins in membrane fusion. Nat Rev Mol Cell Biol 25, 101–118. https://doi.org/10.1038/s41580-023-00668-x

Jahn, R., Südhof, T.C., 1999. Membrane fusion and exocytosis. Annu Rev Biochem 68, 863–911. https://doi.org/10.1146/annurev.biochem.68.1.863

Jakubowski, A.A., Souza, L., Kelly, F., Fain, K., Budman, D., Clarkson, B., Bonilla, M.A., Moore, M.A., Gabrilove, J., 1989. Effects of human granulocyte colony-stimulating factor in a patient with idiopathic neutropenia. N Engl J Med 320, 38–42. https://doi.org/10.1056/NEJM198901053200107

Johansen, T., Lamark, T., 2020. Selective Autophagy: ATG8 Family Proteins, LIR Motifs and Cargo Receptors. J Mol Biol 432, 80–103. https://doi.org/10.1016/j.jmb.2019.07.016

Johnson, L.M., Bankaitis, V.A., Emr, S.D., 1987. Distinct sequence determinants direct intracellular sorting and modification of a yeast vacuolar protease. Cell 48, 875–885. https://doi.org/10.1016/0092-8674(87)90084-5

Kale, J., Osterlund, E.J., Andrews, D.W., 2018. BCL-2 family proteins: changing partners in the dance towards death. Cell Death Differ 25, 65–80. https://doi.org/10.1038/cdd.2017.186

Kang, R., Zeh, H.J., Lotze, M.T., Tang, D., 2011. The Beclin 1 network regulates autophagy and apoptosis. Cell Death Differ 18, 571–580. https://doi.org/10.1038/cdd.2010.191

Kanki, T., Furukawa, K., Yamashita, S., 2015. Mitophagy in yeast: Molecular mechanisms and physiological role. Biochimica et Biophysica Acta (BBA) - Molecular Cell Research, Mitophagy 1853, 2756–2765. https://doi.org/10.1016/j.bbamcr.2015.01.005

Kanki, T., Klionsky, D.J., 2008. Mitophagy in Yeast Occurs through a Selective Mechanism. Journal of Biological Chemistry 283, 32386–32393. https://doi.org/10.1074/jbc.M802403200

Kanki, T., Kurihara, Y., Jin, X., Goda, T., Ono, Y., Aihara, M., Hirota, Y., Saigusa, T., Aoki, Y., Uchiumi, T., Kang, D., 2013. Casein kinase 2 is essential for mitophagy. EMBO reports 14, 788–794. https://doi.org/10.1038/embor.2013.114

Kanki, T., Wang, K., Cao, Y., Baba, M., Klionsky, D.J., 2009. Atg32 is a mitochondrial protein that confers selectivity during mitophagy. Dev Cell 17, 98–109. https://doi.org/10.1016/j.devcel.2009.06.014

Karaatmaca, B., Cagdas, D., Tan, Ç., Aytaç, S., Özbek, B., Üner, A., Gümrük, F., Tezcan, İ., 2020. A rare form of congenital neutropenia: VPS45 deficiency. Scandinavian Journal of Immunology 91, e12871. https://doi.org/10.1111/sji.12871

Keeble, J.A., Gilmore, A.P., 2007. Apoptosis commitment – translating survival signals into decisions on mitochondria. Cell Res 17, 976–984. https://doi.org/10.1038/cr.2007.101

Kim, J., Kamada, Y., Stromhaug, P.E., Guan, J., Hefner-Gravink, A., Baba, M., Scott, S.V., Ohsumi, Y., Dunn, W.A., Klionsky, D.J., 2001. Cvt9/Gsa9 functions in sequestering selective cytosolic cargo destined for the vacuole. J Cell Biol 153, 381–396. https://doi.org/10.1083/jcb.153.2.381

Kim, J., Klionsky, D.J., 2000. Autophagy, cytoplasm-to-vacuole targeting pathway, and pexophagy in yeast and mammalian cells. Annu Rev Biochem 69, 303–342. https://doi.org/10.1146/annurev.biochem.69.1.303

Kim, J., Scott, S.V., Oda, M.N., Klionsky, D.J., 1997. Transport of a Large Oligomeric Protein by the Cytoplasm to Vacuole Protein Targeting Pathway. Journal of Cell Biology 137, 609–618. https://doi.org/10.1083/jcb.137.3.609

Kinchen, J.M., Ravichandran, K.S., 2008. Phagosome maturation: going through the acid test. Nat Rev Mol Cell Biol 9, 781–795. https://doi.org/10.1038/nrm2515

King, K.Y., Goodell, M.A., 2011. Inflammatory modulation of hematopoietic stem cells: viewing the hematopoietic stem cell as a foundation for the immune response. Nat Rev Immunol 11, 685–692. https://doi.org/10.1038/nri3062

Kirisako, T., Ichimura, Y., Okada, H., Kabeya, Y., Mizushima, N., Yoshimori, T., Ohsumi, M., Takao, T., Noda, T., Ohsumi, Y., 2000. The Reversible Modification Regulates the Membrane-Binding State of Apg8/Aut7 Essential for Autophagy and the Cytoplasm to Vacuole Targeting Pathway. J Cell Biol 151, 263–276. https://doi.org/10.1083/jcb.151.2.263

Kissová, I., Deffieu, M., Manon, S., Camougrand, N., 2004. Uth1p Is Involved in the Autophagic Degradation of Mitochondria *. Journal of Biological Chemistry 279, 39068–39074. https://doi.org/10.1074/jbc.M406960200

Kissová, I., Plamondon, L.-T., Brisson, L., Priault, M., Renouf, V., Schaeffer, J., Camougrand, N., Manon, S., 2006. Evaluation of the roles of apoptosis, autophagy, and mitophagy in the loss of plating efficiency induced by Bax expression in yeast. J Biol Chem 281, 36187–36197. https://doi.org/10.1074/jbc.M607444200

Klebanoff, S.J., 2005. Myeloperoxidase: friend and foe. Journal of Leukocyte Biology 77, 598–625. https://doi.org/10.1189/jlb.1204697

Klein, C., 2009. Congenital neutropenia. Hematology 2009, 344–350. https://doi.org/10.1182/asheducation-2009.1.344

Klein, C., Grudzien, M., Appaswamy, G., Germeshausen, M., Sandrock, I., Schäffer, A.A., Rathinam, C., Boztug, K., Schwinzer, B., Rezaei, N., Bohn, G., Melin, M., Carlsson, G., Fadeel, B., Dahl, N., Palmblad, J., Henter, J.-I., Zeidler, C., Grimbacher, B., Welte, K., 2007. HAX1 deficiency causes autosomal recessive severe congenital neutropenia (Kostmann disease). Nat Genet 39, 86–92. https://doi.org/10.1038/ng1940

Klionsky, D.J., 2013. Why just eat in, when you can also eat out? Autophagy 9, 119–119. https://doi.org/10.4161/auto.22915

Klionsky, D.J., Brand-Saberi, B., Dong, X.C., Kenchappa, C.S., Li, Zuguo, Lin, Y., Oshima, S., Rong, Y., Sluimer, J.C., Stallings, C.L., Tong, C.-K., 2021. Guidelines for the use and interpretation of assays for monitoring autophagy (4th edition)1. Autophagy 17, 1–382. https://doi.org/10.1080/15548627.2020.1797280

Klionsky, D.J., Cueva, R., Yaver, D.S., 1992. Aminopeptidase I of Saccharomyces cerevisiae is localized to the vacuole independent of the secretory pathway. Journal of Cell Biology 119, 287–299. https://doi.org/10.1083/jcb.119.2.287

Klionsky, D.J., Emr, S.D., 1989. Membrane protein sorting: biosynthesis, transport and processing of yeast vacuolar alkaline phosphatase. The EMBO Journal 8, 2241–2250. https://doi.org/10.1002/j.1460-2075.1989.tb08348.x

Koppen, M., Langer, T., 2007. Protein Degradation within Mitochondria: Versatile Activities of AAA Proteases and Other Peptidases. Critical Reviews in Biochemistry and Molecular Biology 42, 221–242. https://doi.org/10.1080/10409230701380452

Kostman, R., 1975. Infantile genetic agranulocytosis. A review with presentation of ten new cases. Acta Paediatr Scand 64, 362–368. https://doi.org/10.1111/j.1651-2227.1975.tb03847.x

Kostmann, R., 1956. Infantile genetic agranulocytosis; agranulocytosis infantilis hereditaria. Acta Paediatr Suppl (Upps) 45, 1–78.

Kreykenbohm, V., Wenzel, D., Antonin, W., Atlachkine, V., Fischer von Mollard, G., 2002. The SNAREs vti1a and vti1b have distinct localization and SNARE complex partners. European Journal of Cell Biology 81, 273–280. https://doi.org/10.1078/0171-9335-00247

Kroemer, G., Galluzzi, L., Brenner, C., 2007. Mitochondrial Membrane Permeabilization in Cell Death. Physiological Reviews 87, 99–163. https://doi.org/10.1152/physrev.00013.2006

Kurz, T., Gustafsson, B., Brunk, U.T., 2011. Cell sensitivity to oxidative stress is influenced by ferritin autophagy. Free Radical Biology and Medicine 50, 1647–1658. https://doi.org/10.1016/j.freeradbiomed.2011.03.014

Lee, Y.J., Hoe, K.L., Maeng, P.J., 2007. Yeast cells lacking the CIT1-encoded mitochondrial citrate synthase are hypersusceptible to heat- or aging-induced apoptosis. Mol Biol Cell 18, 3556–3567. https://doi.org/10.1091/mbc.e07-02-0118

Leupold, S., Hubmann, G., Litsios, A., Meinema, A.C., Takhaveev, V., Papagiannakis, A., Niebel, B., Janssens, G., Siegel, D., Heinemann, M., 2019. Saccharomyces

cerevisiae goes through distinct metabolic phases during its replicative lifespan. eLife 8, e41046. https://doi.org/10.7554/eLife.41046
Little, J., Chikina, M., Clark, N.L., 2024. Evolutionary rate covariation is a reliable predictor of co-functional interactions but not necessarily physical interactions. eLife 12, RP93333. https://doi.org/10.7554/eLife.93333
Longo, V.D., Gralla, E.B., Valentine, J.S., 1996. Superoxide dismutase activity is essential for stationary phase survival in Saccharomyces cerevisiae. Mitochondrial production of toxic oxygen species in vivo. J Biol Chem 271, 12275–12280. https://doi.org/10.1074/jbc.271.21.12275
Lord, B.I., Bronchud, M.H., Owens, S., Chang, J., Howell, A., Souza, L., Dexter, T.M., 1989. The kinetics of human granulopoiesis following treatment with granulocyte colony-stimulating factor in vivo. Proc Natl Acad Sci U S A 86, 9499–9503. https://doi.org/10.1073/pnas.86.23.9499
Lynch-Day, M.A., Klionsky, D.J., 2010. The Cvt pathway as a model for selective autophagy. FEBS Letters, Autophagy 584, 1359–1366. https://doi.org/10.1016/j.febslet.2010.02.013
Lystad, A.H., Simonsen, A., 2019. Mechanisms and Pathophysiological Roles of the ATG8 Conjugation Machinery. Cells 8, 973. https://doi.org/10.3390/cells8090973
Madeo, F., Fröhlich, E., Ligr, M., Grey, M., Sigrist, S.J., Wolf, D.H., Fröhlich, K.-U., 1999. Oxygen Stress: A Regulator of Apoptosis in Yeast. J Cell Biol 145, 757–767.
Madeo, F., Herker, E., Maldener, C., Wissing, S., Lächelt, S., Herlan, M., Fehr, M., Lauber, K., Sigrist, S.J., Wesselborg, S., Fröhlich, K.-U., 2002. A Caspase-Related Protease Regulates Apoptosis in Yeast. Molecular Cell 9, 911–917. https://doi.org/10.1016/S1097-2765(02)00501-4
Maianski, N.A., Mul, F.P.J., van Buul, J.D., Roos, D., Kuijpers, T.W., 2002. Granulocyte colony-stimulating factor inhibits the mitochondria-dependent activation of caspase-3 in neutrophils. Blood 99, 672–679. https://doi.org/10.1182/blood.V99.2.672
Maiuri, M.C., Criollo, A., Kroemer, G., 2010. Crosstalk between apoptosis and autophagy within the Beclin 1 interactome. EMBO J 29, 515–516. https://doi.org/10.1038/emboj.2009.377
Marcusson, E.G., Horazdovsky, B.F., Cereghino, J.L., Gharakhanian, E., Emr, S.D., 1994. The sorting receptor for yeast vacuolar carboxypeptidase Y is encoded by the VPS10 gene. Cell 77, 579–586. https://doi.org/10.1016/0092-8674(94)90219-4
Markin, V.S., Kozlov, M.M., Borovjagin, V.L., 1984. On the theory of membrane fusion. The stalk mechanism. Gen Physiol Biophys 3, 361–377.
Matoba, K., Kotani, T., Tsutsumi, A., Tsuji, T., Mori, T., Noshiro, D., Sugita, Y., Nomura, N., Iwata, S., Ohsumi, Y., Fujimoto, T., Nakatogawa, H., Kikkawa, M., Noda, N.N., 2020. Atg9 is a lipid scramblase that mediates autophagosomal membrane expansion. Nat Struct Mol Biol 27, 1185–1193. https://doi.org/10.1038/s41594-020-00518-w
Mauro-Lizcano, M., Esteban-Martínez, L., Seco, E., Serrano-Puebla, A., Garcia-Ledo, L., Figueiredo-Pereira, C., Vieira, H.L.A., Boya, P., 2015. New method to assess mitophagy flux by flow cytometry. Autophagy 11, 833–843. https://doi.org/10.1080/15548627.2015.1034403
McNew, J.A., Parlati, F., Fukuda, R., Johnston, R.J., Paz, K., Paumet, F., Söllner, T.H., Rothman, J.E., 2000. Compartmental specificity of cellular membrane fusion encoded in SNARE proteins. Nature 407, 153–159. https://doi.org/10.1038/35025000
Medzhitov, R., Janeway, C.A., 2002. Decoding the patterns of self and nonself by the innate immune system. Science 296, 298–300. https://doi.org/10.1126/science.1068883
Meerschaut, I., Bordon, V., Dhooge, C., Delbeke, P., Vanlander, A.V., Simon, A., Klein, C., Kooy, R.F., Somech, R., Callewaert, B., 2015. Severe congenital neutropenia with neurological impairment due to a homozygous VPS45 p.E238K mutation:

A case report suggesting a genotype–phenotype correlation. American Journal of Medical Genetics Part A 167, 3214–3218. https://doi.org/10.1002/ajmg.a.37367
Mehta, H.M., Malandra, M., Corey, S.J., 2015. G-CSF and GM-CSF in Neutropenia. The Journal of Immunology 195, 1341–1349. https://doi.org/10.4049/jimmunol.1500861
Meijer, W.H., van der Klei, I.J., Veenhuis, M., Kiel, J.A.K.W., 2007. ATG genes involved in non-selective autophagy are conserved from yeast to man, but the selective Cvt and pexophagy pathways also require organism-specific genes. Autophagy 3, 106–116. https://doi.org/10.4161/auto.3595
Mijaljica, D., Prescott, M., Klionsky, D.J., Devenish, R.J., 2007. Autophagy and Vacuole Homeostasis: A Case for Self-Degradation? Autophagy 3, 417–421. https://doi.org/10.4161/auto.4441
Misura, K.M.S., Bock, J.B., Gonzalez, L.C., Scheller, R.H., Weis, W.I., 2002. Three-dimensional structure of the amino-terminal domain of syntaxin 6, a SNAP-25 C homolog. Proc Natl Acad Sci U S A 99, 9184–9189. https://doi.org/10.1073/pnas.132274599
Misura, K.M.S., Scheller, R.H., Weis, W.I., 2000. Three-dimensional structure of the neuronal-Sec1–syntaxin 1a complex. Nature 404, 355–362. https://doi.org/10.1038/35006120
Mizushima, N., Kuma, A., Kobayashi, Y., Yamamoto, A., Matsubae, M., Takao, T., Natsume, T., Ohsumi, Y., Yoshimori, T., 2003. Mouse Apg16L, a novel WD-repeat protein, targets to the autophagic isolation membrane with the Apg12-Apg5 conjugate. J Cell Sci 116, 1679–1688. https://doi.org/10.1242/jcs.00381
Mochizuki, T., Kojima, Y., Nishiwaki, Y., Harakuni, T., Masai, I., 2018. Endocytic trafficking factor VPS45 is essential for spatial regulation of lens fiber differentiation in zebrafish. Development 145, dev170282. https://doi.org/10.1242/dev.170282
Munson, M., Chen, X., Cocina, A.E., Schultz, S.M., Hughson, F.M., 2000. Interactions within the yeast t-SNARE Sso1p that control SNARE complex assembly. Nat Struct Biol 7, 894–902. https://doi.org/10.1038/79659
Nair, U., Klionsky, D.J., 2011. Autophagosome biogenesis requires SNAREs. Autophagy 7, 1570–1572. https://doi.org/10.4161/auto.7.12.18001
Nakatogawa, H., Ichimura, Y., Ohsumi, Y., 2007. Atg8, a Ubiquitin-like Protein Required for Autophagosome Formation, Mediates Membrane Tethering and Hemifusion. Cell 130, 165–178. https://doi.org/10.1016/j.cell.2007.05.021
Nakatsukasa, K., Kanada, A., Matsuzaki, M., Byrne, S.D., Okumura, F., Kamura, T., 2014. The Nutrient Stress-induced Small GTPase Rab5 Contributes to the Activation of Vesicle Trafficking and Vacuolar Activity*. Journal of Biological Chemistry 289, 20970–20978. https://doi.org/10.1074/jbc.M114.548297
Narendra, D., Walker, J.E., Youle, R., 2012. Mitochondrial Quality Control Mediated by PINK1 and Parkin: Links to Parkinsonism. Cold Spring Harb Perspect Biol 4, a011338. https://doi.org/10.1101/cshperspect.a011338
Nascimbeni, A.C., Codogno, P., Morel, E., 2017. Phosphatidylinositol-3-phosphate in the regulation of autophagy membrane dynamics. FEBS J 284, 1267–1278. https://doi.org/10.1111/febs.13987
Nathan, C., 2003. Specificity of a third kind: reactive oxygen and nitrogen intermediates in cell signaling. J Clin Invest 111, 769–778. https://doi.org/10.1172/JCI18174
Newburger, P.E., 2018. Molecular Pathobiology of VPS45 Bone Marrow Failure.
Nichols, B.J., Ungermann, C., Pelham, H.R., Wickner, W.T., Haas, A., 1997. Homotypic vacuolar fusion mediated by t- and v-SNAREs. Nature 387, 199–202. https://doi.org/10.1038/387199a0
Nickerson, D.P., Russell, M.R.G., Lo, S.-Y., Chapin, H.C., Milnes, J., Merz, A.J., 2012. Termination of isoform-selective Vps21/Rab5 signaling at endolysosomal organelles by Msb3/Gyp3. Traffic 13, 1411–1428. https://doi.org/10.1111/j.1600-0854.2012.01390.x

Nielsen, E., Christoforidis, S., Uttenweiler-Joseph, S., Miaczynska, M., Dewitte, F., Wilm, M., Hoflack, B., Zerial, M., 2000. Rabenosyn-5, a Novel Rab5 Effector, Is Complexed with Hvps45 and Recruited to Endosomes through a Fyve Finger Domain. J Cell Biol 151, 601–612.

Nixon, R.A., Yang, D.-S., 2012. Autophagy and Neuronal Cell Death in Neurological Disorders. Cold Spring Harb Perspect Biol 4, a008839. https://doi.org/10.1101/cshperspect.a008839

Noda, N.N., Kumeta, H., Nakatogawa, H., Satoo, K., Adachi, W., Ishii, J., Fujioka, Y., Ohsumi, Y., Inagaki, F., 2008. Structural basis of target recognition by Atg8/LC3 during selective autophagy. Genes to Cells 13, 1211–1218. https://doi.org/10.1111/j.1365-2443.2008.01238.x

Noda, N.N., Ohsumi, Y., Inagaki, F., 2010. Atg8-family interacting motif crucial for selective autophagy. FEBS Letters, Autophagy 584, 1379–1385. https://doi.org/10.1016/j.febslet.2010.01.018

Noda, T., Kim, J., Huang, W.-P., Baba, M., Tokunaga, C., Ohsumi, Y., Klionsky, D.J., 2000. Apg9p/Cvt7p Is an Integral Membrane Protein Required for Transport Vesicle Formation in the Cvt and Autophagy Pathways. Journal of Cell Biology 148, 465–480. https://doi.org/10.1083/jcb.148.3.465

Ohashi, Y., Munro, S., 2010. Membrane Delivery to the Yeast Autophagosome from the Golgi–Endosomal System. Mol Biol Cell 21, 3998–4008. https://doi.org/10.1091/mbc.E10-05-0457

Okamoto, K., Kondo-Okamoto, N., Ohsumi, Y., 2009. Mitochondria-anchored receptor Atg32 mediates degradation of mitochondria via selective autophagy. Dev Cell 17, 87–97. https://doi.org/10.1016/j.devcel.2009.06.013

Onishi, M., Yamano, K., Sato, M., Matsuda, N., Okamoto, K., 2021. Molecular mechanisms and physiological functions of mitophagy. The EMBO Journal 40, e104705. https://doi.org/10.15252/embj.2020104705

Orsi, A., Razi, M., Dooley, H.C., Robinson, D., Weston, A.E., Collinson, L.M., Tooze, S.A., 2012. Dynamic and transient interactions of Atg9 with autophagosomes, but not membrane integration, are required for autophagy. Mol Biol Cell 23, 1860–1873. https://doi.org/10.1091/mbc.E11-09-0746

Park, J., Kim, H.-I., Jeong, H., Lee, M., Jang, S.H., Yoon, S.Y., Kim, H., Park, Z.-Y., Jun, Y., Lee, C., 2019. Quaternary structures of Vac8 differentially regulate the Cvt and PMN pathways. Autophagy 16, 991–1006. https://doi.org/10.1080/15548627.2019.1659615

Parlati, F., Varlamov, O., Paz, K., McNew, J.A., Hurtado, D., Söllner, T.H., Rothman, J.E., 2002. Distinct SNARE complexes mediating membrane fusion in Golgi transport based on combinatorial specificity. Proceedings of the National Academy of Sciences 99, 5424–5429. https://doi.org/10.1073/pnas.082100899

Parlati, F., Weber, T., McNew, J.A., Westermann, B., Söllner, T.H., Rothman, J.E., 1999. Rapid and efficient fusion of phospholipid vesicles by the alpha-helical core of a SNARE complex in the absence of an N-terminal regulatory domain. Proc Natl Acad Sci U S A 96, 12565–12570. https://doi.org/10.1073/pnas.96.22.12565

Pawelec, A., Arsić, J., Kölling, R., 2010. Mapping of Vps21 and HOPS Binding Sites in Vps8 and Effect of Binding Site Mutants on Endocytic Trafficking. Eukaryotic Cell 9, 602–610. https://doi.org/10.1128/ec.00286-09

Peplowska, K., Markgraf, D.F., Ostrowicz, C.W., Bange, G., Ungermann, C., 2007. The CORVET Tethering Complex Interacts with the Yeast Rab5 Homolog Vps21 and Is Involved in Endo-Lysosomal Biogenesis. Developmental Cell 12, 739–750. https://doi.org/10.1016/j.devcel.2007.03.006

Peterson, M.R., Burd, C.G., Emr, S.D., 1999. Vac1p coordinates Rab and phosphatidylinositol 3-kinase signaling in Vps45p-dependent vesicle docking/fusion at the endosome. Current Biology 9, 159-S1. https://doi.org/10.1016/S0960-9822(99)80071-2

Pevsner, J., Hsu, S.C., Hyde, P.S., Scheller, R.H., 1996. Mammalian homologues of yeast vacuolar protein sorting (vps) genes implicated in Golgi-to-lysosome trafficking. Gene 183, 7–14. https://doi.org/10.1016/s0378-1119(96)00367-8

Pfaffenwimmer, T., Reiter, W., Brach, T., Nogellova, V., Papinski, D., Schuschnig, M., Abert, C., Ammerer, G., Martens, S., Kraft, C., 2014. Hrr25 kinase promotes selective autophagy by phosphorylating the cargo receptor A tg19. EMBO Reports 15, 862–870. https://doi.org/10.15252/embr.201438932

Piper, R.C., Bryant, N.J., Stevens, T.H., 1997. The membrane protein alkaline phosphatase is delivered to the vacuole by a route that is distinct from the VPS-dependent pathway. J Cell Biol 138, 531–545. https://doi.org/10.1083/jcb.138.3.531

Piper, R.C., Whitters, E.A., Stevens, T.H., 1994. Yeast Vps45p is a Sec1p-like protein required for the consumption of vacuole-targeted, post-Golgi transport vesicles. Eur J Cell Biol 65, 305–318.

Poirier, M.A., Xiao, W., Macosko, J.C., Chan, C., Shin, Y.K., Bennett, M.K., 1998. The synaptic SNARE complex is a parallel four-stranded helical bundle. Nat Struct Biol 5, 765–769. https://doi.org/10.1038/1799

Polčic, P., Jaká, P., Mentel, M., n.d. Yeast as a tool for studying proteins of the Bcl-2 family. Microb Cell 2, 74–87. https://doi.org/10.15698/mic2015.03.193

Prescianotto-Baschong, C., Riezman, H., 2002. Ordering of compartments in the yeast endocytic pathway. Traffic 3, 37–49. https://doi.org/10.1034/j.1600-0854.2002.30106.x

Priault, M., Salin, B., Schaeffer, J., Vallette, F.M., di Rago, J.-P., Martinou, J.-C., 2005. Impairing the bioenergetic status and the biogenesis of mitochondria triggers mitophagy in yeast. Cell Death Differ 12, 1613–1621. https://doi.org/10.1038/sj.cdd.4401697

Quinones, M.M., Winston, J.T., Stromhaug, P.E., 2012. Propeptide of Aminopeptidase 1 Protein Mediates Aggregation and Vesicle Formation in Cytoplasm-to-Vacuole Targeting Pathway. Journal of Biological Chemistry 287, 10121–10133. https://doi.org/10.1074/jbc.M111.311696

Rahajeng, J., Caplan, S., Naslavsky, N., 2010. Common and distinct roles for the binding partners Rabenosyn-5 and Vps45 in the regulation of endocytic trafficking in mammalian cells. Exp Cell Res 316, 859–874. https://doi.org/10.1016/j.yexcr.2009.11.007

Rajasekariah, P., Eyre, H.J., Stanley, K.K., Walls, R.S., Sutherland, G.R., 1999. Molecular cloning and characterization of a cDNA encoding the human leucocyte vacuolar protein sorting (h1Vps45). Int J Biochem Cell Biol 31, 683–694. https://doi.org/10.1016/s1357-2725(99)00017-5

Raymond, C.K., Howald-Stevenson, I., Vater, C.A., Stevens, T.H., 1992. Morphological classification of the yeast vacuolar protein sorting mutants: evidence for a prevacuolar compartment in class E vps mutants. MBoC 3, 1389–1402. https://doi.org/10.1091/mbc.3.12.1389

Reggiori, F., Wang, C.-W., Nair, U., Shintani, T., Abeliovich, H., Klionsky, D.J., 2004. Early Stages of the Secretory Pathway, but Not Endosomes, Are Required for Cvt Vesicle and Autophagosome Assembly in Saccharomyces cerevisiae. MBoC 15, 2189–2204. https://doi.org/10.1091/mbc.e03-07-0479

Reggiori, F., Shintani, T., Nair, U., Klionsky, D.J., 2005. Atg9 cycles between mitochondria and the pre-autophagosomal structure in yeasts. Autophagy 1, 101– 109. https://doi.org/10.4161/auto.1.2.1840

Robinson, J.S., Klionsky, D.J., Banta, L.M., Emr, S.D., 1988. Protein sorting in Saccharomyces cerevisiae: isolation of mutants defective in the delivery and processing of multiple vacuolar hydrolases. Mol Cell Biol 8, 4936–4948.

Romanov, J., Walczak, M., Ibiricu, I., Schüchner, S., Ogris, E., Kraft, C., Martens, S., 2012. Mechanism and functions of membrane binding by the Atg5-Atg12/Atg16 complex during autophagosome formation. EMBO J 31, 4304–4317. https://doi.org/10.1038/emboj.2012.278

Rothman, J.H., Howald, I., Stevens, T.H., 1989. Characterization of genes required for protein sorting and vacuolar function in the yeast Saccharomyces cerevisiae. EMBO J 8, 2057–2065. https://doi.org/10.1002/j.1460-2075.1989.tb03614.x

Rothman, J.H., Stevens, T.H., 1986. Protein sorting in yeast: mutants defective in vacuole biogenesis mislocalize vacuolar proteins into the late secretory pathway. Cell 47, 1041–1051. https://doi.org/10.1016/0092-8674(86)90819-6

Rotig, A., Colonna, M., Bonnefont, J.P., Blanche, S., Fischer, A., Saudubray, J.M., Munnich, A., 1989. Mitochondrial DNA deletion in Pearson's marrow/pancreas syndrome. Lancet 1, 902–903. https://doi.org/10.1016/s0140-6736(89)92897-3

Sabitzki, R., Roßmann, A.-L., Schmitt, M., Flemming, S., Guillén-Samander, A., Behrens, H.M., Jonscher, E., Höhn, K., Fröhlke, U., Spielmann, T., 2024. Role of Rabenosyn-5 and Rab5b in host cell cytosol uptake reveals conservation of endosomal transport in malaria parasites. PLoS Biol 22, e3002639. https://doi.org/10.1371/journal.pbio.3002639

Savill, J., Haslett, C., 1995. Granulocyte clearance by apoptosis in the resolution of inflammation. Semin Cell Biol 6, 385–393. https://doi.org/10.1016/s1043-4682(05)80009-1

Sawa-Makarska, J., Abert, C., Romanov, J., Zens, B., Ibiricu, I., Martens, S., 2014. Cargo binding to Atg19 unmasks additional Atg8 binding sites to mediate membrane–cargo apposition during selective autophagy. Nat Cell Biol 16, 425–433. https://doi.org/10.1038/ncb2935

Scales, S.J., Chen, Y.A., Yoo, B.Y., Patel, S.M., Doung, Y.C., Scheller, R.H., 2000. SNAREs contribute to the specificity of membrane fusion. Neuron 26, 457–464. https://doi.org/10.1016/s0896-6273(00)81177-0

Schaffer, A., Klein, C., 2008. Genetic Heterogeneity in Severe Congenital Neutropenia: How Many Aberrant Pathways Can Kill a Neutrophil? Current opinion in allergy and clinical immunology 7, 481–94. https://doi.org/10.1097/ACI.0b013e3282f1d690

Scheidel, N., Kennedy, J., Blacque, O.E., 2018. Endosome maturation factors Rabenosyn-5/VPS45 and caveolin-1 regulate ciliary membrane and polycystin-2 homeostasis. The EMBO Journal 37, e98248. https://doi.org/10.15252/embj.201798248

Schweers, R.L., Zhang, J., Randall, M.S., Loyd, M.R., Li, W., Dorsey, F.C., Kundu, M., Opferman, J.T., Cleveland, J.L., Miller, J.L., Ney, P.A., 2007. NIX is required for programmed mitochondrial clearance during reticulocyte maturation. Proceedings of the National Academy of Sciences 104, 19500–19505. https://doi.org/10.1073/pnas.0708818104

Scott, S.V., Guan, J., Hutchins, M.U., Kim, J., Klionsky, D.J., 2001. Cvt19 Is a Receptor for the Cytoplasm-to-Vacuole Targeting Pathway. Molecular Cell 7, 1131–1141. https://doi.org/10.1016/S1097-2765(01)00263-5

Shah, R.K., Munson, M., Wierenga, K.J., Pokala, H.R., Newburger, P.E., Crawford, D., 2017. A novel homozygous VPS45 p.P468L mutation leading to severe congenital neutropenia with myelofibrosis. Pediatric Blood & Cancer 64, e26571. https://doi.org/10.1002/pbc.26571

Shanks, S.G., Carpp, L.N., Struthers, M.S., McCann, R.K., Bryant, N.J., 2012. The Sec1/Munc18 Protein Vps45 Regulates Cellular Levels of Its SNARE Binding Partners Tlg2 and Snc2 in Saccharomyces cerevisiae. PLoS One 7. https://doi.org/10.1371/journal.pone.0049628

Shintani, T., Huang, W.-P., Stromhaug, P.E., Klionsky, D.J., 2002. Mechanism of cargo selection in the cytoplasm to vacuole targeting pathway. Dev Cell 3, 825–837. https://doi.org/10.1016/s1534-5807(02)00373-8

Shpilka, T., Weidberg, H., Pietrokovski, S., Elazar, Z., 2011. Atg8: an autophagy-related ubiquitin-like protein family. Genome Biol 12, 226. https://doi.org/10.1186/gb-2011-12-7-226

Shvarev, D., König, C., Susan, N., Langemeyer, L., Walter, S., Perz, A., Fröhlich, F., Ungermann, C., Moeller, A., 2024. Structure of the endosomal CORVET tethering complex. Nat Commun 15, 5227. https://doi.org/10.1038/s41467-024-49137-9

Sickmann, A., Reinders, J., Wagner, Y., Joppich, C., Zahedi, R., Meyer, H.E., Schönfisch, B., Perschil, I., Chacinska, A., Guiard, B., Rehling, P., Pfanner, N., Meisinger, C., 2003. The proteome of Saccharomyces cerevisiae mitochondria. Proc Natl Acad Sci U S A 100, 13207–13212. https://doi.org/10.1073/pnas.2135385100

Skokowa, J., Dale, D.C., Touw, I.P., Zeidler, C., Welte, K., 2017. Severe congenital neutropenias. Nat Rev Dis Primers 3, 17032. https://doi.org/10.1038/nrdp.2017.32

Solinger, J.A., Rashid, H.-O., Prescianotto-Baschong, C., Spang, A., 2020. FERARI is required for Rab11-dependent endocytic recycling. Nature Cell Biology 22, 213–224. https://doi.org/10.1038/s41556-019-0456-5

Söllner, T., Whiteheart, S.W., Brunner, M., Erdjument-Bromage, H., Geromanos, S., Tempst, P., Rothman, J.E., 1993. SNAP receptors implicated in vesicle targeting and fusion. Nature 362, 318–324. https://doi.org/10.1038/362318a0

Sponsel, H.T., Alfrey, A.C., Hammond, W.S., Durr, J.A., Ray, C., Anderson, R.J., 1996. Effect of iron on renal tubular epithelial cells. Kidney Int 50, 436–444. https://doi.org/10.1038/ki.1996.334

Stack, J.H., Horazdovsky, B., Emr, S.D., 1995. Receptor-mediated protein sorting to the vacuole in yeast: roles for a protein kinase, a lipid kinase and GTP-binding proteins. Annu Rev Cell Dev Biol 11, 1–33. https://doi.org/10.1146/annurev.cb.11.110195.000245

Stenmark, H., 2009. Rab GTPases as coordinators of vesicle traffic. Nat Rev Mol Cell Biol 10, 513–525. https://doi.org/10.1038/nrm2728

Stepensky, P., Saada, A., Cowan, M., Tabib, A., Fischer, U., Berkun, Y., Saleh, H., Simanovsky, N., Kogot-Levin, A., Weintraub, M., Ganaiem, H., Shaag, A., Zenvirt, S., Borkhardt, A., Elpeleg, O., Bryant, N.J., Mevorach, D., 2013. The Thr224Asn mutation in the VPS45 gene is associated with the congenital neutropenia and primary myelofibrosis of infancy. Blood 121, 5078–5087. https://doi.org/10.1182/blood-2012-12-475566

Stevens, T., Esmon, B., Schekman, R., 1982. Early stages in the yeast secretory pathway are required for transport of carboxypeptidase Y to the vacuole. Cell 30, 439–448. https://doi.org/10.1016/0092-8674(82)90241-0

Struthers, M.S., Shanks, S.G., MacDonald, C., Carpp, L.N., Drozdowska, A.M., Kioumourtzoglou, D., Furgason, M.L.M., Munson, M., Bryant, N.J., 2009. Functional homology of mammalian syntaxin 16 and yeast Tlg2p reveals a conserved regulatory mechanism. J Cell Sci 122, 2292–2299. https://doi.org/10.1242/jcs.046441

Su, M.-Y., Peng, W.-H., Ho, M.-R., Su, S.-C., Chang, Y.-C., Chen, G.-C., Chang, C.-I., 2015. Structure of yeast Ape1 and its role in autophagic vesicle formation. Autophagy 11, 1580–1593. https://doi.org/10.1080/15548627.2015.1067363

Sutton, R.B., Fasshauer, D., Jahn, R., Brunger, A.T., 1998. Crystal structure of a SNARE complex involved in synaptic exocytosis at 2.4 A resolution. Nature 395, 347–353. https://doi.org/10.1038/26412

Suzuki, K., Kamada, Y., Ohsumi, Y., 2002. Studies of cargo delivery to the vacuole mediated by autophagosomes in Saccharomyces cerevisiae. Dev Cell 3, 815–824. https://doi.org/10.1016/s1534-5807(02)00359-3

Suzuki, K., Kondo, C., Morimoto, M., Ohsumi, Y., 2010. Selective Transport of α-Mannosidase by Autophagic Pathways: IDENTIFICATION OF A NOVEL RECEPTOR, Atg34p *. Journal of Biological Chemistry 285, 30019–30025. https://doi.org/10.1074/jbc.M110.143511

Tall, G.G., Hama, H., DeWald, D.B., Horazdovsky, B.F., 1999. The Phosphatidylinositol 3-Phosphate Binding Protein Vac1p Interacts with a Rab GTPase and a Sec1p Homologue to Facilitate Vesicle-mediated Vacuolar Protein Sorting. Mol Biol Cell 10, 1873–1889.

Tellam, J.T., James, D.E., Stevens, T.H., Piper, R.C., 1997. Identification of a Mammalian Golgi Sec1p-like Protein, mVps45. J. Biol. Chem. 272, 6187–6193. https://doi.org/10.1074/jbc.272.10.6187

Twig, G., Elorza, A., Molina, A.J.A., Mohamed, H., Wikstrom, J.D., Walzer, G., Stiles, L., Haigh, S.E., Katz, S., Las, G., Alroy, J., Wu, M., Py, B.F., Yuan, J., Deeney, J.T., Corkey, B.E., Shirihai, O.S., 2008. Fission and selective fusion govern mitochondrial segregation and elimination by autophagy. EMBO J 27, 433–446. https://doi.org/10.1038/sj.emboj.7601963

Ungar, D., Hughson, F.M., 2003. SNARE protein structure and function. Annu Rev Cell Dev Biol 19, 493–517. https://doi.org/10.1146/annurev.cellbio.19.110701.155609

Valls, L.A., Hunter, C.P., Rothman, J.H., Stevens, T.H., 1987. Protein sorting in yeast: the localization determinant of yeast vacuolar carboxypeptidase Y resides in the propeptide. Cell 48, 887–897. https://doi.org/10.1016/0092-8674(87)90085-7

van Raam, B.J., Verhoeven, A.J., Kuijpers, T.W., 2006. Mitochondria in neutrophil apoptosis. Int J Hematol 84, 199–204. https://doi.org/10.1532/IJH97.06131

Vida, T.A., Graham, T.R., Emr, S.D., 1990. In vitro reconstitution of intercompartmental protein transport to the yeast vacuole. J Cell Biol 111, 2871–2884. https://doi.org/10.1083/jcb.111.6.2871

Vilboux, T., Lev, A., Malicdan, M.C.V., Simon, A.J., Järvinen, P., Racek, T., Puchalka, J., Sood, R., Carrington, B., Bishop, K., Mullikin, J., Huizing, M., Garty, B.Z., Eyal, E., Wolach, B., Gavrieli, R., Toren, A., Soudack, M., Atawneh, O.M., Babushkin, T., Schiby, G., Cullinane, A., Avivi, C., Polak-Charcon, S., Barshack, I., Amariglio, N., Rechavi, G., van der Werff ten Bosch, J., Anikster, Y., Klein, C., Gahl, W.A., Somech, R., 2013. A Congenital Neutrophil Defect Syndrome Associated with Mutations in VPS45. New England Journal of Medicine 369, 54–65. https://doi.org/10.1056/NEJMoa1301296

von Mollard, G.F., Nothwehr, S.F., Stevens, T.H., 1997. The yeast v-SNARE Vti1p mediates two vesicle transport pathways through interactions with the t-SNAREs Sed5p and Pep12p. J Cell Biol 137, 1511–1524. https://doi.org/10.1083/jcb.137.7.1511

Wagner, M.C., Molnar, E.E., Molitoris, B.A., Goebl, M.G., 2006. Loss of the homotypic fusion and vacuole protein sorting or golgi-associated retrograde protein vesicle tethering complexes results in gentamicin sensitivity in the yeast Saccharomyces cerevisiae. Antimicrob Agents Chemother 50, 587–595. https://doi.org/10.1128/AAC.50.2.587-595.2006

Wang, C.-W., Klionsky, D.J., 2003. The Molecular Mechanism of Autophagy. Mol Med 9, 65–76. https://doi.org/10.1007/BF03402040

Wang, K., Klionsky, D.J., 2011. Mitochondria removal by autophagy. Autophagy 7, 297–300. https://doi.org/10.4161/auto.7.3.14502

Webb, G.C., Hoedt, M., Poole, L.J., Jones, E.W., 1997. Genetic interactions between a pep7 mutation and the PEP12 and VPS45 genes: evidence for a novel SNARE component in transport between the Saccharomyces cerevisiae Golgi complex and endosome. Genetics 147, 467–478.

Weisman, L.S., Emr, S.D., Wickner, W.T., 1990. Mutants of Saccharomyces cerevisiae that block intervacuole vesicular traffic and vacuole division and segregation. Proc Natl Acad Sci U S A 87, 1076–1080. https://doi.org/10.1073/pnas.87.3.1076

Werr, J., Xie, X., Hedqvist, P., Ruoslahti, E., Lindbom, L., 1998. β1 Integrins Are Critically Involved in Neutrophil Locomotion in Extravascular Tissue In Vivo. J Exp Med 187, 2091–2096.

Wu, Z., Xu, H., Liu, J., Zhou, F., Liang, Y., 2021. The ESCRT-III complex contributes to macromitophagy in yeast. Traffic 22, 258–273. https://doi.org/10.1111/tra.12805

Wurmser, A.E., Emr, S.D., 2002. Novel PtdIns(3)P-binding protein Etf1 functions as an effector of the Vps34 PtdIns 3-kinase in autophagy. J Cell Biol 158, 761–772. https://doi.org/10.1083/jcb.200112050

Xiang, J., Wan, C., Guo, R., Guo, D., 2016. Is Hydrogen Peroxide a Suitable Apoptosis Inducer for All Cell Types? Biomed Res Int 2016, 7343965. https://doi.org/10.1155/2016/7343965

Xie, Z., Nair, U., Klionsky, D.J., 2008. Atg8 controls phagophore expansion during autophagosome formation. Mol Biol Cell 19, 3290–3298. https://doi.org/10.1091/mbc.e07-12-1292

Yamano, K., Wang, C., Sarraf, S.A., Münch, C., Kikuchi, R., Noda, N.N., Hizukuri, Y., Kanemaki, M.T., Harper, W., Tanaka, K., Matsuda, N., Youle, R.J., 2018. Endosomal Rab cycles regulate Parkin-mediated mitophagy. Elife 7, e31326. https://doi.org/10.7554/eLife.31326

Yamasaki, A., Watanabe, Y., Adachi, W., Suzuki, K., Matoba, K., Kirisako, H., Kumeta, H., Nakatogawa, H., Ohsumi, Y., Inagaki, F., Noda, N.N., 2016. Structural Basis for Receptor-Mediated Selective Autophagy of Aminopeptidase I Aggregates. Cell Reports 16, 19–27. https://doi.org/10.1016/j.celrep.2016.05.066

Ye, X., Morikawa, K., Ho, S.-H., Araki, M., Nishida, K., Hasunuma, T., Hara, K.Y., Kondo, A., 2015. Evaluation of genes involved in oxidative phosphorylation in yeast by developing a simple and rapid method to measure mitochondrial ATP synthetic activity. Microb Cell Fact 14, 56. https://doi.org/10.1186/s12934-015-0239-z

Yorimitsu, Tomohiro, Klionsky, D.J., 2005. Atg11 links cargo to the vesicle-forming machinery in the cytoplasm to vacuole targeting pathway. Mol Biol Cell 16, 1593–1605. https://doi.org/10.1091/mbc.e04-11-1035

Yorimitsu, T., Klionsky, D.J., 2005. Autophagy: molecular machinery for self-eating. Cell Death Differ 12 Suppl 2, 1542–1552. https://doi.org/10.1038/sj.cdd.4401765

Yu, Y., Sun, B., 2020. Autophagy-mediated regulation of neutrophils and clinical applications. Burns Trauma 8, tkz001. https://doi.org/10.1093/burnst/tkz001

Yuan, X., Cong, Y., Hao, J., Shan, Y., Zhao, Z., Wang, S., Chen, J., 2004. Regulation of LIP level and ROS formation through interaction of H-ferritin with G-CSF receptor. J Mol Biol 339, 131–144. https://doi.org/10.1016/j.jmb.2004.03.027

Zhao, L., You, W., Sun, D., Xu, Hui, You, X., Xu, Haiqian, Wu, Z., Xie, Z., Liang, Y., 2022. Vps21 Directs the PI3K-PI(3)P-Atg21-Atg16 Module to Phagophores via Vps8 for Autophagy. International Journal of Molecular Sciences 23, 9550. https://doi.org/10.3390/ijms23179550

Zhou, F., Zou, S., Chen, Y., Lipatova, Z., Sun, D., Zhu, X., Li, R., Wu, Z., You, W., Cong, X., Zhou, Y., Xie, Z., Gyurkovska, V., Liu, Y., Li, Q., Li, W., Cheng, J., Liang, Y., Segev, N., 2017. A Rab5 GTPase module is important for autophagosome closure. PLOS Genetics 13, e1007020. https://doi.org/10.1371/journal.pgen.1007020

Ziviani, E., Tao, R.N., Whitworth, A.J., 2010. Drosophila Parkin requires PINK1 for mitochondrial translocation and ubiquitinates Mitofusin. Proceedings of the National Academy of Sciences 107, 5018–5023. https://doi.org/10.1073/pnas.0913485107